Fritz Laboratory Reports

Civil and Environmental Engineering

1993

Field study of a prestressed concrete bridge, Final Report, Vol 1 of PennDOT Project 86-05, January 1993

Ben T. Yen

Ti Huang

David A. VanHorn

COMMONWEALTH OF PENNSYLVANIA

Department of Transportation

Office of Research and Special Studies

Stephen A. Davis - Associate Director

Research Project No. 86-05
Field Testing of a Steel Bridge and a Prestressed Concrete Bridge

FINAL REPORT
Vol. I
FIELD STUDY OF A PRESTRESSED CONCRETE BRIDGE

by

Ben T. Yen
Ti Huang
David A. VanHorn

LEHIGH UNIVERSITY

Office of Research and Sponsored Programs

Bethlehem, Pennsylvania

January 1993

Fritz Engineering Laboratory Report No. 519.1

Table of Contents

Table of Contents (continued)

ABSTRACT

This report summarizes the results of a study of a precast prestressed concrete beam-slab bridge across the Susquehanna River at Milton, Pennsylvania. Strains in various parts of the bridge superstructure were monitored to determine the effects (1) of dead load, (2) of special test vehicles simulating the AASTHO and PennDOT design loads, and (3) of normal in-service traffic loads. The measured results were used to examine the validity of four commercially available finite element computer programs. The major findings of this study are as follows:

1) The introduction of continuity diaphragms and the continuous concrete deck effectively transforms the simply supported prestressed concrete beams into a continuous structure for live load.

2) Dead load stresses in the prestressed concrete beams are caused primarily by the concrete deck in the positive moment regions. The overall long term effect due to shrinkage, creep, and thermal changes is also significant.

3) The results from four computer programs provided estimates of live load stresses which were considerably higher than stresses derived from strain measurements, typically by a factor of two.

4) The superposition of effects of vehicular loads in different traffic lanes to simulate loading combinations was confirmed.

5) The actual in-service traffic condition on this bridge appears to be considerably lighter than the "fully loaded" condition typically used for structural design.

1. INTRODUCTION

Two highway bridges have been monitored for the determination of stresses developed during construction, as well as under traffic loads after completion. The primary purpose of this study was to use stress data based on measured strains to evaluate the adequacy of several commercially available finite element programs which are being used for the analysis and design of bridge superstructures. This report describes the study of a precast prestressed concrete beam bridge across the Susquehanna River at Milton, Pennsylvania. A separate report provides the results of the study of the other bridge in this project, a steel plate girder bridge carrying I-78 over the Delaware River near Easton, Pennsylvania.

The research reported herein was conducted by Lehigh University under the Pennsylvania Department of Transportation Research Project 86-05. The tasks completed by Lehigh University include the field measurement of strains under various conditions, and comparison of stresses based on measured strains with computed results obtained from four commercially available computer programs.

The computed results were supplied by Modjeski and Masters, Inc. of Camp Hill, Pennsylvania, under a separate contract with the Pennsylvania Department of Transportation. The Lehigh researchers had no direct interaction with the providers of the various computer-based analysis and design programs. The specific tasks included in the Milton Bridge study by Lehigh University are as follows:

1. Determination of the dead load stresses in the main beams caused by the casting of the bridge deck and continuity diaphragms.

1

2. Determination of the structural response of the bridge superstructure to simulated AASHTO and PennDOT design vehicular loads.

3. Determination of the variation of superstructure stresses caused by normal in-service traffic loads.

4. Comparison of the stresses based on field measurements with corresponding stress values obtained from four commercially available finite element computer programs.

5. Determination of the long-term effects of the continuity diaphragms on the stresses in the end regions of the precast prestressed concrete beams.

2. GENERAL DESCRIPTION OF THE STRUCTURE AND INSTRUMENTATION

2.1 Description of the Bridge

The bridge under study is a nine-span structure between Milton, Pennsylvania and an island in the Susquehanna River. The bridge has a total length of 1306 ft., with a slab width of 44 ft. 7 in. A shorter bridge connects the island to West Milton on the west bank of the river, and thence to US 15. The span lengths are 142 ft. for the two end spans, and 146 ft. for the seven interior spans. Fig. 2.1 shows the plan and elevation of the west half of the bridge, where the field study was conducted. Figure 2.2 is a photograph of the completed bridge, taken from a point west of the tested spans.

The main elements of the superstructure consist of four precast prestressed concrete I-beams, at center-to-center spacings of 11 ft. 5 in. The cross-section of the I-beams is that of the AASHTO/PCI Type VI, but elongated to a total depth of 96 in. Figure 2.3 shows a typical cross-section of this bridge. As shown in the figure, the 44 ft. 7 in. deck slab is approximately symmetrically placed atop the four I-beams. However, a 6 ft. wide pedestrian walkway is placed on the northside of the deck, and the 36-ft. wide vehicular roadway is slightly off center to the south. The two 12 ft. designated traffic lanes are nearly directly over the two interior beams. As a result, the fascia beams are expected to carry a relatively small portion of the regular traffic load.

The prestressed concrete I-beams are supported on neoprene pads at the abutments and piers. Initially, there was no continuity at the intermediate supports. However, the concrete deck slab is continuous over

3

the entire bridge, with expansion joints only at the abutments. Monolithically cast with the deck slab are (1) the continuity diaphragms at the piers, which enclose the ends of the precast beams, and (2) the diaphragms at midspan. This method of construction renders the superstructure non-continuous (simple spans) for most of the dead load (weight of beams, deck slab, and diaphragms), but continuous for loads applied after the deck slab has gained strength (including parapet, railing, and live load). Figure 2.4 shows the stay-in-place metal form for the deck slab, as well as the wooden forms for the diaphragms. Figure 2.5 shows the formwork outside the south fascia beam. The continuity of the bridge structure is depicted in Fig. 2.6, which shows the beam-end diaphragm and the bearings over a pier.

The placement of concrete for the deck slab proceeded westward from span 9 to span 1. The deck in the positive moment region of a span, including the mid-span diaphragm, was placed first. Next, the continuity diaphragm between two spans was cast. Finally, concrete was placed in the negative moment region above the continuity diaphragm. Figure 2.7 lists the dates of concrete placement for spans 3, 2 and 1.

2.2 Description of Instrumentation

2.2.1 Electrical Resistance Strain Gages

Strains in the I-beams and deck slab were measured using 2 in. long, temperature-compensated electrical resistance strain gages. These foil gages were attached to the beams by epoxy glue, with the help of a bucket truck for access (Fig. 2.8).

4

The layout for strain gage locations is given in Fig. 2.9. There were 72 strain gages on the I-beams in spans 1, 2 and 3, all in the longitudinal direction of the beams. Because of the diaphragms and the formwork, the strain gages near the diaphragms were attached after the placing of the deck concrete, and were offset by about 3-5 ft. This is shown in Fig. 2.10 for a gage at the bottom of a beam near its end, and in Fig. 2.11 for two gages near a midspan diaphragm. Figure 2.12 shows the exact location of all instrumented cross sections.

Each of these strain gages is identified by an alpha-numeric code which indicates the span number, beam number, quarter span location, and the position on the beam section. For example, gage 243TS was in span 2 (from the westend), on beam 4 (from the northside), at the 3rd quarter point (towards pier no. 2), on the top flange of the beam, and on the south surface. This identification system is used throughout this report.

There were 44 strain gages placed on the bridge deck and parapet, along three cross sections of the deck (midspan of spans 2 and 3, and directly above pier 2). Figure 2.13 shows one row of strain gages at one cross section. The strain gages on the deck are 90-degree rosettes with two individual gages. A closeup of one rosette, covered by protective tapes, is shown in Fig. 2.14. Extreme care was taken to protect the gages from damage due to direct loads from vehicular wheels, and due to rain and heat. Unfortunately, the summer of 1987 was unusually rainy, and the skid-resistance surface scrapemarks of the concrete deck permitted retention of rainwater on the concrete surface, which resulted in debonding of the adhesive. Only a few of these deck gages survived the rainy season during load testing of the bridge.

5

The deck gages were coded to show their location and direction. For example, the gage 214NL was located in span 2 near beam 1, at the 4th quarter point (near pier 2), to the North of the beam, in the Longitudinal direction. Gage 2P2S was in span 2, on top of the Parapet on the South side of the bridge, at midspan (2nd quarter point). All parapet gages were longitudinal.

2.2.2 Instruments for Strain Measurement

For the measurement of beam strains during bridge construction, the primary concern was the steadiness of reference for static strains. Static strain indicators and switch boxes (Fig. 2.15) were located in a trailer under the bridge (Fig. 2.16), and were permanently connected throughout the period of concrete placement (from June 1 to June 11, 1987). The electrical resistances of the lead wires of the strain gages were recorded and incorporated into the evaluation of strains. Repeated reading of the strain indicators demonstrated that an accuracy of 2 microinches per inch, or better, was achieved at all times.

For the measurement of strains due to vehicular loads, a high-precision, analog, magnetic tape recorder was used. This recorder was capable of monitoring 21 gages simultaneously. The most important quantity to be determined was the time variation of strain at each gage as the test vehicle(s) moved at various speeds on the bridge. The magnetic tape recorder permitted the recording of low strains (0.5 microinches per inch), which was about one-fiftieth of the maximum strain. For concrete with a modulus of elasticity of 6×10^6 psi, this strain corresponds to a stress of 3 psi. The recorded live load strains were plotted as strain-

6

time diagrams, and separately analyzed by computer for live load stress evaluation.

2.2.3 Whittemore Gage Instrumentation

The long-term strain changes at the ends of the prestressed concrete beams were measured by means of a Whittemore Strain Gage. Target points were attached to the beams, and metal extension bars were placed in the pressure relief holes in the continuity diaphragms (Fig. 2.17). Ideally, these target points should be securely attached to the prestressed beam by embedded inserts. However, the research project was authorized after the fabrication of the beams, and the preferred method of attachment was not available to the researchers. As a second-choice alternate, the target points were glued to the prestressed concrete beams, using epoxy glue. The high humidity condition underneath the bridge superstructure and the long time interval from installation in 1987 to final measurements in 1990 resulted in movement of some of the target points. Several gage distances went out-of-range of the measuring device. Nevertheless, useful information was obtained from the remaining targets.

3. BEAM STRESSES DURING CONSTRUCTION

3.1 Stresses Based on Measured Strains

The strain recordings from the strain gages on the beams were converted into changes of stresses at the gage locations. Samples of these stress values are given in Appendix A. For conversion of uniaxial strains to stresses, the modulus of elasticity of concrete (E_c) was obtained by direct measurements of axial shortening of standard concrete cylinders provided by the fabricator. Thirty cylinders, cast along with the beams, were tested. From these tests the average value of the modulus of elasticity was found to be 5875 ksi. The average compressive strength of these cylinders, tested in May, 1989, was over 9350 psi.

Some observations on the concrete stresses during the construction period are presented below.

(A) Stress Variation with Concrete Placement

The changes in stresses at the top and bottom of the beams in spans 2 and 3, due to the placement of deck concrete, are shown in Figs. 3.1 to 3.19. The stresses, tensile or compressive, are plotted versus the days from placement of concrete directly above the beams.

(1) Span 2

Figures 3.1 to 3.4 show the stress variations at midspan on the bottom surface of the four beams in span 2. The strain gages were 212B, 222B, 232B and 242B, signifying 2nd span; beams 1, 2, 3 and 4, respectively; 2nd quarter point (midspan); and bottom flange. The first set of readings was taken at 6 a.m. on June 5, 1987, (Day 1) and was used as the reference datum for strains. After placement of the concrete in

8

the positive moment region of span 2 and at the continuity diaphragm of pier 2, (P3 and P4 of Fig. 2.7), the stress change reflected at gage 212B was about 1000 psi in tension at 1 pm, and slightly lower at 6 pm. There were slight daily fluctuations of stresses afterwards. The placement of deck concrete in span 1 and at the continuity diaphragm over pier 1 (P5 and P6 on day 4), had little influence on the stresses at these four gage locations, and neither did the placement of deck concrete in the negative moment regions over the piers (P7, P8 and P9 on days 5, 6 and 7). However, there appears to be a very slight increase in tensile stress in the bottom flange after the simply supported beam was made continuous by the continuity diaphragms (after placement P6 on day 4).

This same trend was observed for all four beams, as can be detected from Figs. 3.1 to 3.4 and from Fig. 3.5 in which the results from the four beams are superimposed. There were minor differences in the magnitude of stresses among the beams, but the general agreement is excellent. The maximum tensile stress due to the weight of the deck concrete, based on measured strains, was about 1200 psi.

The changes of stress in the top flanges of the four beams in span 2 are shown in Figs. 3.6 to 3.10. Two strain gages were placed on the vertical edges of the top flanges of these I-beams, at about 2-1/2 in. from the top. Originally, there was some concern that the water from the placement of the deck concrete might affect the usefulness of these strain gages, even though the gages were properly protected. Fortunately, this problem did not materialize. The results of the measurements showed that all gages functioned well, except gage 212TS. During the night of day 1, a large amount of water used in curing the deck concrete flowed over the

9

area where this gage was located. As a result, gage 212TS consistently read lower than its counterpart, gage 212TN. The difference was nearly constant at 600 psi.

The stress-time plots of Figs. 3.6 to 3.10 are consistent with the results of Figs. 3.1 to 3.5. That is, the placement of the deck concrete in the positive moment region of the beams caused a substantial change in the stresses in the positive moment regions, and the placement of concrete in the continuity diaphragms and in the negative moment regions over the piers had only a very minor influence. For each of the beams, the changes in stresses on the opposite sides of the top flange were quite consistent, and there was a trend of decreasing compression after the simply supported beams were made continuous. The maximum dead load stresses occurred on the day after placement of concrete in the positive moment region, and were on the order of 1600 psi.

(2) Span 3

The results from span 3 were identical to those from span 2 in every respect, due to the dead load of the concrete deck in the positive moment region. The influence of continuity of the beams on the subsequent concrete stresses at the piers was also expected to be about the same for the two spans. Figures 3.11 to 3.15 show the stress variations in the bottom flanges of the four beams, and Figs. 3.16 to 3.19 show those for the top flanges. As expected, the characteristics of these two groups of plots are similar to those for the beams in span 2. The stresses in the bottom flange of the beams increased slightly from day 1 to day 4 (Figs. 3.11 to 3.15) as the deck concrete developed strength, and shrinkage took place. The corresponding decrease of stresses in the top flanges during

10

this time period was a little more prominent (Figs. 3.16 to 3.19). The maximum change was about 400 psi, as compared with a maximum dead load stress of about 1700 psi due to the placement of the concrete deck.

(B) Cross-Sectional Stresses

The distribution of bending stresses at the midspan cross section of the beams due to the weight of the deck concrete is illustrated in Fig. 3.20. The stresses at cross sections 232 and 242 in span 2 are plotted for the 6 a.m. time on days 2, 4 and 7 (June 6, 8 and 11). Those at cross sections 312 and 322 in span 3 are plotted for the 6 a.m. time on days 2, 5, 8 and 11 (June 2, 5, 8 and 11).

It is obvious from these plots that the primary load-induced stress changes in the cross sections were caused by the bending moments due to the weight of the deck concrete in the positive moment region (at day 2), and subsequent changes were of a different nature. The fact that the beams alone carried the weight of the deck concrete is confirmed by the location of the neutral axes being very close to those of the precast beams. As the deck concrete aged, it gradually became composite with the beams. The subsequent effects of continuity and concrete shrinkage were borne by the composite sections. The slight shifting of the neutral axes upward in Fig. 3.20 is a qualitative indication of this phenomenon.

3.2 Comparison with Results from Analysis

No computed beam stresses during the construction stages were made available to the Lehigh researchers for this study. For a qualitative check of the measured stresses, a simple analysis was made on one line of beams. The simplified structural model and the sequence of concrete

11

placement studied are shown in Fig. 3.21. Stage 1 represents the condition that each beam carries the concrete deck in the positive moment region. Stages 2, 3 and 4 represent the casting of concrete in the negative moment region over piers 4, 3 and 2, respectively, and Stage 5 (over pier 1) makes the beam continuous throughout. The effects of concrete shrinkage were not considered in this simple analysis.

Based on the simple analysis, the computed beam stresses at midspan of the four beams in span 2 are listed in Tables 3.1 to 3.4. In all cases, the stresses determined by analysis remain about the same through the five stages. In contrast, the measured stresses, based on E_c - 5875 ksi, changed noticeably and were generally higher than the computed values.

The calculated stresses at stages 1 and 5 along beams number 3 and number 4 are plotted in Figs 3.22 to 3.25 and are compared with the measured stresses. Figures 3.22 and 3.23 are for beam number 3; Figs. 3.24 and 3.25 for beam number 4. For both beams, the calculated and measured stresses in the bottom flange were in good agreement, particularly for beam number 4. In the top flange, the simple analysis underestimated the stress by as much as 500 psi. Although this was not a high magnitude of compressive stress in the top flange, the difference was about one-half of the computed value.

There are several possible reasons for the difference between the computed and measured stresses. One strong possibility is the effect of concrete shrinkage. Examination of the influence of shrinkage during construction is beyond the scope of this study. Such examination may be

12

necessary in the future for a more complete understanding of the behavior

of continuous decks.

4. TEST TRUCK LOADING AND BEAM STRESSES

4.1 Simulated Design Trucks and Test Runs

4.1.1 Test Trucks

For the correlation of live vehicular loads on the bridge and the stresses generated by these loads, controlled tests were conducted using trucks of known axle spacings and weights. The ideal test trucks would be: (1) an AASHTO HS25 vehicle, and (2) one that conforms to the 102-ton Pennsylvania permit truck. However, trucks of these configurations were not available. Two four-axle trucks were used to simulate the desired live loads. The axle spacing and axle weights of these two test trucks are summarized in Fig. 4.1.

The gross weight of each truck was 86.5 kips. The maximum bending moment caused by one such truck over a simple span of 146 ft. (2930 k-ft.) is approximately equal to that which would be caused by an AASHTO HS25 design truck (2950 k-ft.). To simulate the effect of a 102-ton permit truck, the two test trucks were placed in tandem with a spacing of 12 ft. between the last axle (axle 4) of the first truck and the steering axle (axle 5) of the second truck. The maximum bending moment produced by the 2-truck tandem was 4890 k-ft., as compared with the moment of 5710 k-ft. that would be produced by the 102-ton permit truck.

4.1.2 Test Runs

The bridge has a roadway width of 36 ft. between parapets, and contains two normal operation traffic lanes, each 12 ft. in width, placed symmetrically with respect to the roadway centerline. The cross-section is

14

shown in Fig. 2.3. For load testing, these two lanes were designated as Lane 2 and Lane 4, as shown in Fig. 4.2. Lanes 1, 3 and 5 were standard "design lanes" as defined by the AASHTO Bridge Specifications[1]. During the controlled load testing the test trucks were centered in each of the five lanes.

Eight runs at crawl speed were made by the test trucks. Each run consisted of a forward travel of the truck, or trucks, from span 1 to span 3, and then backward travel to span 1. Table 4.1 lists the run numbers and the corresponding trucks and lanes. For example, run 1 had truck no. 1 traveling in lane 5, run 6 had trucks 1 and 2 in lane 4 (to simulate a 102-ton permit truck), etc. Because there were more strain gages than the number of channels in the tape recorder, the strain gages were grouped and the test runs were repeated. The groupings of gages are summarized in Table 4.2.

Strain gages in groups A and B were selected for the purpose of examining the validity of superposition of the effects of multiple loads on the bridge. The five "superposition test runs" are listed in Table 4.1.

4.2 Stresses due to Test Trucks

The recorded strain-time data from the strain gages was examined using an oscilloscope or a plotter. A digital oscilloscope permitted very accurate measurement of strain variation at a gage location, but the process was time consuming. For the Milton Bridge the strains due to the test trucks were quite low, and the amount of data was very large;

15

therefore, the strain-time records of the various runs were plotted out and examined visually.

Figure 4.3 is an example of a strain-time record. Figures B1 to B32 in Appendix B include four sets of strain-time plots for beam cross sections 232 and 242, 212 and 222, 214 and 224, and 234 and 244, respectively. Each set contains the strains of test truck runs 1 to 8. The time (horizontal) scale is identical for all plots with one unit equal to one second. The vertical scales, as indicated, are in microinches per inch of strain. The full height of each strip represents either 25, 50, or 100 microinches per inch.

Each of the strain-time curves starts from the left and travels to the right. A peak indicates compressive stress, and a valley corresponds to tensile stress. Figure 4.3 shows that gage 232B on the bottom flange was subjected to tension during test truck run number 1, while gages 232TN and 232TS on the top flange were under compression. The maximum tensile strain was about 24 microin./in. (140 psi), and the maximum compressive strains were about 8 to 10 microin./in. (50-60 psi). The second peaks and valleys in Fig. 4.3 were variations of strains (and stresses) when the test truck traveled back toward span 1. For the top flange gages 242TN and 242TS on beam number 4, the latter gage was directly under the right wheels of the test truck. The localized effects of the four axles on the strain at 242TS can be seen clearly in the curve.

While a wealth of information on the response of the bridge components can be deduced from these strain-time records, the most important data were the instantaneous responses of the gages as the test truck(s) moved along the specified lanes. Nine specific instants were

16

selected for detailed study and discussion, each corresponding to the peak responses in one of the nine instrumented bridge cross-sections (see Fig. 2.9 and 2.12). The fact that all gages on one cross-section reached their peak responses at the same instant during each test truck run enabled the synchronization of the strain-time records for the repeated runs, when the truck-lane combination was unchanged but different groups of strain gages were monitored (refer to Tables 4.1 and 4.2 for the description of test truck runs and strain gage groups). These nine instants during each run are hereafter referred to as "positions" 1 through 9, position 1 corresponds to peak responses in gages on the midspan section of span 1 (Gages 1X2), position 2 relating to gages at the three-quarter point of span 1 (gages 1X3), and so on, and position 9 correlating with gages on the midspan of span 3 (gages 3X2). Table 4.3 lists the measured stresses in all gages when a simulated 102-ton truck in lane 4 (run 6) was at position 5. At that instant, the gages at midspan of span 2 registered peak stresses. A summary of the largest measured stresses corresponding to each of the nine positions is presented in Table 4.4. A complete compilation of measured stresses, at all 72 beam gage locations, at the nine positions for all eight runs, is given in Appendix C. The deck gages did not generate useful data (as explained in Section 2.2.1, only a very few of these escaped damage of rainwater on the deck surface) and are not included. This data and similar data under other loading conditions were used in the comparison with the results from four commercially available computer programs. A detailed discussion of that comparison is presented in Section 4.3 of this report. It suffices here to point out that the measured stresses were, in all cases, significantly lower than the

17

computer-generated values. The highest strain recorded during the entire test truck load test series translated to a stress of 322 psi in tension. This stress occurred at the bottom of beam 4 at midspan of span 1 (position 1, gage 142B), when a simulated 102-ton truck was in lane 4 (run 6). Under the same loading condition, the average measured stress in the top flange gages (142TS and 142TN) was 74 psi in compression. The largest compression stress developed during the test truck runs was 190 psi (position 3, gage 240B, run 6). All of these stress values are less than 60% of the corresponding stress based on results from the computer programs.

4.3 Comparison of Measured and Computed Beam Stresses

4.3.1 Reduction of Computer-Generated Results

Four commercially available computer programs were used to analyze the bridge superstructure under the test truck loadings, and the results were compared with the measured stresses. The computer-generated results[2] were supplied by Modjeski and Masters, Consulting Engineers, using the computer programs: STRESS, CURVBRG, DESCUS, and BSDI. The first three programs use two-dimensional grid models for the structure, while BSDI uses a three-dimensional model. The actual axle spacings and axle weights of the trucks used in the field test (shown in Fig. 4.1) were used in the analyses. The peak responses at each of the nine instrumented bridge cross-sections were used in the comparisons.

In principle, a comparison of analytical (or computed) versus experimental results should be made as nearly directly as possible at the

18

level of the experimental measurements. In this present study, the preferred level of comparison is the stress at each strain gage location. However, it should be noted that the "computed" stresses were not directly generated by the compter programs. Actually, the programs provided bending moments in individual beams. These moments were then used by Modjeski and Masters to determine stresses at the gage locations, using properties of the precast beam and composite section as shown in Fig. 4.4.

Tables 4.5 to 4.12 present the computed and measured stresses·at the top and bottom gage locations on eight beam cross sections, with the bridge under selected loading conditions. The loading conditions refer to either a simulated HS25 truck in a designated test lane such as lane 5 (test run 1) or lane 2 (test run 4) or a simulated 102-ton overload vehicle in a designated test lane such as lane 4 (test run 6) or lane 2 (test run 8). See Table 4.1. It should be noted that the tabulated values are stresses at the top and bottom of the 96-in. precast beam. Since the top flange gages were actually placed 2-1/2 in. below the top of the beam, the tabulated "measured" stress values at the top were extrapolations from the measured values at the gage locations, as illustrated in the sketch accompanying Table 4.5.

A glance at Tables 4.5 to 4.12 reveals that in all cases, the measured stresses were substantially lower than the computed values. On the other hand, there were only slight differences between the computed values based on moment values yielded by the four computer programs.

4.3.2 Stresses at Midspan of Beams

At the midspan sections of spans 1 and 2, where the beams are under positive bending moment, the stresses based on measured strains at the top and bottom of the beams were about 30 to 60 percent of the computed values. Furthermore, in all cases, the neutral axis locations indicated by the measured stresses were higher (closer to the bridge deck) than those indicated by the computer-generated results. These results are depicted by the sketches associated with Tables 4.5 to 4.10.

In general, all four computer programs gave very similar results, except for occasional differences between the values from BSDI and those from the other three. It should be noted that the computed stresses were the peak responses caused by the specific test truck and loaded lane conditions used in the field measurements. The live load distribution factors of the AASHTO design specifications[1] were not utilized in any of the computer programs. Therefore, any difference among the computed stresses would be attributed to differences in the structural modelling schemes used in the computer programs. As expected, there was good agreement in the results from the three two-dimensional programs, while the three-dimensional program (BSDI) yielded somewhat different results in several cases. It was not expected that the computed stresses based on the beam bending moments generated by all four programs would be much higher than the actual measured stresses from the test truck runs.

Since all four computer programs generated very similar beam bending moments under the same loading conditions, it was initially suspected that the substantial differences between computed and measured stresses may have been caused by the use of the composite beam cross section shown in

20

Fig. 4.4 More specifically, it was felt that the effective flange width used in the calculations may not be appropriate for determining stresses under loading by one test truck (or two test trucks) in a single lane. An in-depth investigation of this problem -- the selection of cross section properties of beams for the analysis of stresses under specific loading conditions other than design load conditions -- would be very useful in the enhancement of current bridge analysis methods, and would be of great future interest. While a current study of this problem is in progress[3], the inclusion of the results is beyond the scope of this study.

Upon further reflection, it is clear that the effect of the effective width of the composite deck slab could not be solely responsible for the differences between the computed and measured stresses. The section used in these computations (Fig. 4.4) has an effective flange width of 96 in. which is approximately two-thirds of the center-to-center spacing of the beams, and a transformed effective width of 73.9 in. which is based on a modular ratio of $n = 0.77$ ($= E_c$ of slab/E_c of beam). The use of a larger transformed effective flange width would influence the section moduli only slightly, particularly with respect to the bottom fiber. That is, even if the transformed effective width is considered to be 137 in. (the center-to-center spacing of the beams), the bottom-fiber section modulus is increased by only 6.7%. Therefore, it is obvious that other factors must be examined.

It is possible that the structural modelling schemes used in the computer programs may have led to the substantial over-estimates of the beam stresses under test truck loads. All four programs took into consideration the continuity of the bridge superstructure under vehicular

21

loads[3]. However, several other characteristics of the bridge may also have contributed to the differences between computed and measured stresses. These characteristics include the actual as-constructed end conditions at the piers and abutments, and the parapet section which acts compositely with the beams and slab. More detailed information on the modelling of these characteristics would be required in order to provide a better basis for the development of a rational explanation of the differences between the computed and measured stresses. Nevertheless, it can be safely stated that for the positive moment region, all four of the computer programs provide similar bending moments in the beams, with the bridge under test truck loads, and all four programs lead to a very conservative (over-estimate) of beam stresses.

4.3.3 Stresses in Beam Sections at Piers

The difference between the computed stresses and the measured values was even more pronounced in the beam sections in the negative moment regions over the piers. In Tables 4.11 and 4.12 are listed stresses in beams 3 and 4 in span 2 near pier 1 (beam sections 230 and 240). The measured stresses at the top of the beam were 20-22% of the corresponding computed values, while measured values at the bottom ranged from 35 to 55% of the computed values.

In determining the computed values of stress at cross-sections in the negative moment region, the deck concrete is typically considered to be cracked, and only the longitudinal reinforcing steel is considered to be effective in resisting tension. The computed values (Tables 4.11 and 4.12) were developed with this assumption. As a result the centroidal

22

axis of the composite section (precast beam plus longitudinal reinforcing bars) was at approximately mid-height of the precast beam, and the computed stresses at the top and bottom fibers of the beam were nearly equal. In contrast, the measured top fiber stresses, which ranged between 29 and 66 psi, were only about one-third of the corresponding bottom fiber stresses, reflecting a considerably higher position of the neutral axis. The low magnitude of the stresses in the top fiber also points to the probable uncracked condition of the deck concrete.

It must be recognized that the continuous bridge deck slab was subjected only to the test truck loadings. The weight of the entire bridge is carried by the precast beams, causing no tensile force in the slab. In view (1) of this construction procedure, (2) of the fact that no cracks in the concrete deck were detected in the negative moment regions, (3) of the low values of measured and computed live load stresses, and (4) of the observed live load stress distribution in the beams (Tables 4.11 and 4.12), it is reasonable to consider that the entire concrete deck slab was effective as the bridge was subjected to the test truck loadings. The effective beam cross section would then have the same geometrical properties as those in the positive moment region (Fig. 4.4). Using those properties, the beam stresses were recalculated from the bending moments generated by the computer programs, and compiled in Tables 4.13 and 4.14. The recalculated stresses in these tables are much lower than the corresponding values in Tables 4.11 and 4.12, but are still significantly higher than the measured values. The ratios of the computed-to-measured stresses in Tables 4.13 and 4.14 are similar to those in Tables 4.5-4.10. It is concluded that the entire concrete deck may be appropriately

23

considered as effective in the negative moment region, and that the computer-generated moments lead to conservative stress estimates in the beams.

4.4 Superposition of Live Load Stresses

Because it was not physically possible to place the full design live load (lane loads) on the completed bridge structure for the direct verification of design live load stresses, the principle of superposition of the truck loads and of the measured stresses was invoked. It was reasoned that the confirmation of the principle with respect to both the computed stresses (from the computer programs) and the measured stresses in the bridge beams would permit its use to estimate the maximum design live load stresses in the bridge structure.

The test truck "superposition runs" are listed in Table 4.1. Single test trucks traveled in the design lanes (lanes 5, 3 and 1 of Fig. 4.2, respectively) during the test runs 1, 2 and 3. In test runs 4 and 5, two trucks traveled side by side in lanes 1 and 3, and in 3 and 5, respectively. The strain-time data were recorded and some of the results are shown as Figs. 4.5 to 4.9. These are for the strain gages at the midspan cross section of beams 3 and 4 in span 2. In Figs. 4.5 and 4.6 the strains due to the forward crawl of a single truck are presented, while Figs. 4.7 to 4.9 include data for both the forward and backward crawl runs. A downward excursion of a curve indicates tension. The full height of each strip is either 50 or 100 microinches per inch of strain, as indicated.

The maximum values of these measured strains are summarized in Table 4.15. Also listed are the results of superposition. It is obvious that the principle of superposition is applicable for determining stresses due to the test truck loadings. In most cases the discrepancy between direct measurement and superposition is no more than 1 microinch/in. The largest deviation is 3 microin./in. (out of 72 microin./in., or about 4%). The accuracy of measurement was about 1 microin./in..

This validity of superposition of measured stresses can be translated to the superposition of the computed stresses, so long as the computed stresses are reasonably conservative estimates of the measured (actual) stresses. For example, if a 204k truck on lane 4 and a HS25 truck in lane 2 were on span 2 simultaneously, the maximum stress at the bottom of beam 4 would be computed as 441 + 99 = 540 psi, according to the computer program CURVBRG (see Table 4.10). The corresponding superimposed measured values would be 268 + 59 = 327 psi. This and other examples are listed in Table 4.16.

In all cases shown in Table 4.16, and in all cases of superposition in this study, the computed tensile stresses at the bottom of the prestressed concrete beams are considered to be reasonably conservative estimates of the actual stresses. Consequently, the beam stresses based on moments yielded by the computer program for full design loading on the bridge model are conservative estimates of the actual stresses in the beams.

5. LIVE LOAD STRESSES DUE TO REGULAR TRAFFIC

5.1 Selection of Strain Gages

Live load stresses caused by regular vehicular loads under normal operating condition were monitored over two two-day periods in June and August, 1988, respectively. These measured live load stresses were compared with the stresses measured under controlled test truck loads, in order to establish the operating live load condition for this bridge, and to generate information for the assessment of the bridge superstructure under normal traffic conditions.

While test trucks of known axle spacings and weights can be controlled to repeatedly travel back and forth in any given lane so that stresses at all strain gages can be recorded, the same control is not possible for regular traffic vehicles. Only 21 strain gages can be monitored by the recording device at one time. By examining the magnitudes of the stresses generated by the simulated HS25 and 204k test trucks, 42 strain gages were selected in two groups of 21 gages for the magnetic tape recorder. These two groups are designated as Group RA and RB, and are listed in Table 5.1.

After careful examination of the recorded stresses due to regular vehicular traffic during the first two-day period in June 1988, further consolidation was made. The most significant 21 strain gages were selected as Group RC for the second two-day measurement in August, 1988. These gages are also listed in Table 5.1.

During the periods when the live load stresses were being monitored, live load traffic was moving freely and without any interference on the

26

Milton bridge. The vehicular mix (passenger cars vs. trucks), direction of travel (eastward or westward), and speed all varied with time. Consequently, there is no duplication among the three sets of recordings, from strain gage groups RA, RB and RC. All are representative of live load stresses from a random sample of normal traffic.

5.2 Maximum Live Load Stresses in Beams

During the two-day periods of live load stress (strain) measurement, it was confirmed at the onset that passenger cars produced very low stresses in the beams, stresses which could not be measured accurately. Only trucks generated meaningful measurable stresses.

Figures 5.1 to 5.3 are examples of stress-time records of seven selected strain gages on the bottom flange of six beams. A downward excursion of the traces indicates live load tension. The stresses in these figures were the highest from this recording group (RC).

The stresses in Fig. 5.1 were due to a truck traveling westward, from span 3 to span 1. This direction of motion can be deduced by observing that gages 342B and 332B in span 3 reached peak strains just seconds before gages 233B in span 2. Gages 222B, 232B and 242B reached their peak values slightly later, followed by the peak response from gage 142B. The largest live load stress range caused by this truck was about 120 psi, in gage 222B on beam 2, which was directly under the westbound operating lane. The shape of the strain-time trace of gage 222B is somewhat similar to the strain influence line for that point, but is affected by the likely presence of other vehicles on the bridge.

27

Figure 5.2 shows the live load stress variations in the same seven strain gages caused by an eastbound truck. Beam 4 yielded the highest live load stresses, about 180 psi in span 1 (Gage 142B) and about 150 psi in span 2 (Gage 242B). The stress records in Fig. 5.3 are from two trucks traveling east, one close behind the other. The first truck was heavier than the second. The largest live load stress was, once again, about 180 psi in beam 4.

All of the strain data recorded during the two two-day periods provided very similar results. Observation of traffic on the bridge also showed that the type and number of cars and trucks were quite consistent. Table 5.2 summarizes the number of cars and trucks manually counted during several one-hour periods. The trucks included both 2-axle and 3 (or more)-axle (busses, trucks and semi-trailer) types. On the average, there were about 30 trucks per hour in east and west bound lanes combined. Some of these trucks appeared to be fully loaded, and some were observed to be empty.

5.3 Comparison with Test Truck Induced Stresses

Although the weights and axle-configurations of normal traffic trucks were not directly determined, some insight was gained by a comparison between the measured stresses due to normal traffic trucks and the stresses caused by the simulated HS25 test truck. Figures 5.4 and 5.5 show two sets of recorded strains in beams 3 and 4 at the midspan of span 2 (reference position 5) due to regular traffic trucks. The corresponding test truck data were taken from run no. 2 with the simulated HS25 truck in lane 4. (Section 4.1, Table 4.1)

28

Table 5.3 lists the highest stress values in six gages due to a normal traffic truck and the corresponding stresses due to the simulated HS25 test truck. From the stress values in the table, it is obvious that this particular truck produced live load stresses of the same general characteristic as those due to the test truck, but with higher magnitude. Normal traffic typically includes trucks wtih axle configurations which do not match those of the standard design vehicle. As a result, live load stresses generated by some of these trucks exceed the stresses produced by a standard design vehicle. The important observation is that the actual measured live load stresses were still quite low, being only 230 psi in this case, and well below typical allowable live load stress limits. It is also important to note that the presence of one heavy truck on the bridge does not approach the "fully loaded" condition which is used as basis for structural design.

5.4 Discussion

A number of important points need to be discussed with regard to the behavior of the Milton bridge under live load. These are the site-specific conditions of vehicle speed, truck positions, and traffic volume, along with their influence on the performance of the bridge.

The bridge under study and a companion bridge provide direct linkage between two communities, Milton and West Milton. Traffic signals are located (1) at the east end of the Milton bridge, and (2) at a short distance to the west of the companion bridge. Furthermore, the bridge deck surface is at a 5% upgrade, from east to west. Under these conditions truck speed on the bridge can hardly exceed 30 mph. This

29

rather low speed of the truck traffic was fully confirmed during the periods of live load stress measurements. Because of the low speed, there was expected to be little impact stress in the bridge members. The smoothness of the strain-time traces of Figs. 5.1 to 5.5 is consistent with the low impact effect. Some very minor high-frequency vibrational strains (with an amplitude of about 6 microinches per inch, corresponding to a stress range of about 20 psi) were detected in the traces in Fig. 5.3. This minor vibration occurred in spans 2 and 3 when an eastbound truck came onto span 1 at a speed of about 30 mph. Whether the presence of a second truck closely behind influenced the minor vibration cannot be determined without knowing the actual conditions of travel. The fact that no such vibration was detected from the strain records of other trucks (such as shown in Fig. 5.2) suggests that the high-frequency vibration was due primarily to the characteristics of this particular truck. The most significant observation regarding impact and vibration of the bridge structure under normal traffic load is that the magnitudes of these stresses are very small.

Although the bridge has only two normal operating traffic lanes, the clear roadway width of 36 ft. is sufficient to permit three 12 ft. design lanes, as represented by test lanes 1, 3 and 5 in Fig. 4.2. In fact, AASHTO Bridge Specifications[1] require that the structural design of this bridge be based on live load from these three lanes. Actually, even under the two-lane operating condition of the bridge, a three-lane loading condition could conceivably occur as a disabled truck may be stopped close to the curb, and two other trucks, travelling in opposite directions, may pass the same cross-section at the same instant. Such a worst-scenario

30

situation was not observed during the normal traffic strain measurement periods. In fact, it is not likely to occur, even if the traffic volume were to double the current number of about 30 trucks per hour (in both directions combined). Nevertheless, the response of the bridge under such an unlikely condition can be estimated by means of superposition. In Table 5.4, the results of test truck runs 1, 3 and 5 (Simulated HS25 truck on lanes 5, 3 and 1, respectively) are combined to generate the maximum stresses at several beam cross-sections. It can be seen that among the four beams, beam 4 would be most heavily stressed, with a maximum stress of 442 psi at midspan of span 3. Reference to Table 4.6 reveals that this stress, obtained by superposition of measured stresses for the 3-truck condition, is still lower than that computed for a single 102-ton permit truck (test truck run no. 6). It is clear that the computer programs generate conservative (too high) estimates of live load stresses.

In summary, the monitoring of live load stresses in the beams of the Milton Bridge under normal traffic conditions led to the following observations:

1. The truck traffic on this bridge is rather light. The total truck volume appears to be about 30 trucks per hour (in both directions combined), including some that are empty. The speed of the trucks rarely exceeds 30 mph.

2. Live load stresses in the main beams caused by individual trucks are comparable to those caused by the simulated HS25 test vehicle.

31

3. Neither the test truck runs nor the normal traffic conditions approached the "fully loaded" condition typically used as a basis for structural design.

4. The measured live load stresses are considerably lower than stresses based on results from the four computer programs. A detailed discussion is given in Section 4.3.

It appears reasonable to surmise that the HS25 truck configuration is an acceptable representation of the live load traffic on the Milton Bridge, and that the bridge, as constructed, has sufficient live load carrying capacity for the foreseeable future.

6. END RESTRAINT OF PRESTRESSED CONCRETE BEAMS

6.1 Whittemore Gage Records

The targets for the Whittemore gage measurements were installed after the removal of the wooden formwork for the continuity diaphragms over the piers. This was approximately three months after the completion of the concrete deck. The gage target points were mounted, as shown in Fig. 6.1, at the ends of beams 3 and 4, on both sides of pier 1 and pier 2.

At the intersection of each beam with each pier, five Whittemore target points were mounted enabling three measurements as shown in Fig. 6.1. Measurement B, between the end of an aluminum bar placed in the pressure relief hole and a target mounted on the concrete surface, reflect the length change over an effective gage distance of 50 in. The intention was to determine the effect of end restraint by the continuity diaphragm. As indicated in Section 2.2.3, difficulties were encountered in the installation of target points after the beams were fabricated. The Epoxy glue was not strong enough to support the weight of the 3'-6" long aluminum bar. On the other hand, drilling holes in the beam was also found to be impractical. In the end, this particular measurement (across the community diaphragm) was abandoned. Measurements were made over gage distances A and C. These measurements yielded information on the longitudinal strains in the beams near their ends, but not the direct effect of the deformation of the diaphragm.

Four sets of measurements were taken, in September of 1987, June and August of 1988, and October of 1990. The readings, in units of 10^{-6}

inches, are listed in Table 6.1 as R1, R2, R3 and R4 respectively. As indicated earlier in the report, the fixity of some targets on the beams was affected by moisture, resulting in some being out of range for measurement. The small number of successful measurements rendered quantitative interpretation of the results rather difficult. Therefore emphasis is placed on the qualitative evaluation of the results.

The difference in Whittemore gage readings between the initial and subsequent measurements at the same gage location represents the elongation or shortening of the fiber over a gage length of 10 inches. These differences are given in Table 6.1 as R21, between readings R2 and R1, etc. All values are negative, revealing that all gage distances were shortened after September 1987. The largest change was on the order of 200×10^{-4} in., in the lower portion of the beams adjacent to pier 1 in span 1.

6.2 Changes in Long-Term Strains at Ends of Beams

The changes in long-term strains obtained from the Whittemore gage measurements are graphically presented in Fig. 6.2 For each section, the changes in strains are shown as the distances away from the beam surface. The line connecting these points across a beam section then provides a visual indication of the deformation of the beam segment (both shortening and curvature).

The largest shortening was observed at the end of nearly three years at section 144, at the interior end of span 1. The shortening at the lower gage location was 213×10^{-4} in. over the 10 in. gage length, representing a contracting strain of 2130×10^{-6} in./in. The change of

34

curvature at this section was represented by the gradient of the connecting line (R41), as follows:

$$\frac{-2130-(-850)}{31 \ in.} \ x \ 10^{-6} = -41.3 \ x \ 10^{-6} \ rad/in.$$

The negative curvature value signifies negative bending, or haunching. These strain and curvature values are extremely high, when compared with the calculated values at midspan of span 2 due to the dead weight of the bridge deck. Based on the stresses shown in Table 3.3, the dead load strain at the midpoint of span 2 is $-283 \ x \ 10^{-6}$, and the curvature is 4.8 $x \ 10^{-6}$ rad./in. The observed long term deformations were an order of magnitude larger.

Very large changes in strains and curvatures were observed only at the end of three years (R41), and only at a few sections, most notably 134 and 144. At most other sections, the changes in fiber strains were less than 300 $x \ 10^{-6}$ in./in., and the change in long-term curvature was less than 4 $x \ 10^{-6}$ rad./in. These values are more nearly consistent with what may be expected as a result of shrinkage and creep of concrete.

The small amount of Whittemore gage data does not permit meaningful quantitative analysis. Nevertheless, a few qualitative observations can be made:

1. At most sections, the time-dependent deformation is dominated by direct shortening, as the curvature stayed nearly constant over the three year period from Sept. 1987 to Oct. 1990. This signifies that the deformations were primarily caused by shrinkage and/or thermal effects. The bending effect is relatively small.

35

2. Where data are available, the curvature changes in the beams at opposite sides of a continuity diaphragm were very similar (Sections 134 vs. 240, 234 vs. 330).

3. From June to August 1988, almost all gage distances recorded an elongation, or positive strain. One possible explanation for the elongation, or expansion, could be the temperature increase experienced over this period.

6.3 Discussion

It is disappointing that difficulties were encountered in the mounting of the Whittemore gage target points, and that several targets moved with time to become unusable. In view of the very small size of the data pool, any general conclusion must be tempered with caution. In this section, several observations and comments are made, based on the results of this study.

1. The changes in the Whittemore gage readings represent the combined effect of shrinkage and temperature changes in the deck and the beam concretes, as well as the long-term effect of beam stresses due to dead load, prestress and differential shrinkage and creep. This study was not intended to be a determination of the effects of separate parameters, but to be a global estimation of the combined effect. As pointed out in the preceding section, in a majority of the sections being monitored, there appeared to be primarily a contracting phenomenon. There was very little time-dependent change of the

36

negative curvature in the neighborhood of the continuity diaphragms.

2. The relatively insignificant time-dependent changes in the curvature at the beam ends, illustrated by the lack of rotation of the strain profiles in Fig. 6.2, would imply that the end restraining moments are relatively small. However, it must be emphasized that this does not imply the lack of continuity. The magnitudes of the restraining moments at the ends of beams are dependent upon the differential deformation between the deck slab and the beam. For the Milton Bridge, the precast prestressed beams were fabricated in early 1987, the bridge deck was cast in June, and the first set of Whittemore gage measurements were made in September. The initial phase of rapid shrinkage of the deck concrete, which would generate sizeable end moments and curvatures, was not detected by the Whittemore gage measurements. The three-month time lag before the first set of measurements (R1) diminished the detectable differential shrinkage between the deck slab and the beams. The presence of significant longitudinal prestress in the beams further reduced the non-conformity of the deformations. Consequently, the small restraining moments implied by the Whittemore gage measurements are seen as consistent with expected long-term deformations of the concrete material.

3. The similarity of behavior of the beams on opposite sides of a continuity diaphragm may be viewed as an indication that the diaphragm has indeed made the beams continuous. (The

37

construction plans show that the ends of each beam are embedded in the diaphragms to a depth of 10 in.). Furthermore, the live load stress records, described in Chapters 4 and 5, also support the continuous behavior of the superstructure of this bridge.

4. Three of the four measurements (R1, R3 and R4) were made in later summer (September, August and October, respectively). These times were chosen to minimize the influence of ambient temperature on the deformations and curvatures. The second reading (R2) was made in June 1988, before the onset of the summer heat. Table 6.1 and Fig. 6.2 show that the gage measurements were almost uniformly higher (shorter) than the corresponding values two months later. The summer heat had caused the structure to expand in the meantime.

5. Diagonal cracks were discovered in the end regions of the precast beams in interior spans in the spring of 1988. These cracks typically extended from about 9 in. above the mid-height of the beam webs at the face of the continuity diaphragms to the top of the web about 4 ft. away, at a slope of approximately 1 to 2 from the horizontal. In October 1990, the widest part of these cracks, typically near the middle, was found to be from 0.009 in. to 0.016 in. in width. None of these cracks passed between any of the Whittemore gage points. No such crack was detected in the beams of span 1. The cause for these cracks was not immediately clear, but the direction of them suggests that the shearing stresses due to prestress, negative bending and shrinkage of the deck were at least partially responsible.

38

6. The completed superstructure is continuous over nine spans, with neoprene bearing pads at all supports. The bearings on top of piers 2 through 7 are of the "fixed" variety, which does not allow longitudinal movements. At the abutments as well as piers 1 and 8, "expansion" type bearings are used, allowing longitudinal movement compatible with the shearing deformation of the neoprene pads. The response of such a structure to temperature and shrinkage changes is quite complicated. The Whittemore gage measurements indicate that the curvature change after the first three months was very small (item 2 in Section 6.2). The small amount of data does not allow an evaluation of the several possible influencing factors, such as temperature change, thermal gradient, prestress change, differential shrinkage, and creep. An extended study would be needed to better understand the long-term behavior of bridge structures of this type.

7. SUMMARY AND CONCLUSIONS

From the results and discussions presented in Chapter 3 through Chapter 6, the following findings can be summarized.

(1) The maximum experimentally determined change in stresses in the prestressed concrete beams, due to placement of the concrete deck, was 1700 psi. This maximum stress occurred near the top of the beams, at midspan in span 3.

(2) The placement of concrete for the continuity diaphragms at the supports, and the placement of the concrete deck above these diaphragms and over the supports, had very little effect on the stresses in the prestressed concrete beams.

(3) In the days immediately following the placement of the deck concrete in the positive moment region, the dead load stresses in the prestressed beams decreased as the deck concrete hardened. This change ranged as high as 20% of the initial dead load stress.

(4) The continuity of the bridge beams was confirmed by the live load stress distribution in beam cross-sections at the ends of spans. The stress distribution was consistent with that of continuous beams.

(5) Live load stresses in the bridge beams were quite low. Nowhere was the experimentally determined value higher than 500 psi in the prestressed concrete beams, under either test truck loading or regular truck loading.

(6) The experimentally determined live load stress distribution in the prestressed concrete beams due to the test trucks were in general agreement with the corresponding distributions from computation by the available finite element programs. The magnitudes of measured stresses,

40

however, were always significantly lower, sometimes by as much as 50 to 60% of the computed values.

(7) Strain measurements indicated that practically no impact (dynamic) stress was produced by the live loads on this bridge.

(8) The test truck runs affirmed the validity of superposition of measured live load strains produced by trucks in parallel lanes. As a result, superposition of computed live load stresses from the computer programs appears to be acceptable. However, as indicated in item (6) above, it should be noted that all computer programs yielded stresses considerably higher than those derived from measured strains.

(9) The long-term changes in strains at the ends of the beams, recorded over a three-year period from the construction of the bridge, were as high as, or higher than, those caused by live loads. In one extreme case, the long-term strain changes were an order of magnitude higher than the live load values. In many other cases, they were of comparable magnitudes.

(10) Devices for the effective measurement of shrinkage (and creep) effects of concrete on the prestressed beams should be installed in the beams during fabrication. Surface attached devices, particularly those near formwork, were strongly affected by moisture during the placement of the deck concrete. Since shrinkage effects are most prominent during the first few days of deck placement, the incorporation of parts of the measuring system into the construction scheme is of paramount importance.

(11) Diagonal tension cracks in the upper portion of beam ends were detected in several interior spans (spans 2 and 3), but not in the end span (span 1). The largest opening, measured in 1990, was about 0.016 in.

41

The following general conclusions are derived from the foregoing results and findings.

(1) The introduction of continuity diaphragms and the continuous concrete deck effectively transforms the simply supported prestressed concrete beams into a multispan continuous bridge for live loads.

(2) The shrinkage and creep of the concrete, along with thermal changes, combine to induce relatively high strains and stresses in the continuous structural system. An extensive analytical study of the phenomenon to ascertain the effects of individual factors, is necessary and is recommended.

(3) In all cases, the live load stresses based on results from the computer programs are significantly higher than the corresponding stresses derived from measured strains. The differences are too large to be ignored. Possible contributors to the differences include the superstructure support conditions, the interaction of curb and parapet, the distribution of wheel loads to the finite element nodal points in the analysis, and the effective slab width for the composite beams, etc.

(4) The traffic conditions on this bridge appear to be considerably lighter than the "fully loaded" condition typically used for design purposes. This was borne out by the very low experimentally determined live load stresses. Whether the total stress condition (dead plus live plus impact) approaches the allowable limits was not examined in this study. In view of the very low live load stresses, an examination of the probable high margin of safety of this structure may be beneficial toward the improvement of design economy of similar bridges in the future.

References

1. American Association of State Highway and Transportation Officials
   (AASHTO)
   Standard Specifications for Highway Bridges, 14th Edition, 1989.

2. Modjeski and Masters, Inc., Consulting Engineers
   Milton Bridges: Moments and Stresses for Simulated HS25 Truck and
   Simulated 204K Vehicle at Specific Locations Using Computer Programs,
   1989.

3. Bae, Doobyong
   Effective Slab Width in Multi-Girder Composite Bridges, Dissertation,
   Dept. of Civil Engineering, Lehigh University, 1991.

TABLE 3.1 DEAD LOAD STRESSES (PSI) - SECTION 212

GAGE	STAGE	1	2	3	4	5
212T	ANALYSIS	-978	-978	-978	-982	-985
	MEASURED	-1245	-1369	-1288	-1186	-1165
212B	ANALYSIS	921	922	920	928	934
	MEASURED	981	1061	1036	1085	1073

TABLE 3.2 DEAD LOAD STRESSES (PSI) - SECTION 222

GAGE	STAGE	1	2	3	4	5
222T	ANALYSIS	-1011	-1012	-1011	-1015	-1019
	MEASURED	-1515	-1471	-1380	-1301	-1304
222B	ANALYSIS	953	953	951	959	965
	MEASURED	818	979	954	991	979

TABLE 3.3   DEAD LOAD STRESSES (PSI) - SECTION 232

GAGE	STAGE	1	2	3	4	5
232T	ANALYSIS	-1011	-1012	-1011	-1015	-1019
	MEASURED	-1486	-1662	-1542	-1470	-1495
232B	ANALYSIS	953	953	951	959	965
	MEASURED	807	987	894	1032	1013

TABLE 3.4   DEAD LOAD STRESSES (PSI) - SECTION 242

GAGE	STAGE	1	2	3	4	5
242T	ANALYSIS	-949	-949	-948	-952	-955
	MEASURED	-1369	-1407	-1351	-1295	-1331
242B	ANALYSIS	893	894	892	900	905
	MEASURED	833	952	921	914	914

TABLE 4.1   TEST TRUCK RUNS

SUPERPOSITION TEST RUNS (9-16-1987)

RUN	LANE (TRUCK NO.)	TIME
1	5 (1)	14:28
2	3 (1)	14:48
3	1 (1)	14:55
4	1 (1) AND 3 (2)	15:00
5	3 (1) AND 5 (2)	15:07

REGULAR TEST RUNS (GROUP D: 9-17-1987)

RUN	LANE (TRUCK NO.)	TIME
1	5 (1)	9:39
2	4 (1)	9:43
3	3 (1)	9:48
4	2 (1)	9:52
5	1 (1)	9:55
6	4 (1 AND 2)	9:58
7	3 (1 AND 2)	10:05
8	2 (1 AND 2)	10:11

TABLE 4.2 GROUPINGS OF GAGES FOR STRAIN MEASUREMENTS

GAGE IDENTIFICATIONS							
GROUP CHANNEL	A	B	D	E	F	G	H
1	212TN	312TN	212TN	312TN	230TN	214TN	214NL
2	212B	312B	212B	312B	230B	214B	214NT
3	212TS	312TS	212TS	312TS	230TS	214TS	234NT
4	222TN	322TN	222TN	322TN	240TN	224TN	244NT
5	222B	322B	222B	322B	240B	224B	244SL
6	222TS	322TS	222TS	322TS	240TS	224TS	222NT
7	232TN	332TN	232TN	332TN	133TN	234TN	244ST
8	232B	332B	232B	332B	133B	234B	2P4N
9	232TS	332TS	232TS	332TS	133TS	234TS	2P4S
10	242TN	342TN	242TN	342TN	143TN	244TN	232NT
11	242B	342B	242B	342B	143B	244B	332ST
12	242TS	342TS	242TS	342TS	143TS	244TS	342NT
13	231TN	331TN	231TN	331TN	132TN	233TN	X
14	231B	331B	231B	331B	132B	233B	242NT
15	231TS	331TS	231TS	331TS	132TS	233TS	242SL
16	241TN	341TN	241TN	341TN	142TN	243TN	242ST
17	241B	341B	241B	341B	142B	243B	2P2N
18	241TS	341TS	241TS	341TS	142TS	243TS	2P2S
19	233B	232B	233B	232B	232B	232B	232B
20	132B	242B	132B	242B	242B	242B	242B
21	332B	132B	332B	132B	332B	332B	332B

TABLE 4.3 STRESSES AT MIDSPAN OF SPAN 2 (REF POSITION 5)
TEST TRUCK RUN 6 (SIMULATED 204 KIP TRUCK)

GAGE	STRESS (PSI)	GAGE	STRESS (PSI)	GAGE	STRESS (PSI)
132T	22	212T	-20	234T	44
132B	-40	212B	35	234B	-104
142T	17	222T	-38	244T	37
142B	-69	222B	105	244B	-137
133T	22	232T	-42	331T	22
133B	-62	232B	145	331B	-77
143T	31	242T	-51	341T	21
143B	-113	242B	268	341B	-96
230T	35	233T	-18	312T	6
230B	-109	233B	88	312B	-17
240T	36	243T	-16	322T	11
240B	-136	243B	62	322B	-34
231T	-46	214T	-5	332T	11
231B	166	214B	-11	332B	-44
241T	-38	224T	19	342T	20
241B	141	224B	-43	342B	-65

TABLE 4.4   MAXIMUM MEASURED STRESSES - TEST TRUCK AT REFERENCE POSITION

POSITION	GAGE	RUN	MAXIMUM STRESS (PSI)
1	142B	6	322
2	142B	6	310
3 (PIER 1)	240B	6	-190
	142B	6	310
4	242B	6	268
5	242B	6	268
6	242B	6	263
7 (PIER 2)	244B	6	-168
	342B	6	287
8	342B	6	272
9	342B	6	310

TABLE 4.5 MAXIMUM TEST-TRUCK STRESSES (PSI) - SECTION 132

GAGE LOCATION	LANE - NO. OF TRUCKS	ANALYTICAL RESULTS				MEASURED
		STRESS	CURVBRG	DESCUS	BSDI	
132T (TOP)	L5-1	-109	-112	-110	-109	-57
	L4-2	-126	-134	-127	-147	-54
132B (BOTTOM)	L5-1	233	240	236	233	148
	L4-2	269	288	271	315	171

L5-1

L4-2
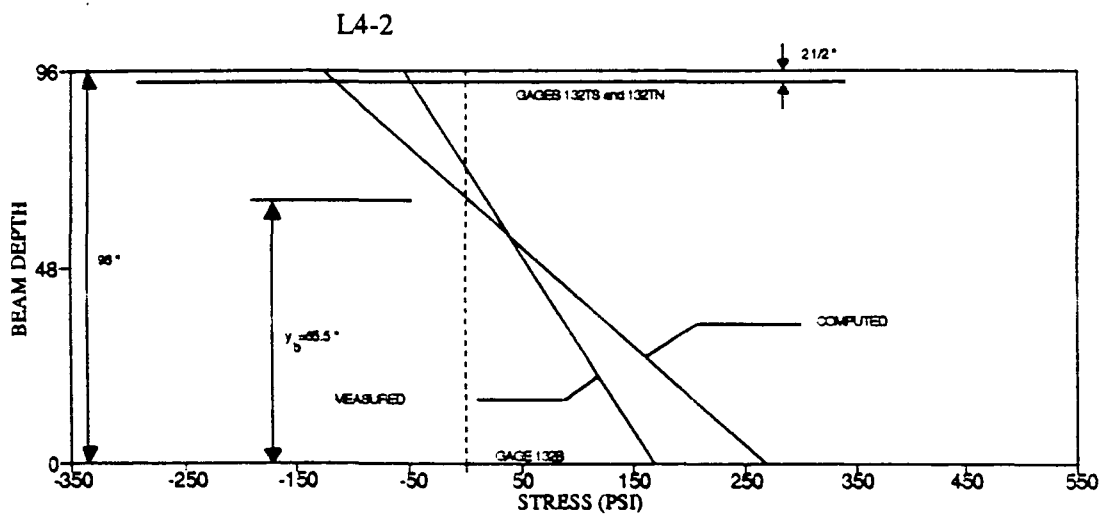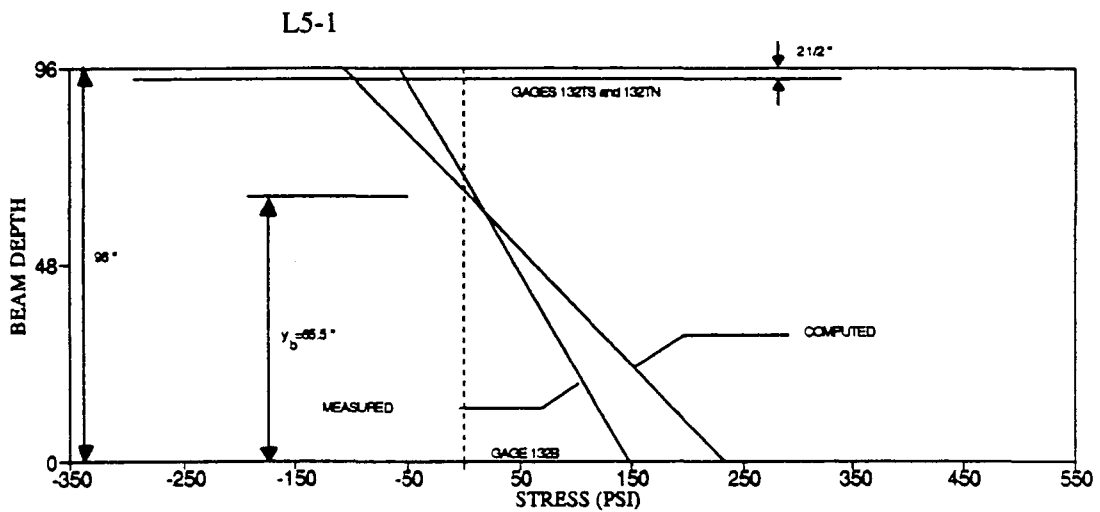
TABLE 4.6 MAXIMUM TEST-TRUCK STRESSES (PSI) - SECTION 142

GAGE LOCATION	LANE - NO. OF TRUCKS	ANALYTICAL RESULTS				MEASURED
		STRESS	CURVBRG	DESCUS	BSDI	
142T (TOP)	L5-1	-180	-187	-190	-184	-66
	L4-2	-230	-239	-238	-233	-86
142B (BOTTOM)	L5-1	385	400	406	394	264
	L4-2	493	511	511	500	322

L5-1

L4-2
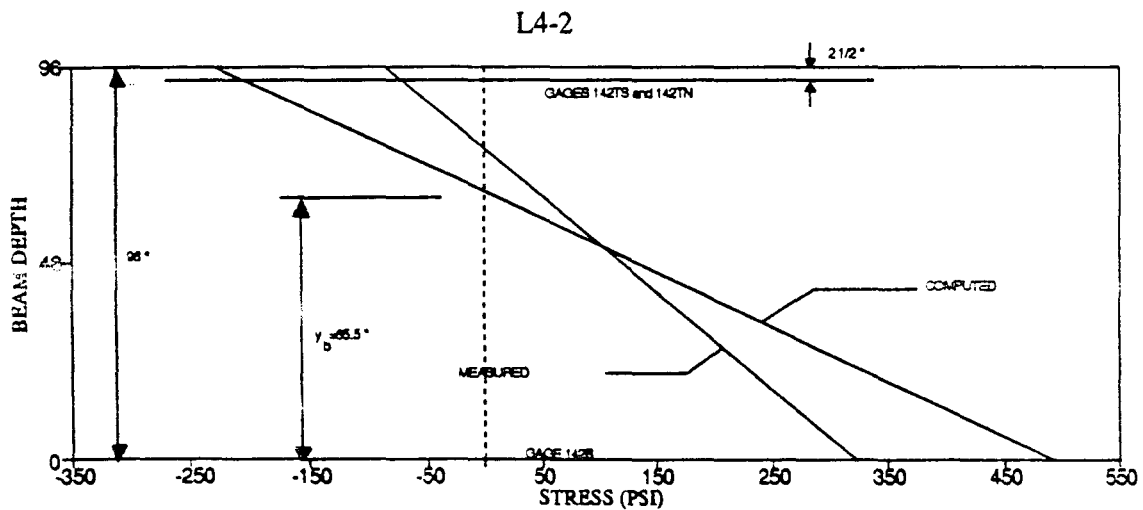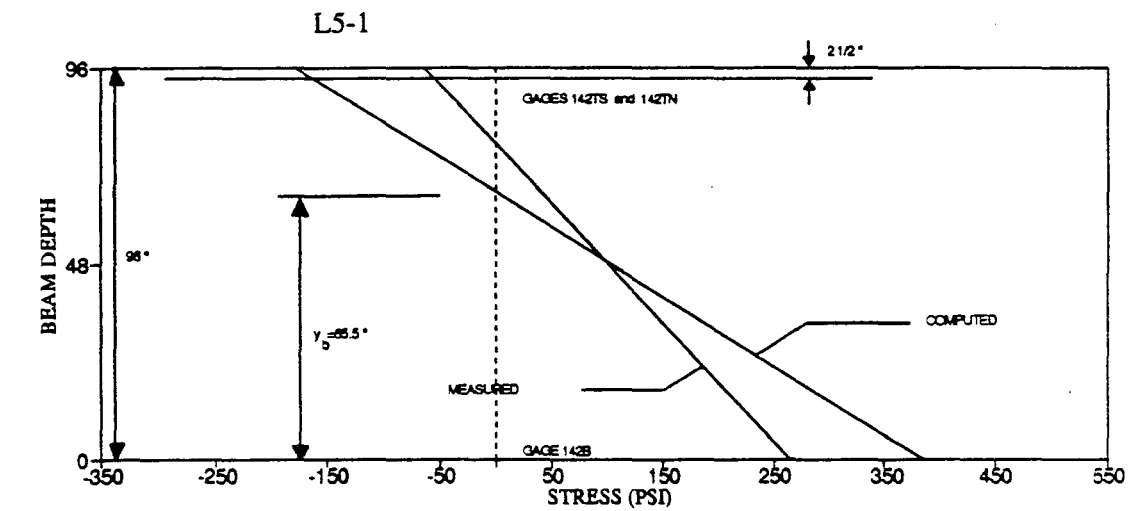
TABLE 4.7 MAXIMUM TEST-TRUCK STRESSES (PSI) - SECTION 212

GAGE LOCATION	LANE - NO. OF TRUCKS	ANALYTICAL RESULTS				MEASURED
		STRESS	CURVBRG	DESCUS	BSDI	
212T (TOP)	L2-1	-86	-87	-82	-86	-48
	L5-1	26	32	30	23	10
	L2-2	-149	-150	-146	-147	-76
	L4-2	-18	-12	-7	-22	-27
212B (BOTTOM)	L2-1	184	185	176	184	119
	L5-1	-56	-69	-64	-50	-32
	L2-2	319	322	312	315	189
	L4-2	38	25	16	47	35

L2-1

L2-2
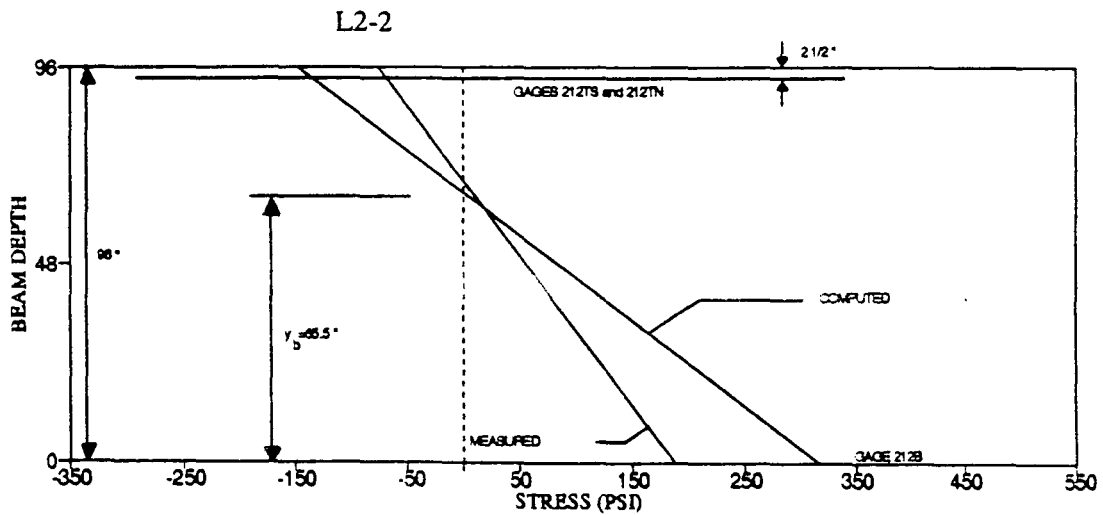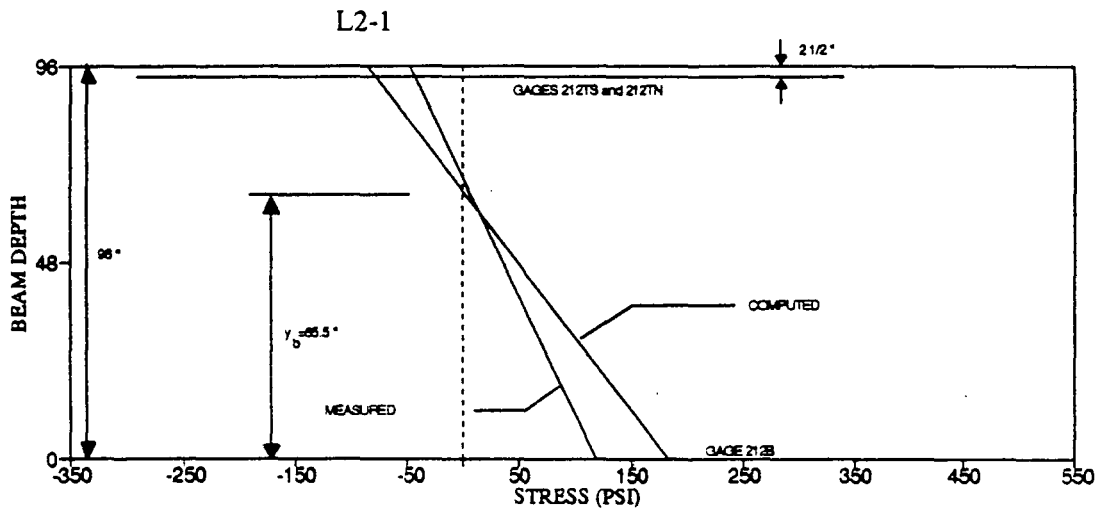
TABLE 4.8 MAXIMUM TEST-TRUCK STRESSES (PSI) - SECTION 222

GAGE LOCATION	LANE - NO. OF TRUCKS	ANALYTICAL RESULTS				MEASURED
		STRESS	CURVBRG	DESCUS	BSDI	
222T (TOP)	L2-1	-72	-73	-77	-79	-40
	L5-1	-35	-34	-30	-36	-28
	L2-2	-86	-91	-89	-110	-56
	L4-2	-88	-84	-92	-87	-51
222B (BOTTOM)	L2-1	154	156	165	170	123
	L5-1	76	72	64	78	45
	L2-2	185	194	192	236	142
	L4-2	189	180	197	186	105

L2-1

L2-2
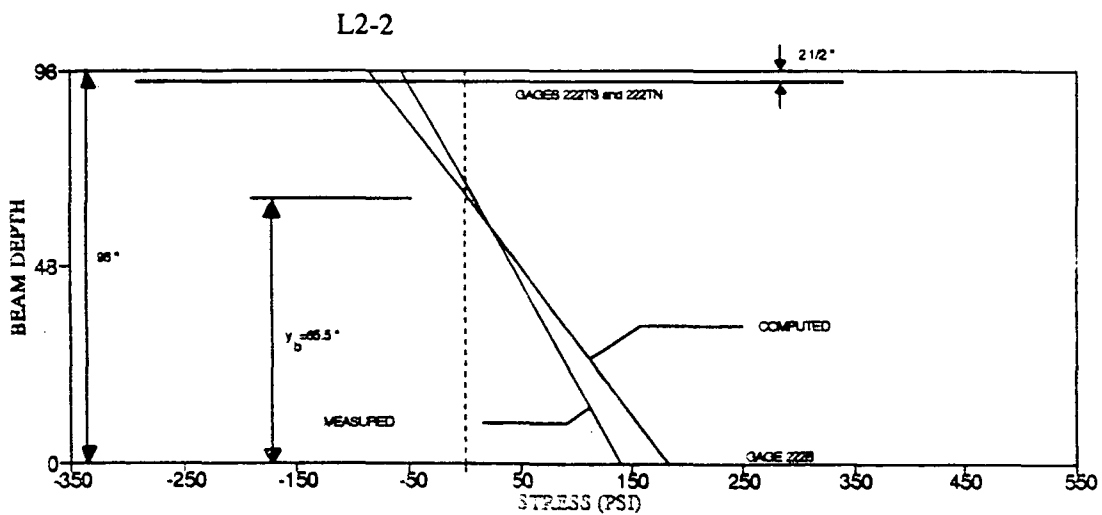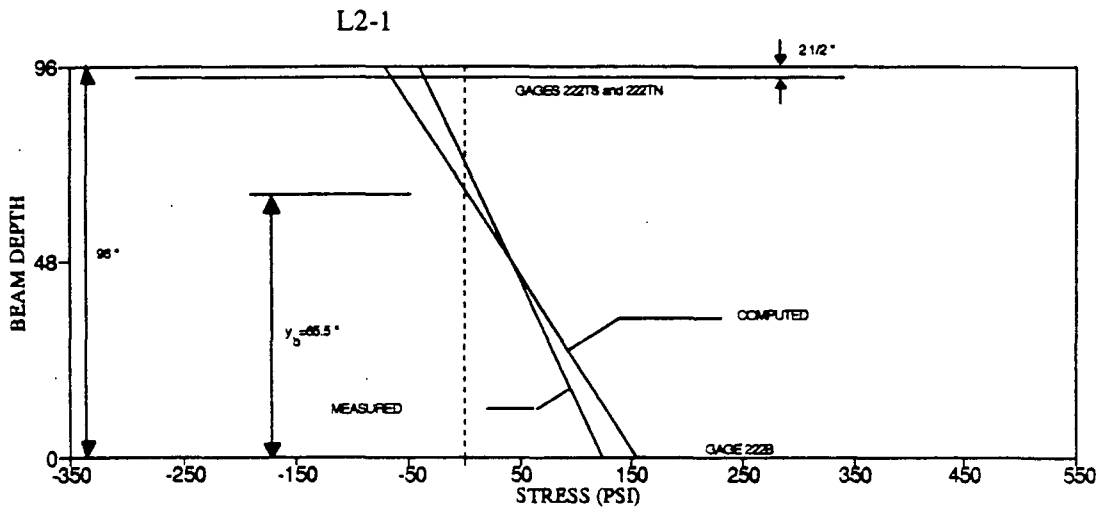
TABLE 4.9   MAXIMUM TEST-TRUCK STRESSES (PSI) - SECTION 232

| GAGE LOCATION | LANE - NO. OF TRUCKS | ANALYTICAL RESULTS | | | | MEASURED |
		STRESS	CURVBRG	DESCUS	BSDI	
232T (TOP)	L2-1	-64	-63	-67	-64	-36
	L5-1	-97	-100	-97	-96	-63
	L2-2	-95	-94	-105	-101	-53
	L4-2	-106	-113	-109	-128	-57
232B (BOTTOM)	L2-1	136	134	145	138	91
	L5-1	207	214	209	207	129
	L2-2	204	201	224	216	123
	L4-2	227	241	234	275	145

L5-1

L4-2
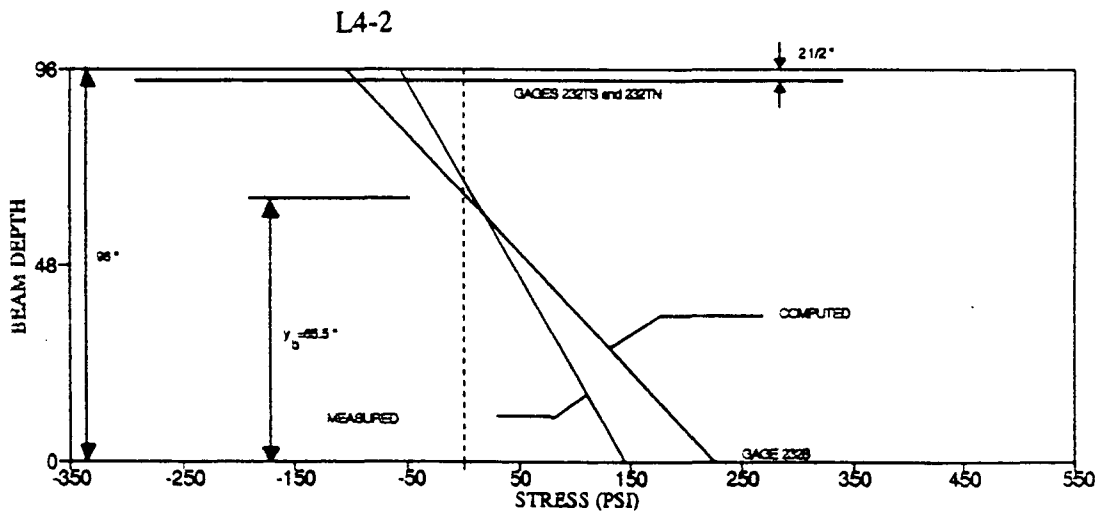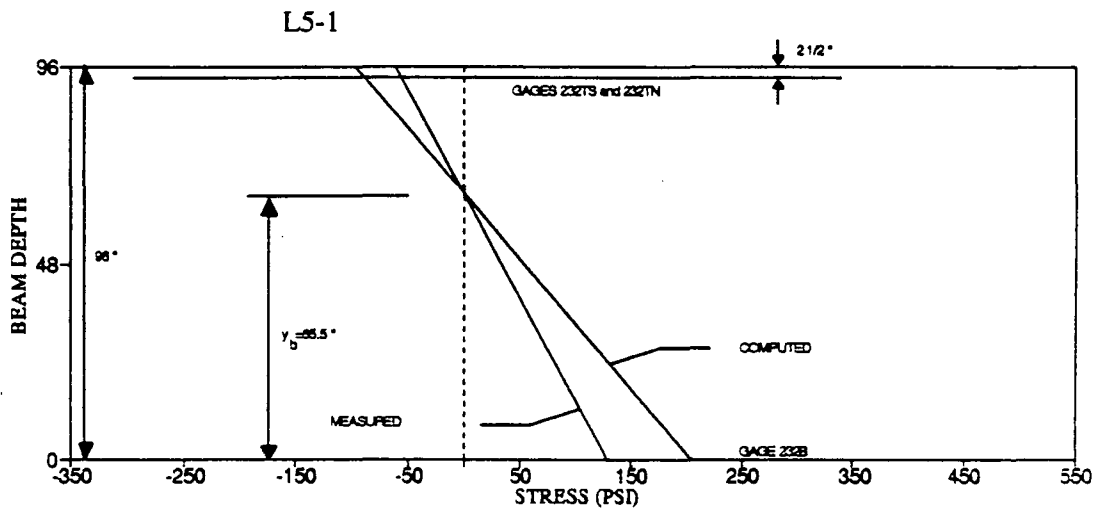
TABLE 4.10   MAXIMUM TEST-TRUCK STRESSES (PSI) - SECTION 242

GAGE LOCATION	LOADING CONDITION	ANALYTICAL RESULTS				MEASURED
		STRESS	CURVBRG	DESCUS	BSDI	
242T (TOP)	L2-1	-45	-46	-41	-46	-28
	L5-1	-161	-167	-170	-165	-73
	L2-2	-80	-82	-74	-81	-43
	L4-2	-199	-206	-205	-203	-77
242B (BOTTOM)	L2-1	97	99	88	99	59
	L5-1	344	358	365	354	263
	L2-2	172	176	158	174	107
	L4-2	425	441	440	435	268

L5-1

L4-2
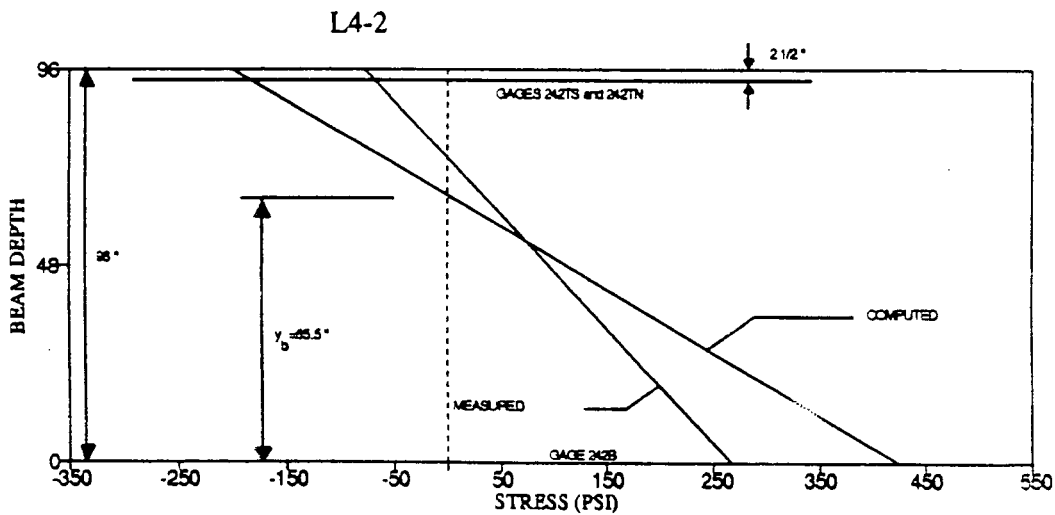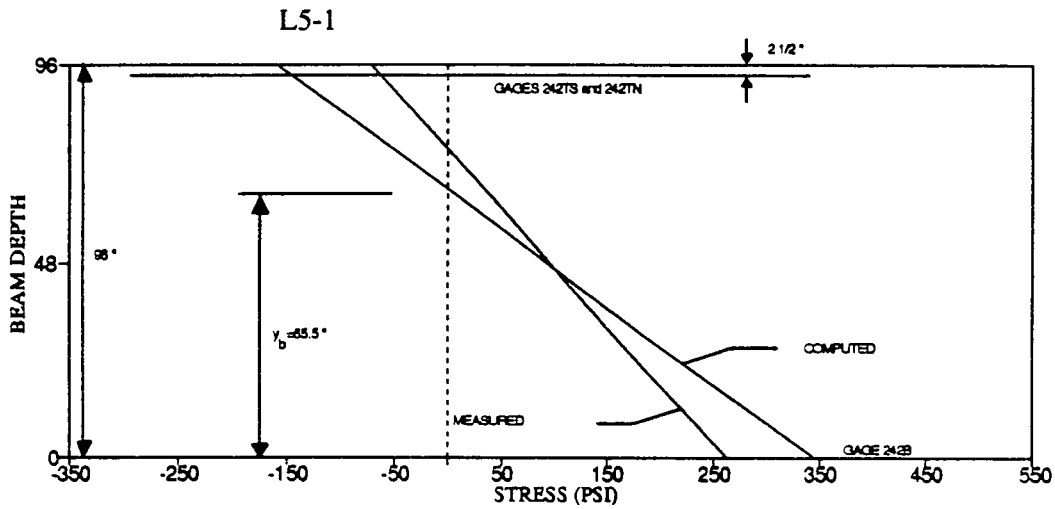
TABLE 4.11   MAXIMUM TEST-TRUCK STRESSES (PSI) - SECTION 230
COMPOSITE SECTION - REBAR + GIRDER

GAGE LOCATION	LANE - NO. OF TRUCKS	ANALYTICAL RESULTS				MEASURED
		STRESS	CURVBRG	DESCUS	BSDI	
230T (TOP)	L5-1	128	129	126	131	29
	L4-2	212	208	216	262	51
230B (BOTTOM)	L5-1	-146	-146	-144	-149	-52
	L4-2	-241	-237	-246	-299	-150

L5-1

L4-2
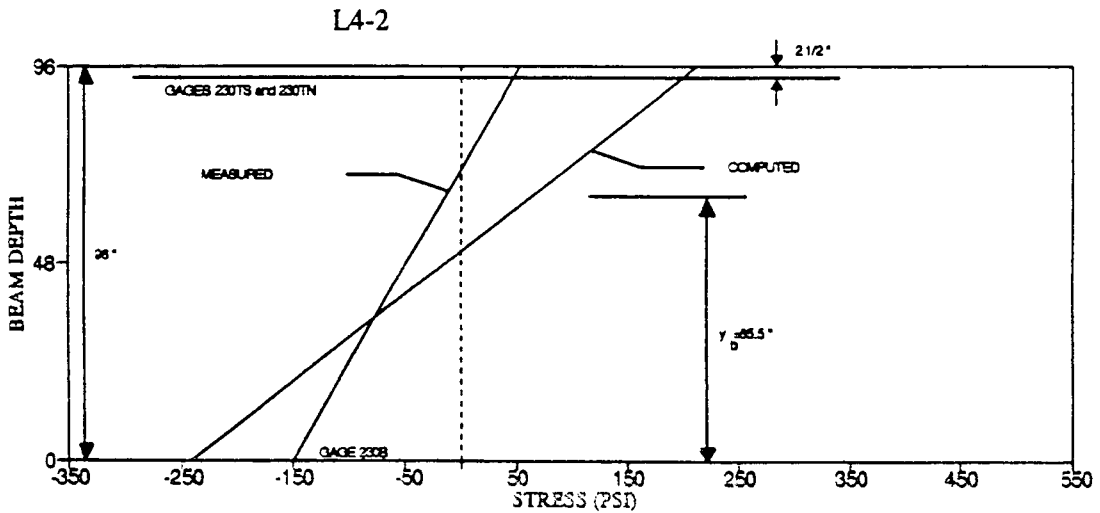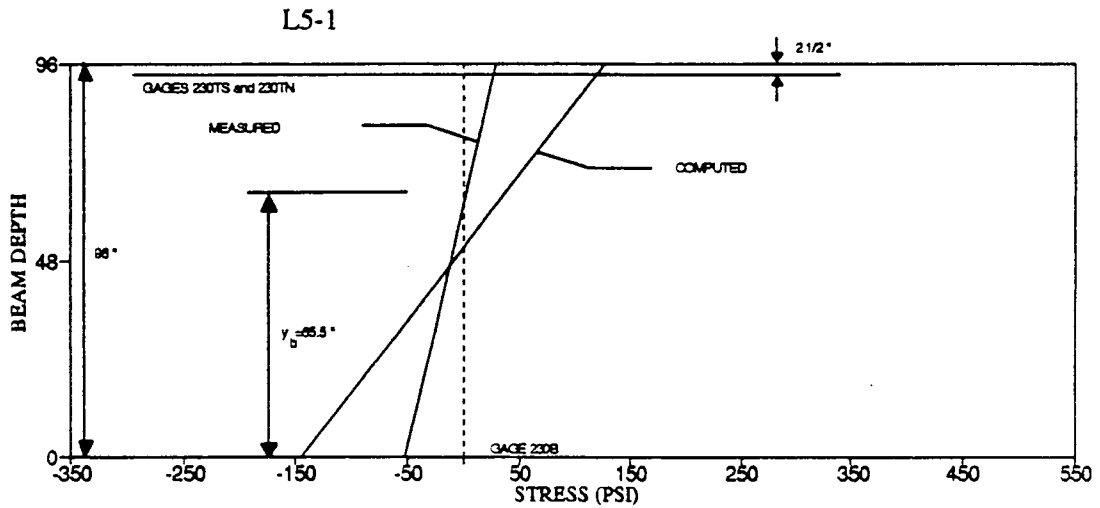
TABLE 4.12 MAXIMUM TEST-TRUCK STRESSES (PSI) - SECTION 240
COMPOSITE SECTION - REBAR + GIRDER

GAGE LOCATION	LANE - NO. OF TRUCKS	ANALYTICAL RESULTS				MEASURED
		STRESS	CURVBRG	DESCUS	BSDI	
240T (TOP)	L5-1	225	227	236	231	50
	L4-2	290	294	294	302	66
240B (BOTTOM)	L5-1	-257	-258	-269	-263	-142
	L4-2	-330	-335	-335	-344	-190

L5-1

L4-2
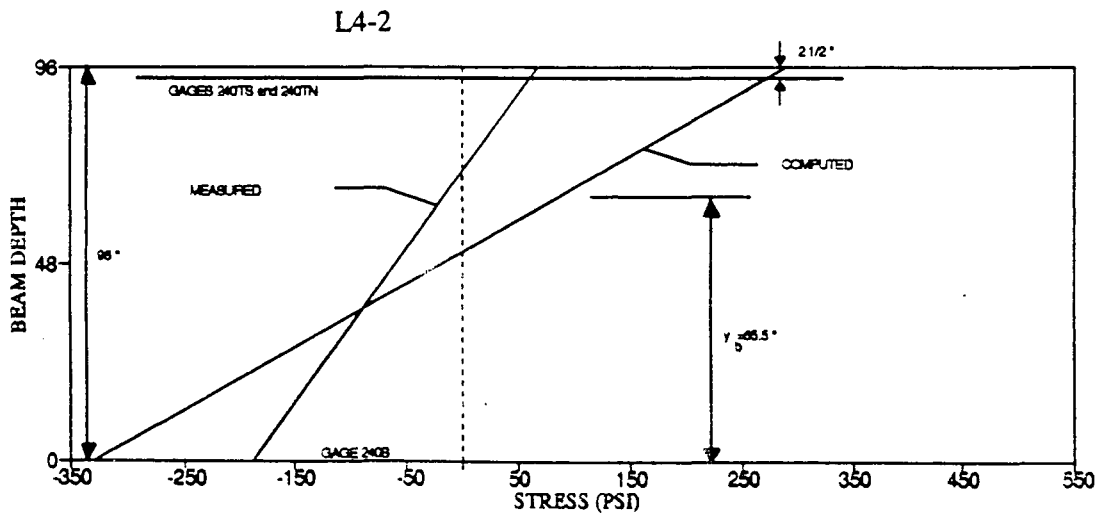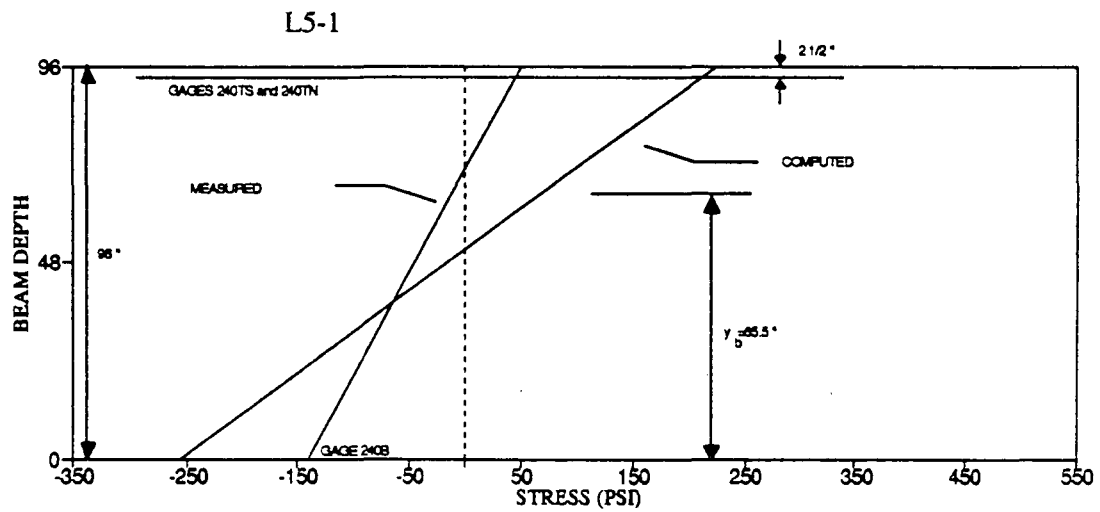
TABLE 4.13 MAXIMUM TEST-TRUCK STRESSES (PSI) - SECTION 230
COMPOSITE SECTION - SLAB + GIRDER

| GAGE LOCATION | LANE - NO. OF TRUCKS | ANALYTICAL RESULTS | | | | MEASURED |
		STRESS	CURVBRG	DESCUS	BSDI	
230T (TOP)	L5-1	56	56	55	57	29
	L4-2	92	91	94	114	51
230B (BOTTOM)	L5-1	-119	-120	-118	-122	-52
	L4-2	-198	-195	-201	-245	-150

L5-1

L4-2
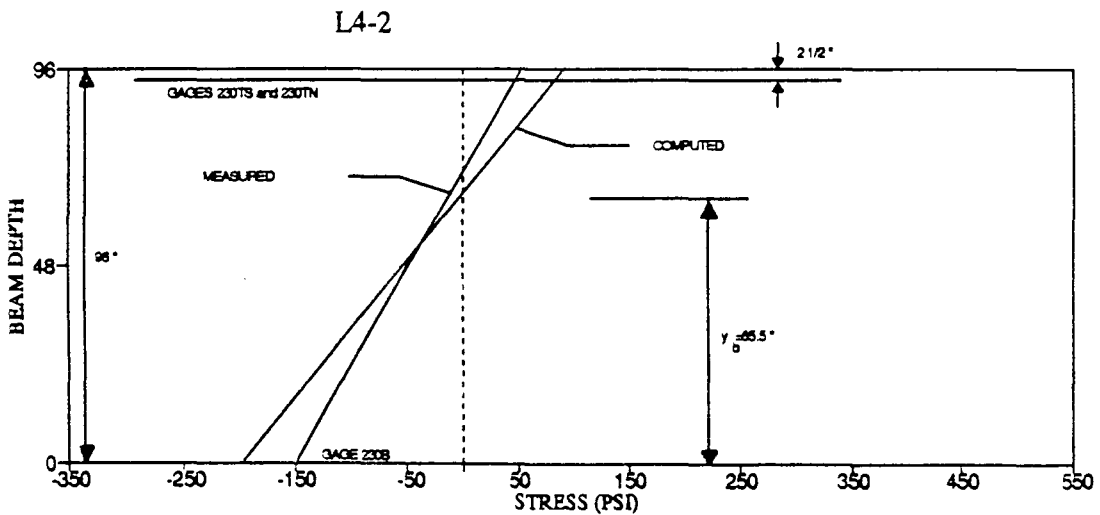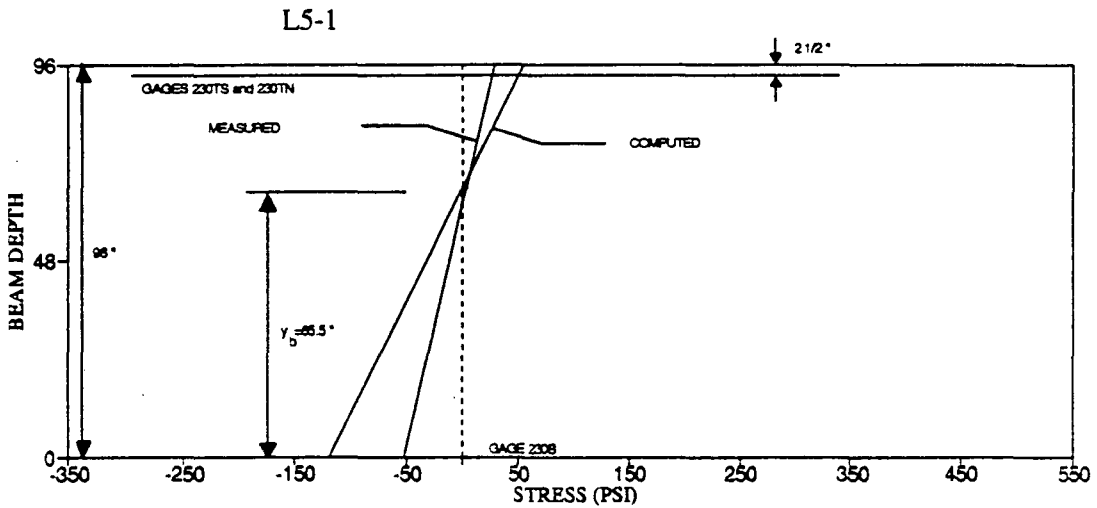
TABLE 4.14 MAXIMUM TEST-TRUCK STRESSES (PSI) - SECTION 240
COMPOSITE SECTION - SLAB + GIRDER

GAGE LOCATION	LANE - NO. OF TRUCKS	ANALYTICAL RESULTS				MEASURED
		STRESS	CURVBRG	DESCUS	BSDI	
240T (TOP)	L5-1	98	99	103	100	50
	L4-2	126	128	128	132	66
240B (BOTTOM)	L5-1	-210	-212	-220	-215	-142
	L4-2	-271	-274	-274	-282	-190

L5-1

L4-2
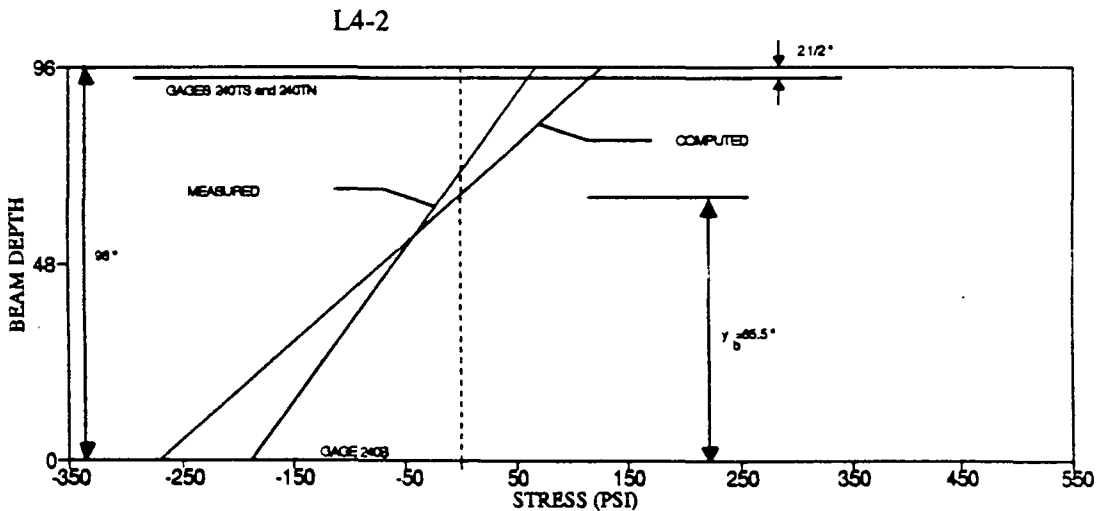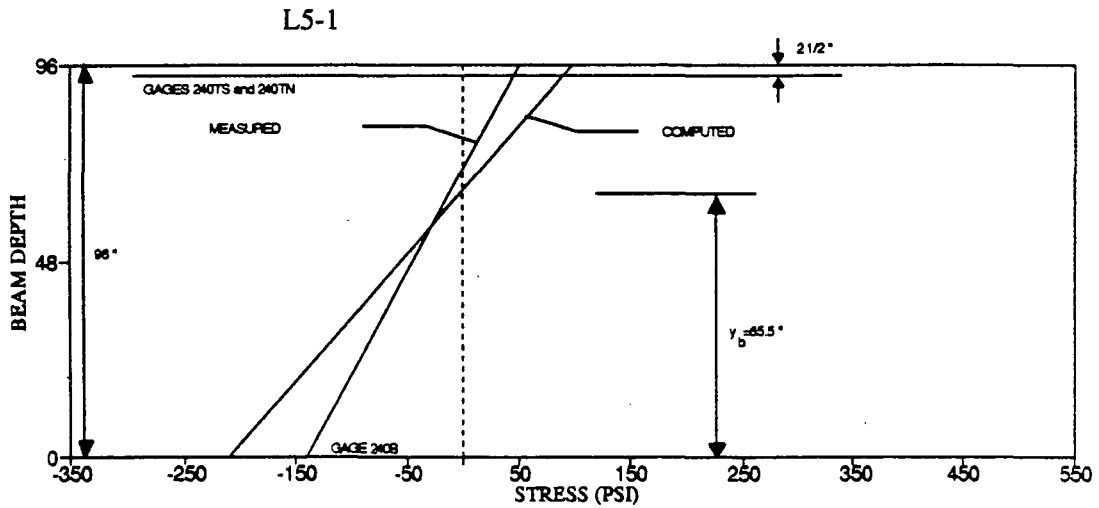
TABLE 4.15 MAXIMUM MEASURED STRAINS (MICRO-IN./IN.)
SUPERPOSITION TEST RUNS

GAGE	RUN 1	RUN 2	RUN 3	RUN 4	RUN 2 + RUN 3	RUN 5	RUN 1 + RUN 2
232TN	-8	-7	-6	-12	-13	-14	-15
232B	25	22	12	34	34	46	47
232TS	-9	-6	-4	-9	-10	-14	-15
242TN	-9	-6	-1	-8	-7	-14	-15
242B	50	22	3	25	25	75	72
242TS	-9	-6	-1	-6	-7	-14	-15

(REFER TO TABLE 4.1)

TABLE 4.16 COMPARISON OF MAXIMUM STRESSES AT SELECTED
LOCATIONS (PSI) - COMPUTED VS. MEASURED

| GAGE | LANE - NO. OF TRUCKS | COMPUTED | | MEASURED |
		CURVBRG	BSDI	
232T	L2-1 L4-2 SUM	-63 -113 -------------- -176	-65 -128 -------------- -193	-36 -57 -------------- -93
232B	L2-1 L4-2 SUM	134 241 -------------- 375	138 275 -------------- 413	91 145 -------------- 236
242T	L2-1 L4-2 SUM	-46 -206 -------------- -252	-46 -203 -------------- -249	-28 -77 -------------- -105
242B	L2-1 L4-2 SUM	99 442 -------------- 541	99 435 -------------- 534	59 268 -------------- 327
242T	L5-1 L2-2 SUM	-167 -82 -------------- -249	-165 -81 -------------- -246	-73 -43 -------------- -116
242B	L5-1 L2-2 SUM	358 176 -------------- 534	354 174 -------------- 528	263 107 -------------- 370

TABLE 5.1   GROUPINGS OF GAGES FOR NORMAL TRAFFIC SAMPLING

GROUP R.A.		GROUP R.B.		GROUP R.C.	
CHANNEL	GAGE	CHANNEL	GAGE	CHANNEL	GAGE
1	222TN	1	322TN	1	242TN
2	222B	2	322B	2	242B
3	222TS	3	322TS	3	232TN
4	232TN	4	332TN	4	232B
5	232B	5	332B	5	222B
6	232TS	6	332TS	6	212B
7	242TN	7	242B	7	342B
8	242B	8	342B	8	342TS
9	242TS	9	342TS	9	332B
10	224TN	10	132TN	10	332TS
11	224B	11	142B	11	233TN
12	224TS	12	132TS	12	233B
13	234TN	13	230TN	13	244B
14	234B	14	230B	14	244TS
15	234TS	15	230TS	15	234B
16	244TN	16	133TN	16	234TN
17	244B	17	133B	17	224B
18	244TS	18	231TS	18	331B
19	233TN	19	231B	19	230B
20	233B	20	331TN	20	142B
21	332B	21	331B	21	133B

(REFER TO TABLE 4.2)

TABLE 5.2 BRIDGE TRAFFIC SAMPLING

DATE	TIME	CARS (1)	TRUCKS (1,2)
6/21/88	15:20 - 17:40	NA	42
6/22/88	8:39 - 9:45	546	27
	9:45 - 10:40	523	38
8/17/88	14:30 - 15:30	900	34
	15:30 - 16:30	1013	25
8/18/88	7:30 - 8:35	610	30
	8:35 - 9:30	433	25
	9:30 - 10:30	458	31

(1) TOTAL TRAFFIC COUNT IS IN TWO DIRECTIONS

(2) TOTALS ALSO INCLUDE BUSES, H AND HS TRUCKS

TABLE 5.3 COMPARISON OF MAXIMUM STRESSES INDUCED
BY TEST TRUCKS AND REGULAR TRUCKS

GAGE	TEST-TRUCK (1) (PSI)	REGULAR TRUCK (PSI)
232TN	-34	-44
232B	129	147
232TS	-35	-45
242TN	-40	-60
242B	204	230
242TS	-35	-54

(1) MAXIMUM STRESS USUALLY OCCURRED WITH TWO
TEST-TRUCKS RUN IN TANDEM

TABLE 5.4   STRESSES DUE TO TEST-TRUCKS

TEST-TRUCK POSITION (1)	GAGE	TEST-TRUCK IN LANE (1)			SUM (PSI)
		5 (PSI)	3 (PSI)	1 (PSI)	
1	132B	148	114	---	262
	142B	264	138	---	402
5	212B	-32	59	173	200
	222B	45	95	134	274
	232B	127	118	64	309
	242B	263	118	5	386
9	312B	-34	67	180	213
	322B	53	112	142	307
	332B	142	128	70	340
	342B	286	136	21	443

(1) TEST-TRUCK USED SIMULATED HS25 TRUCK

TABLE 6.1 RESULTS OF WHITTEMORE GAGE MEASUREMENTS (MICRO IN./IN.)

GAGE	RUN 1 09/16/87	RUN 2 06/22/88	RUN 3 08/19/88	RUN 4 10/08/90	RUN 2 - RUN 1	RUN 3 - RUN 1	RUN 4 - RUN 1
134T	X	-291	-279	-327	-	-	-
134M	17	4	14	-29	-13	-3	-46
134B	-479	-495	-487	-673	-16	-8	-194
144T	X	X	X	X	-	-	-
144M	274	188	241	189	-86	-33	-85
144B	77	-87	19	-136	-164	-58	-213
230T	X	X	X	X	-	-	-
230M	-151	-170	-157	-198	-19	-6	-47
230B	-233	-255	-247	-286	-22	-14	-53
240T	-287	-337	-324	-361	-50	-37	-74
240M	172	165	171	129	-7	-1	-43
240B	X	X	X	X	-	-	-
234T	327	314	299	243	-13	-28	-84
234M	75	55	49	-31	-20	-26	-106
234B	192	183	170	143	-9	-22	-49
244T	-170	X	X	X	-	-	-
244M	-430	X	X	X	-	-	-
244B	-15	X	X	X	-	-	-
330T	-456	-466	-456	-489	-10	0	-33
330M	-255	-271	-264	-298	-16	-9	-43
330B	-442	-453	-448	X	-11	-6	-
340T	434	420	434	X	-14	0	-
340M	-480	-498	-486	-572	-18	-6	-92
340B	42	26	32	-5	-16	-10	-47
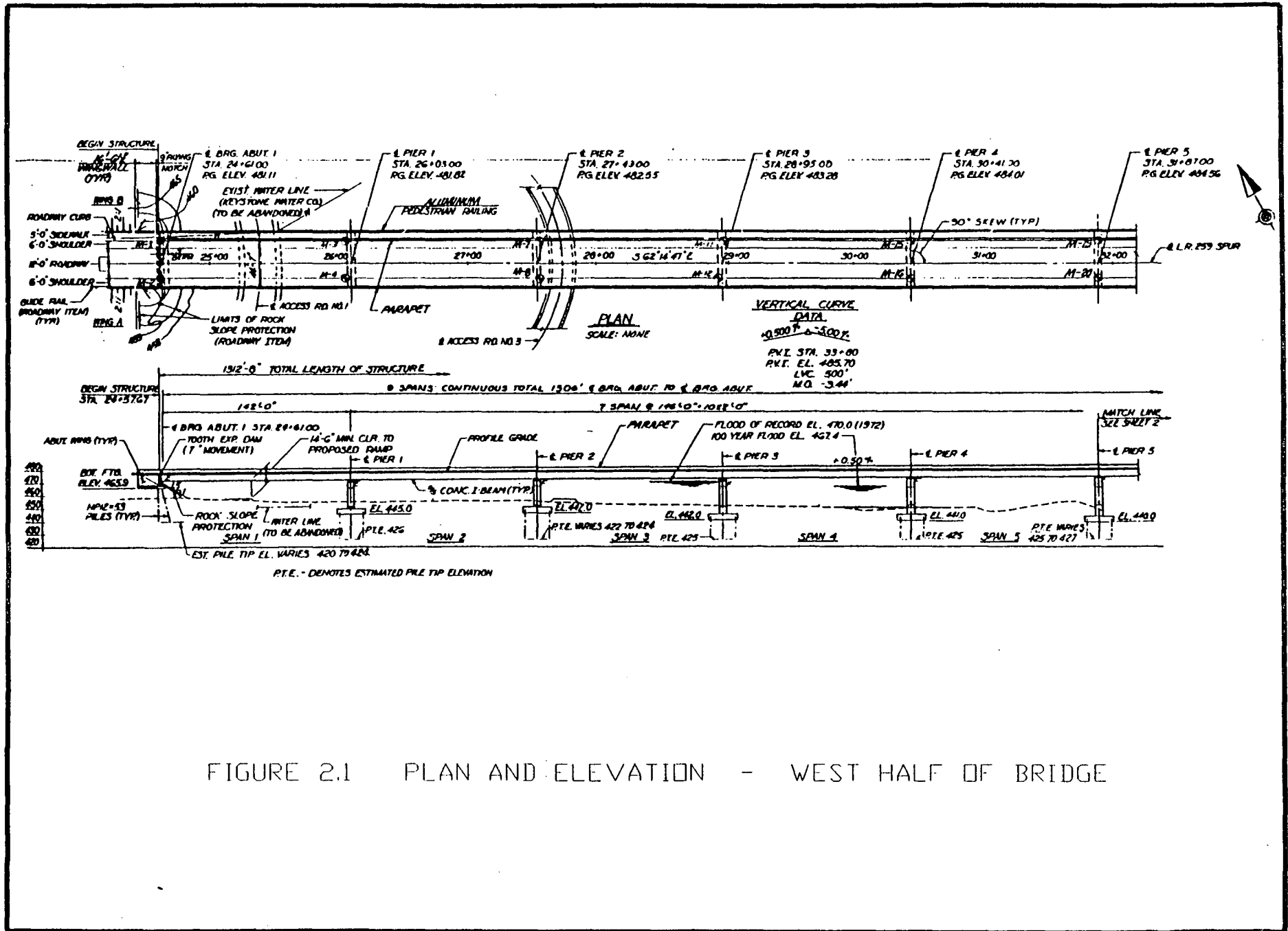
FIGURE 2.1 PLAN AND ELEVATION - WEST HALF OF BRIDGE
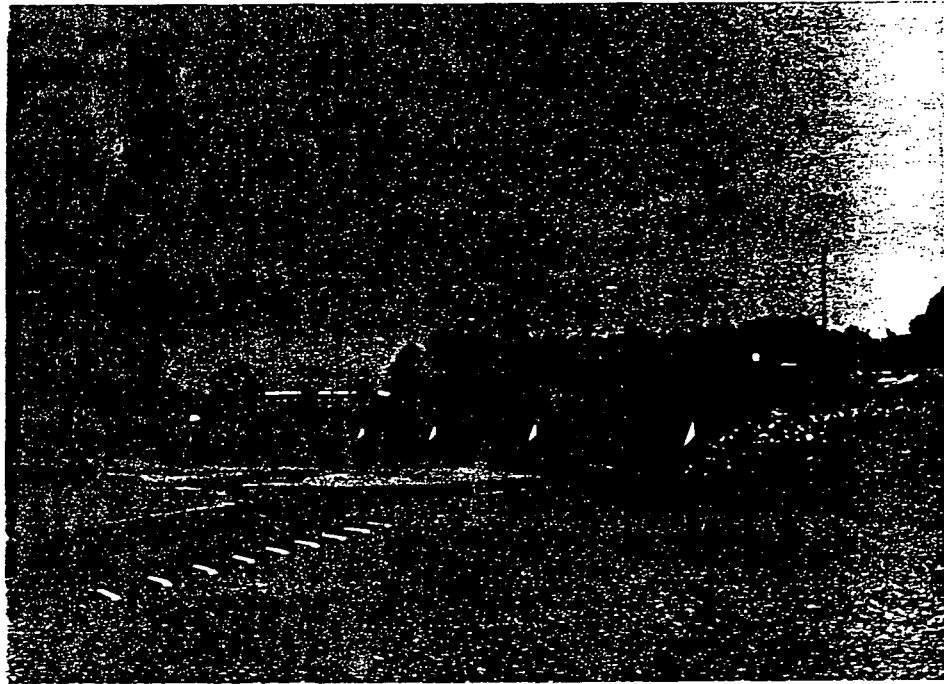
FIGURE 22 COMPLETED BRIDGE (WEST-TO-EAST)
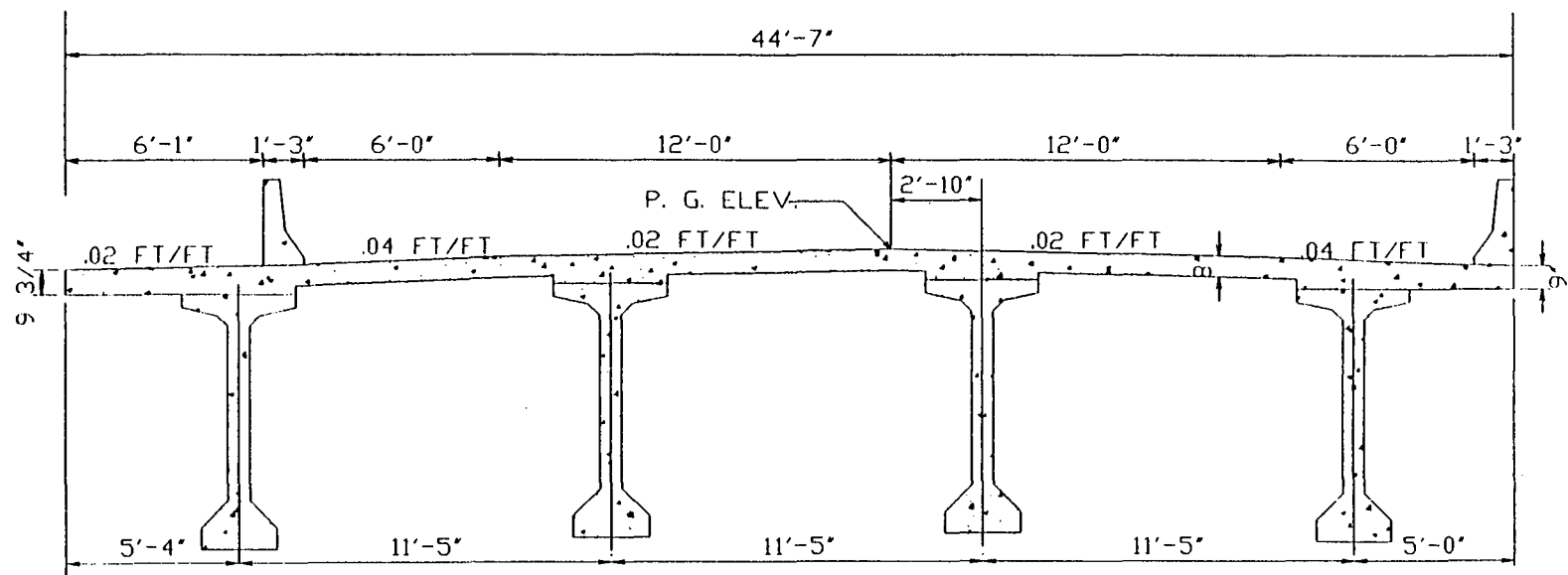
FIGURE 2.3   TYPICAL CROSS SECTION OF BRIDGE
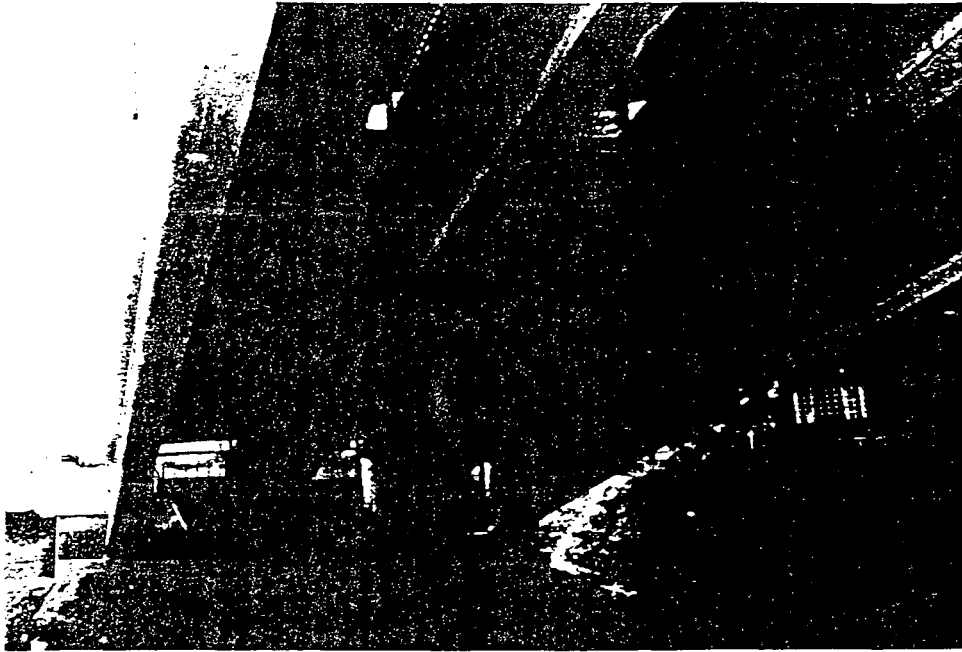
FIGURE 24   UNDERSIDE OF BRIDGE SHOWING FORMS

FIGURE 25   FORM WORK BENEATH THE SOUTH FASCIA BEAM

FIGURE 26   CONTINUITY DIAPHRAGM AT PIER
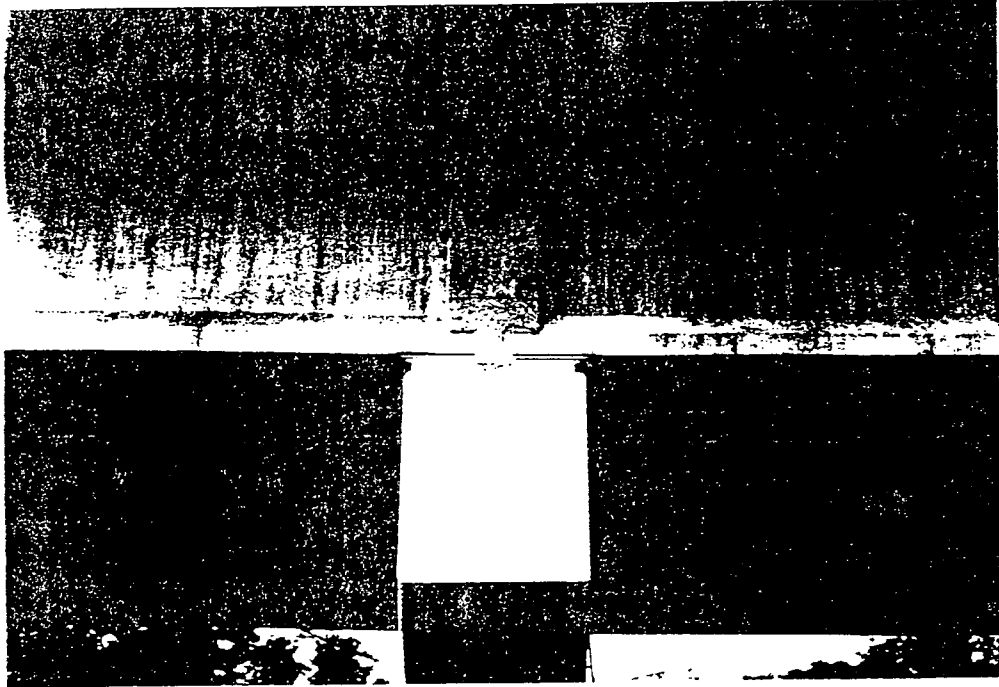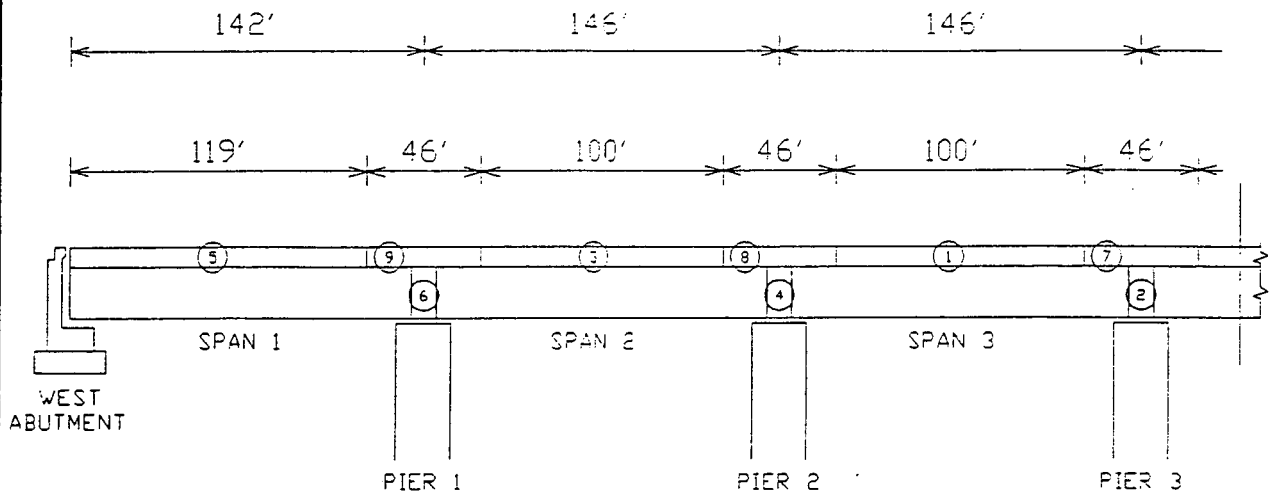
FIGURE 2.7   CASTING SEQUENCE FOR SPANS 1, 2, AND 3

FIGURE 28. ATTACHMENT OF SPRAY BARS
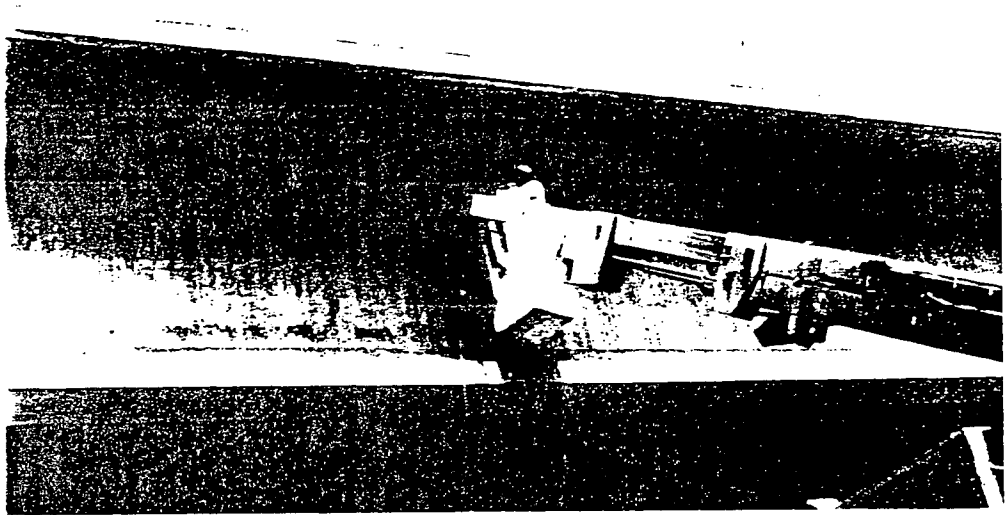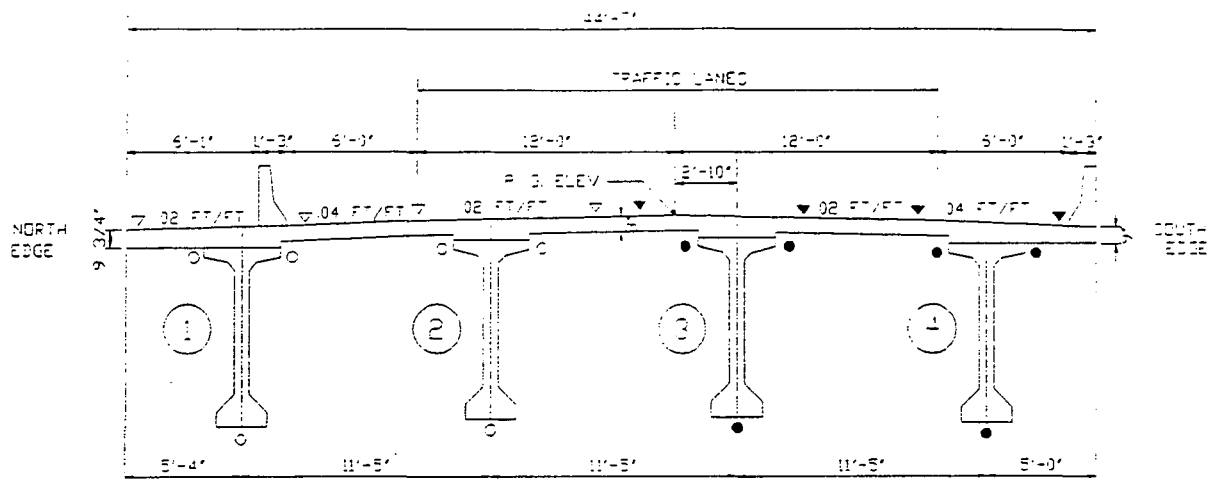
- ● LONGITUDINAL GAGES (9 CROSS-SECTIONS)
- ○ LONGITUDINAL GAGES (3 CROSS-SECTIONS)
- ▼ 2 GAGES AT 90° ON SLAB (3 CROSS-SECTIONS)
- ▽ 2 GAGES AT 90° ON SLAB (2 CROSS-SECTIONS)
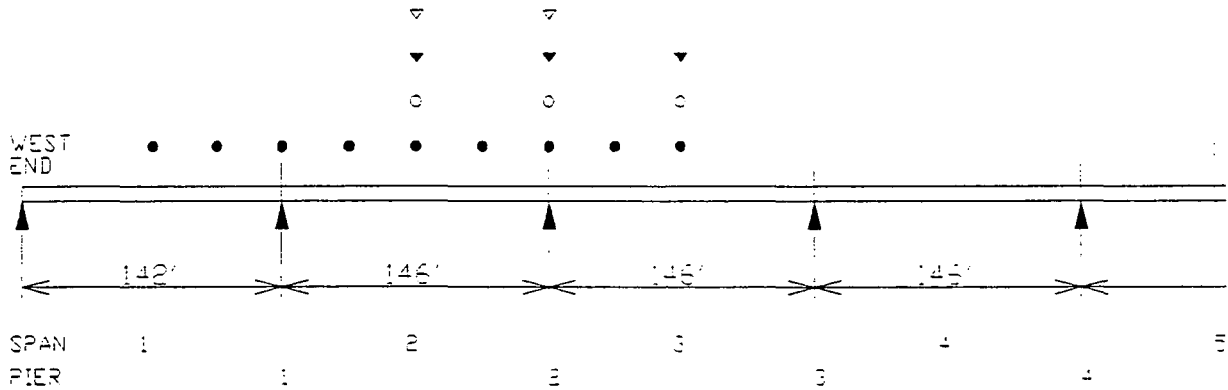
FIGURE 2.9   STRAIN GAGE LOCATIONS
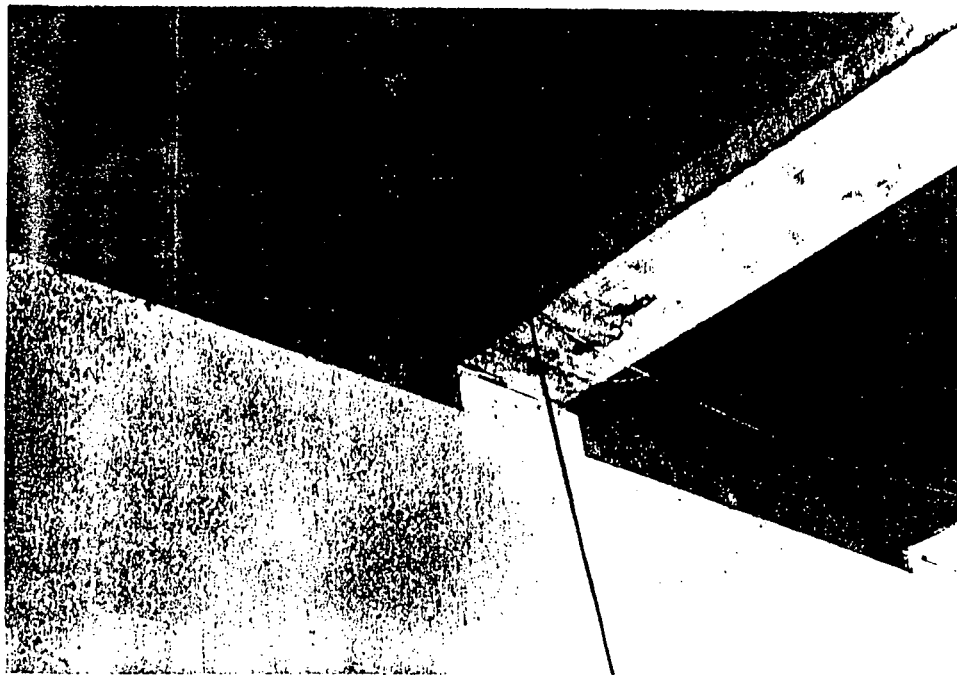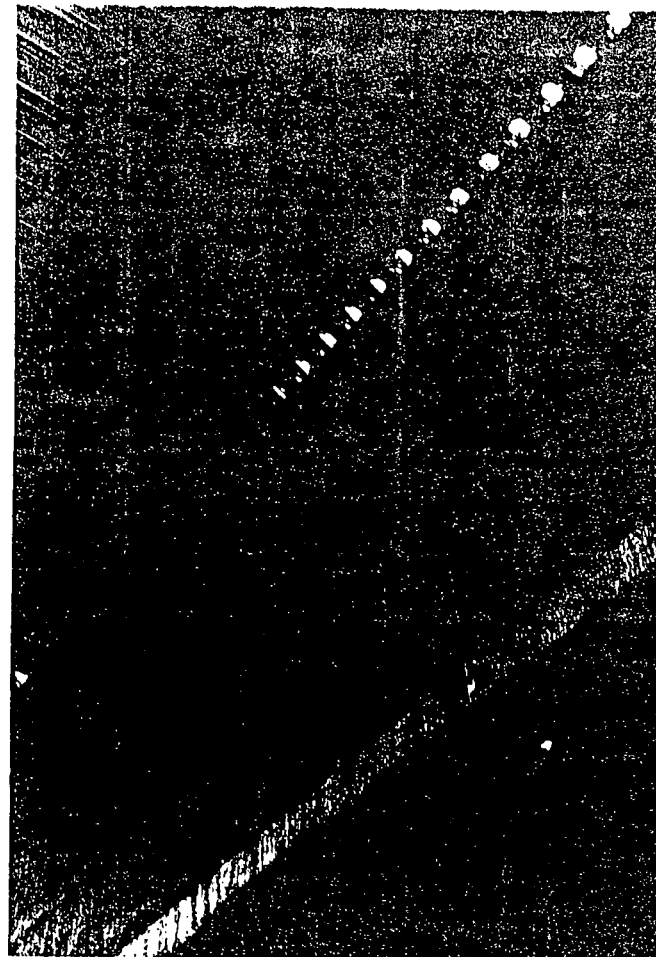
ABUTMENT 1 ... PIER 1

142'-0"

71'-0"

B1-1

INTERMEDIATE
DIAPHRAGM
(TYPICAL)

B1-2

11'-5"
(TYPICAL)

B1-3

B1-4

3'-5"

2

36'-11"

3

PIER 1 ... PIER 2

146'-0"

73'-0"

B2-1

B2-2

B2-3

B2-4

4'-6"

37'-11"

3'-5"

4'-6"

36'-6"

0   1   2*   3   4

PIER 2 ... PIER 3

146'-0"

73'-0"

B3-1

B3-2

B3-3

B3-4

36'-6"

3'-5"

1*   2*
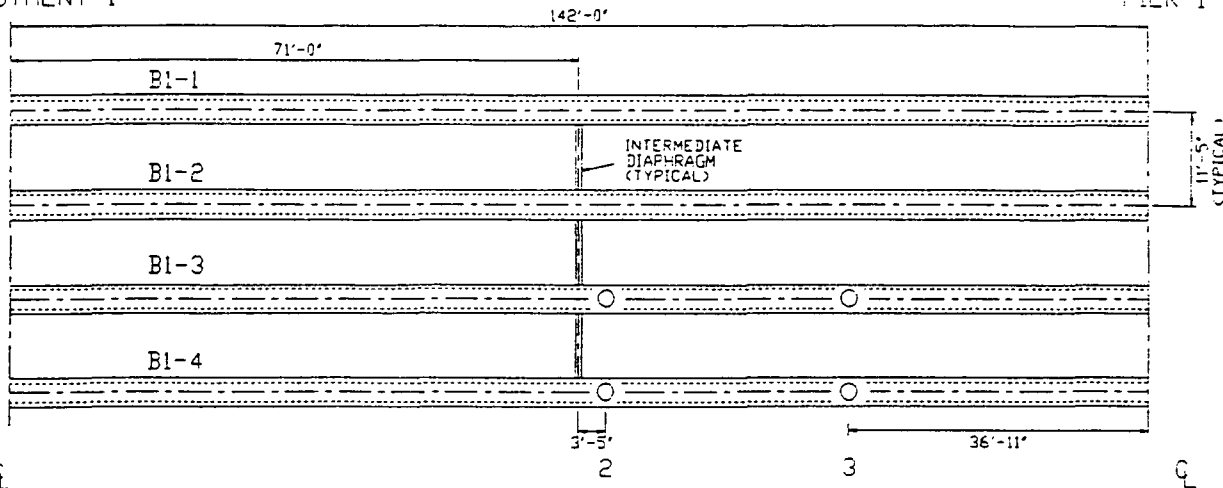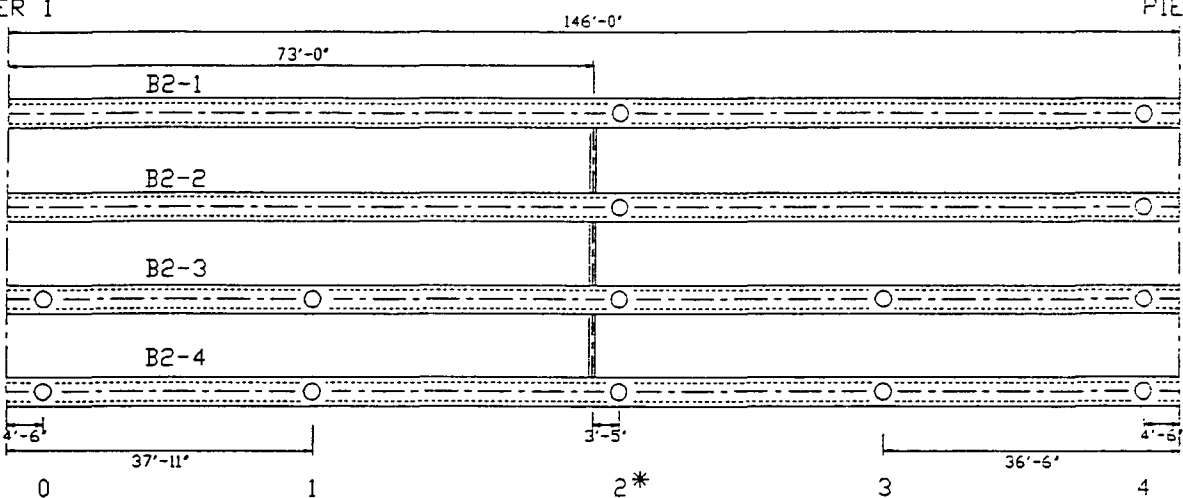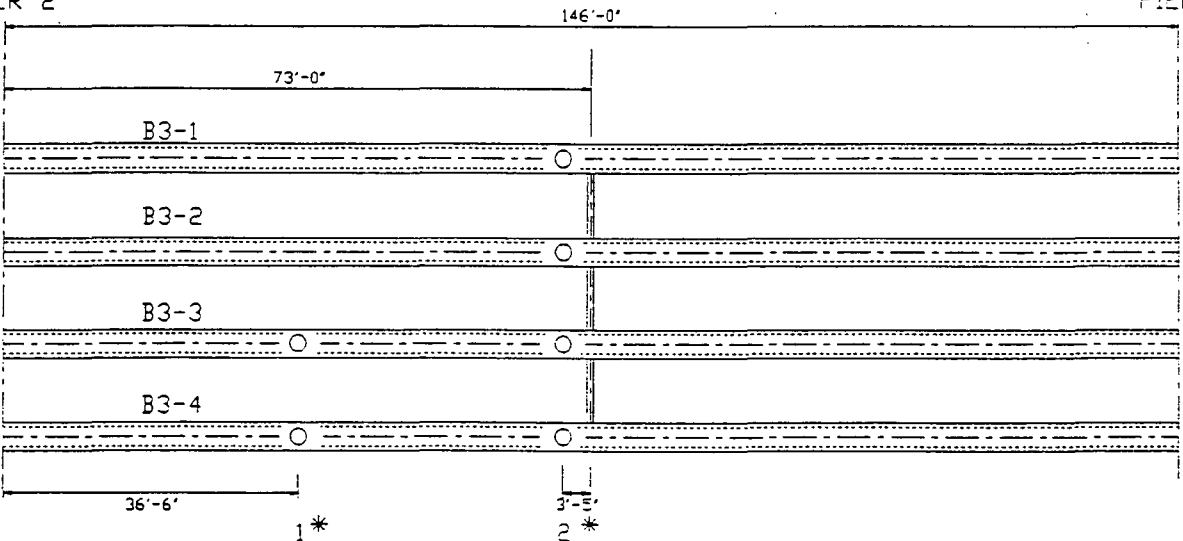
* : NOMINAL DISTANCE FOR EACH GAGE
O : GAGE POINTS (EACH GAGE POINT HAS THREE GAGES)

FIGURE 2.12   STRAIN GAGE LOCATIONS - PLAN VIEW
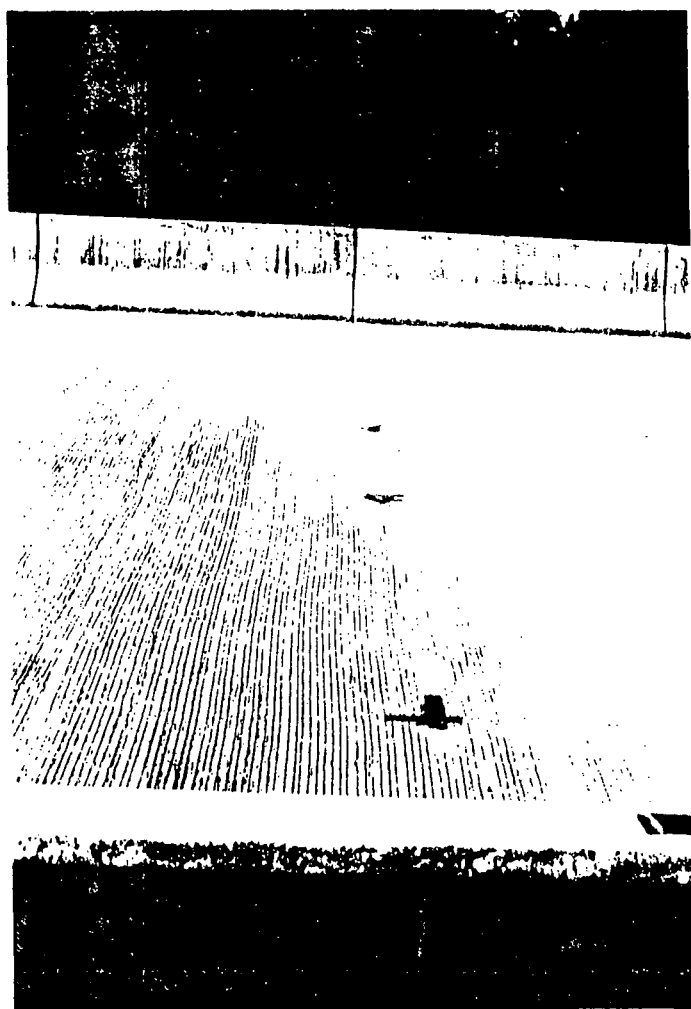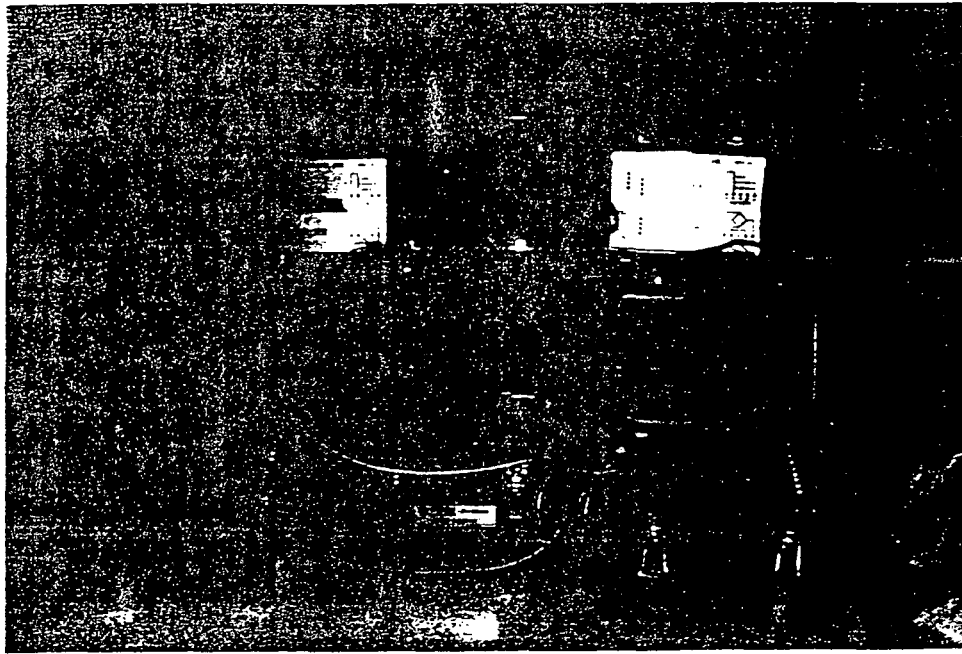
FIGURE 2.15   STRAIN INDICATORS
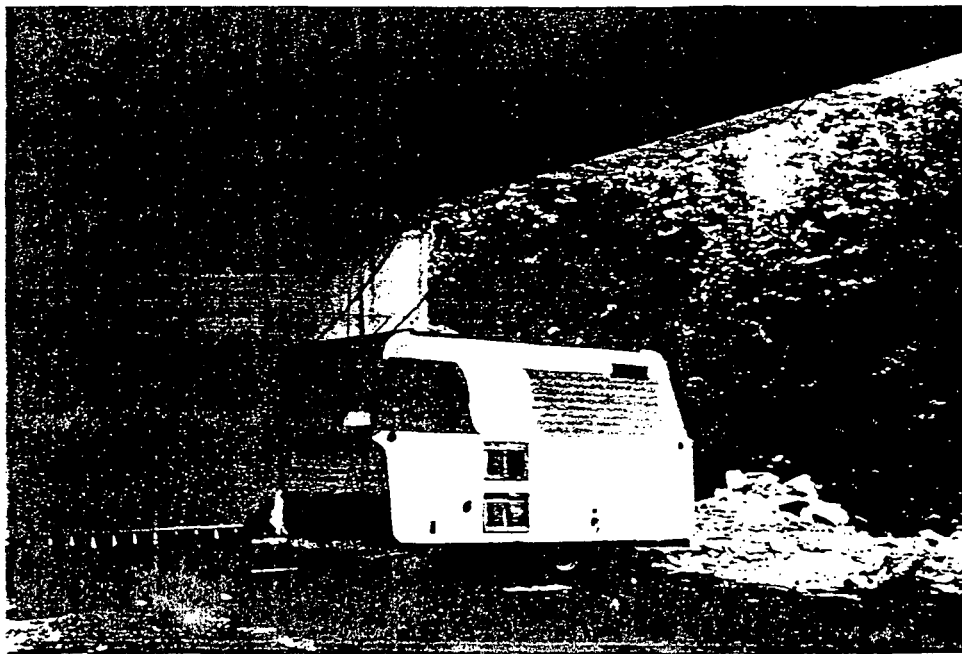
FIGURE 2.16   INSTRUMENT TRAILER
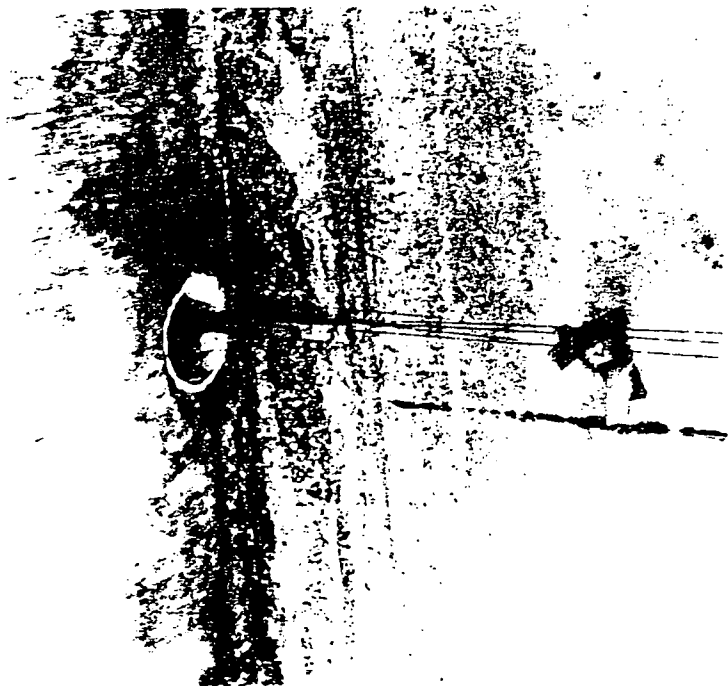
212B
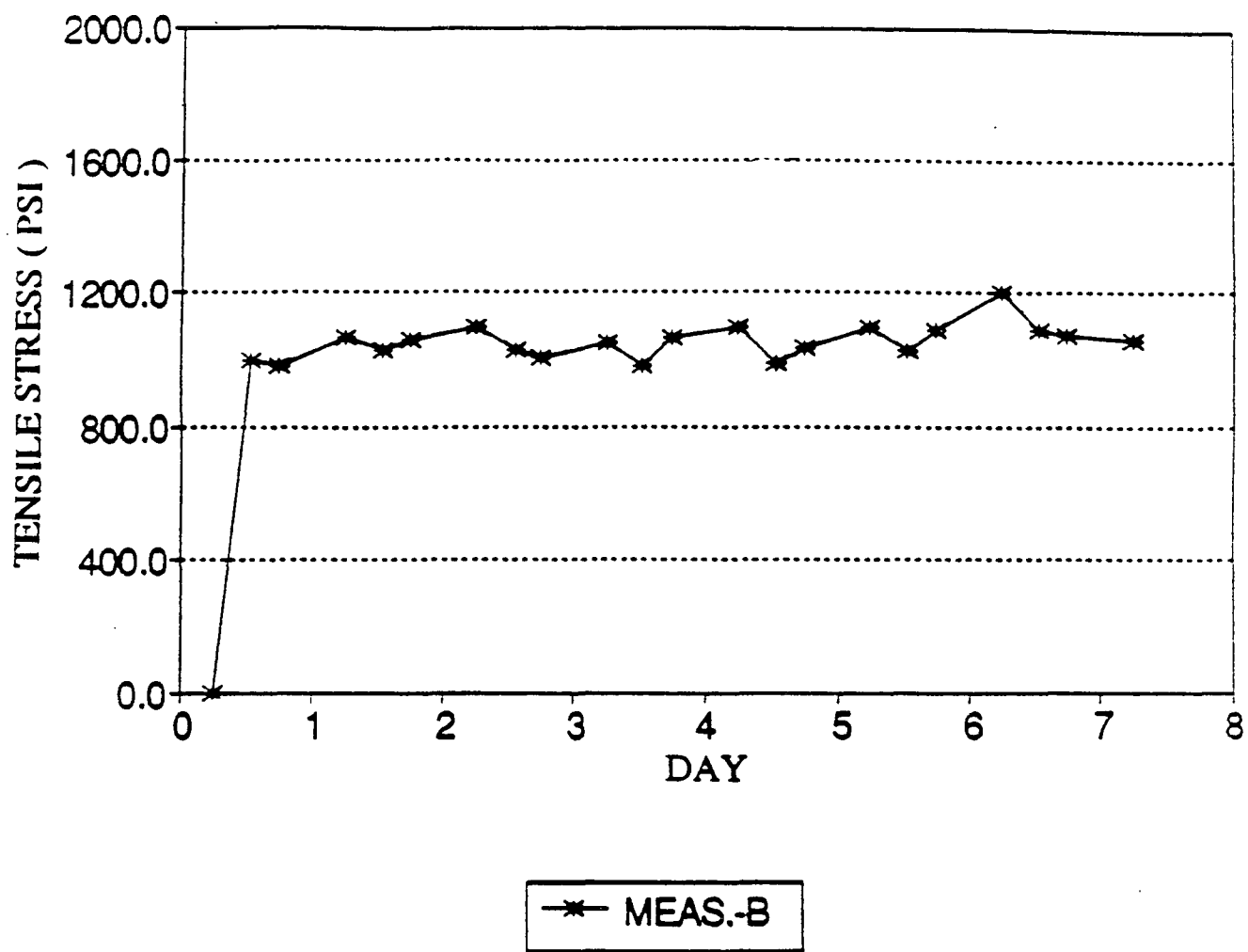
FIGURE 3.1   DEAD LOAD STRESSES BASED ON MEASUREMENTS
GAGE 212B
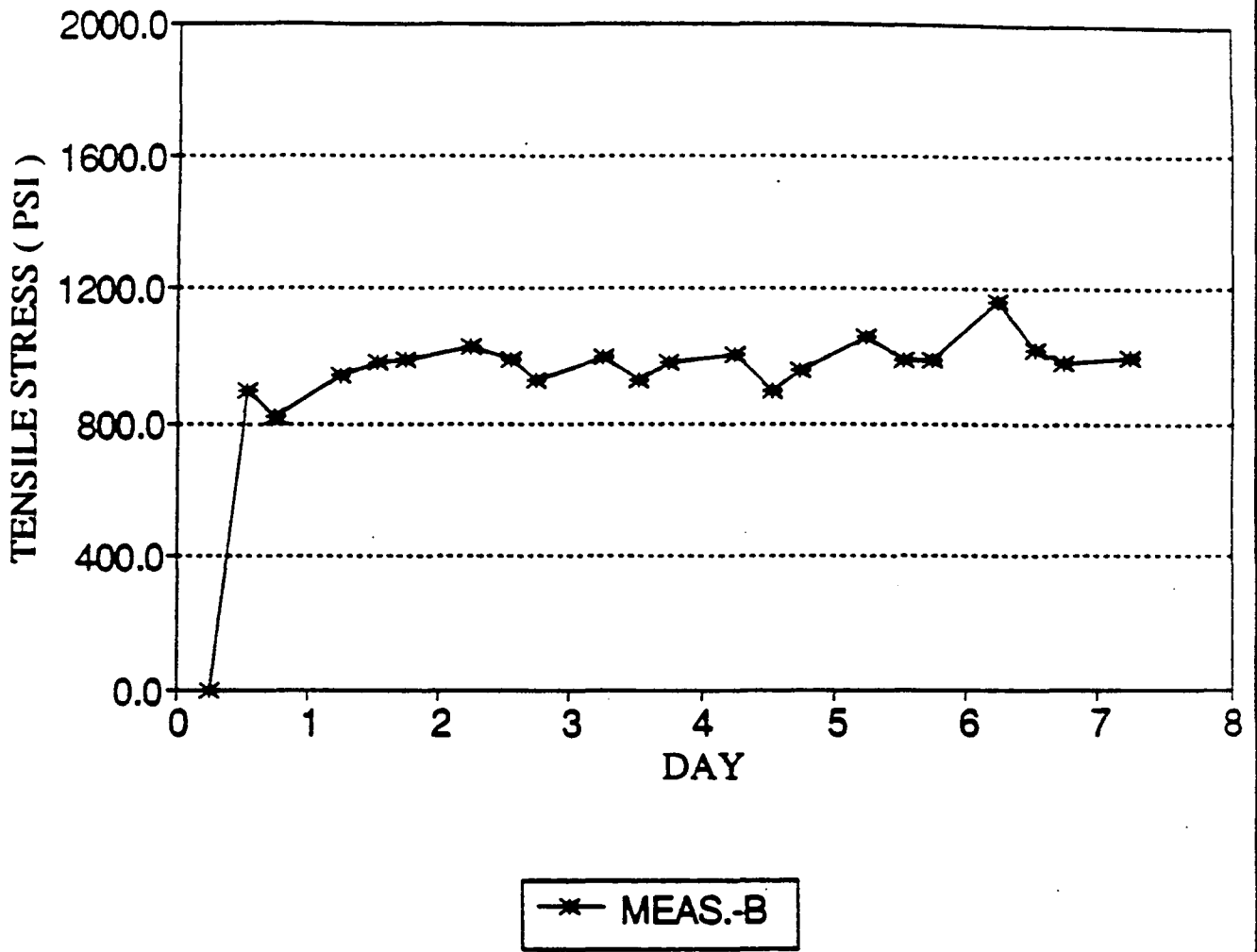
222B

FIGURE 3.2 DEAD LOAD STRESSES BASED ON MEASUREMENTS
GAGE 222B

232B
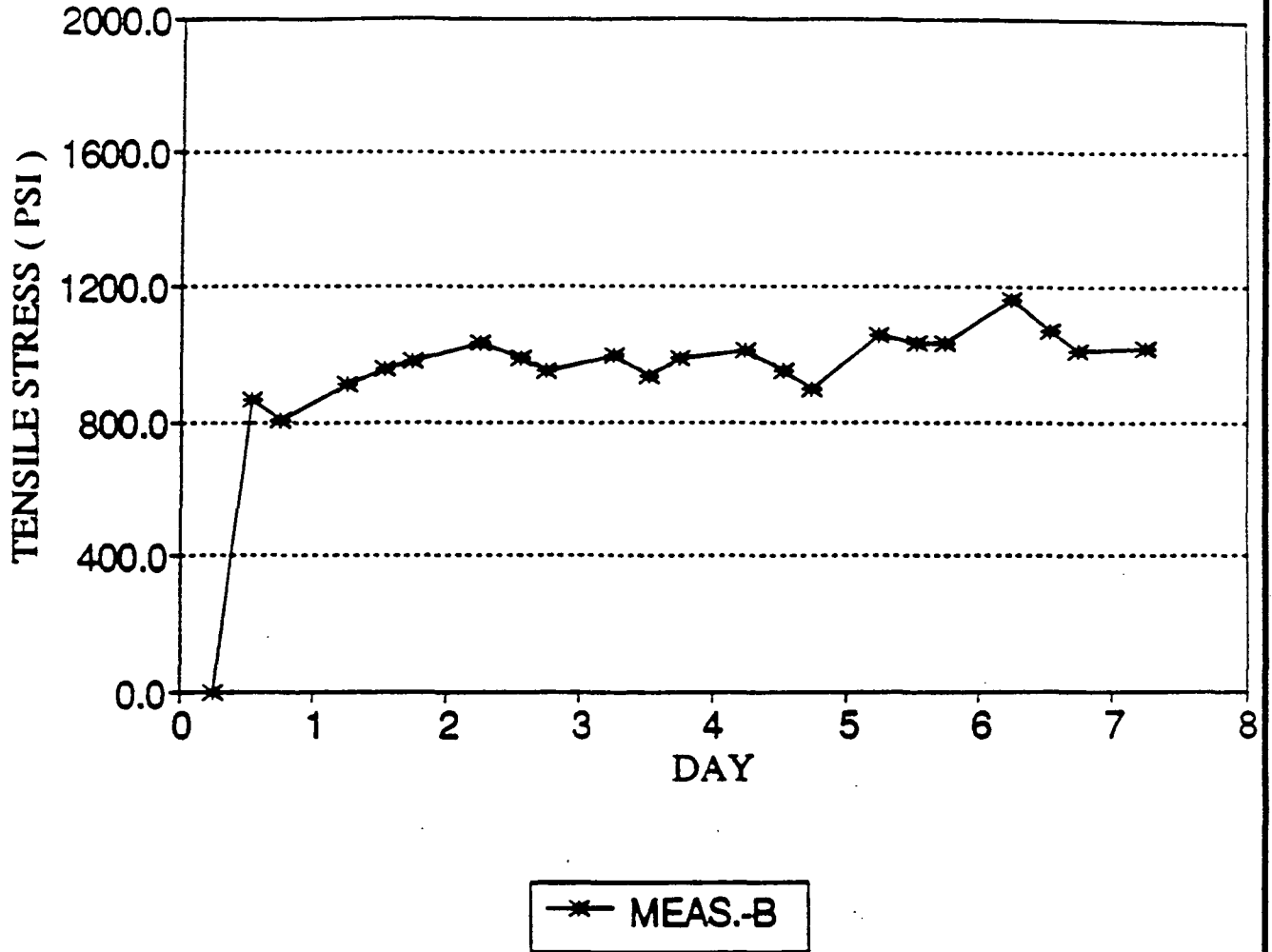
FIGURE 3.3 DEAD LOAD STRESSES BASED ON MEASUREMENTS
GAGE 232B

242B
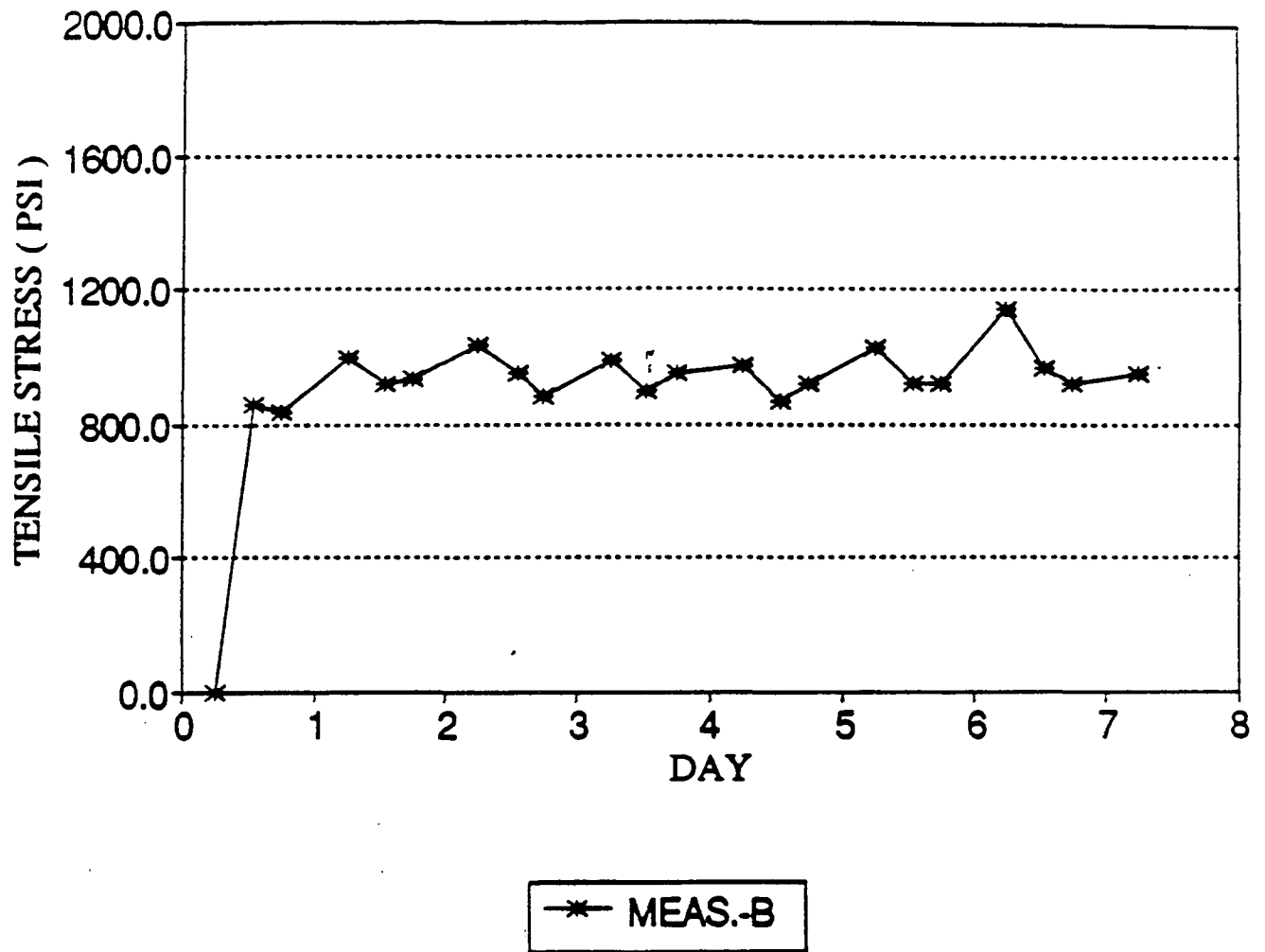
FIGURE 3.4   DEAD LOAD STRESSES BASED ON MEASUREMENTS
GAGE 242B

2_2B
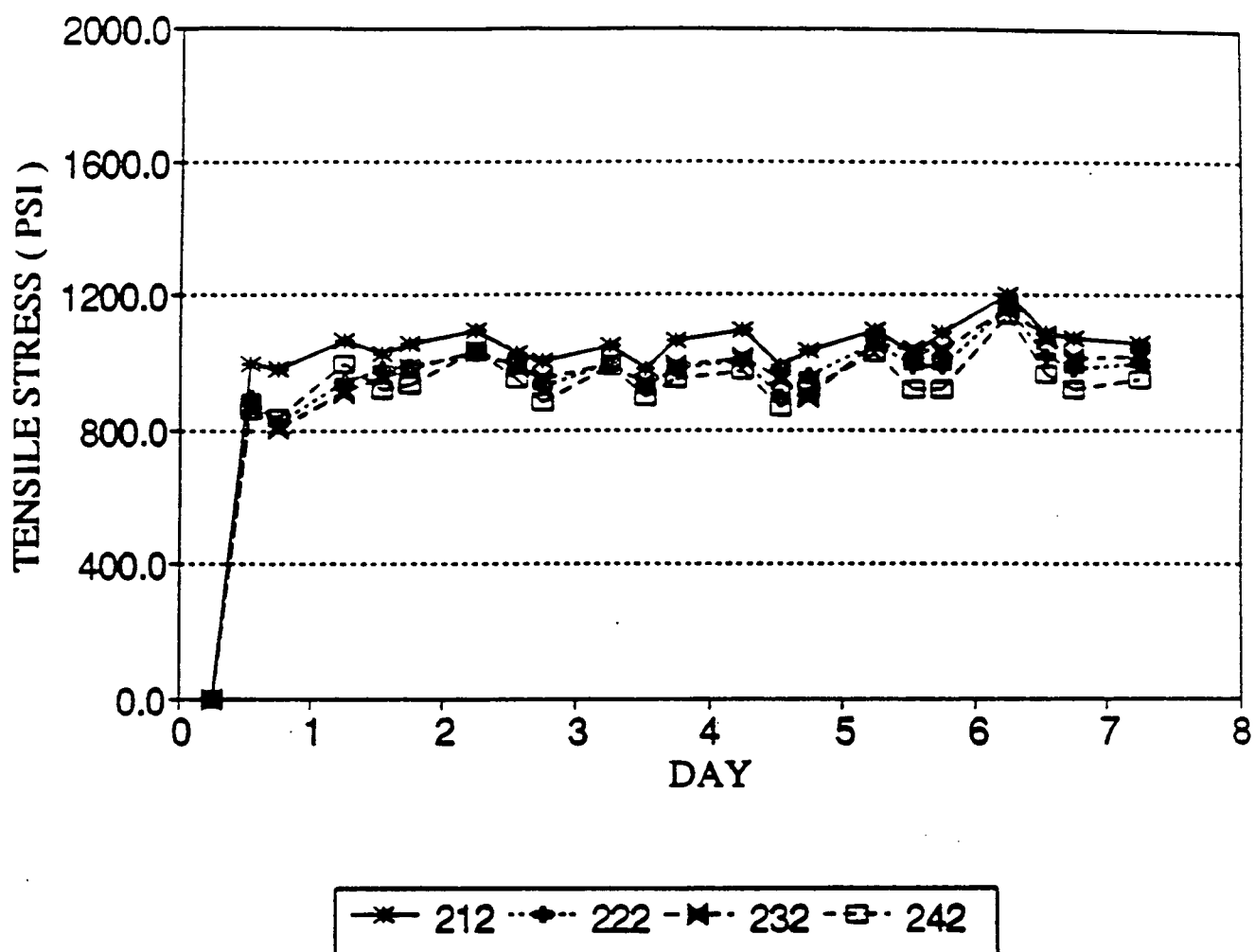
FIGURE 3.5   DEAD LOAD STRESSES BASED ON MEASUREMENTS
GAGES 2_2B
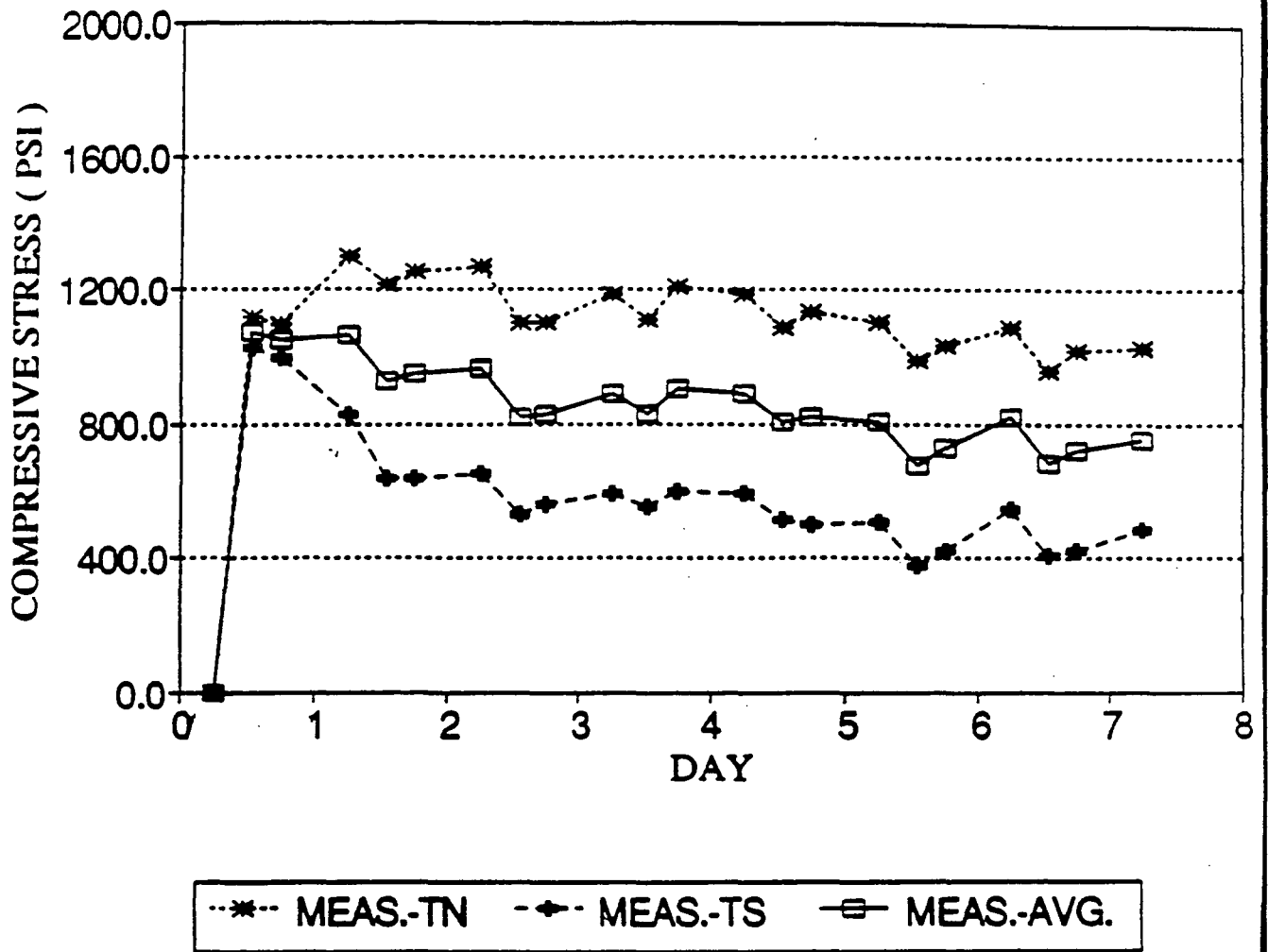
FIGURE 3.6   DEAD LOAD STRESSES BASED ON MEASUREMENTS
GAGES 212T
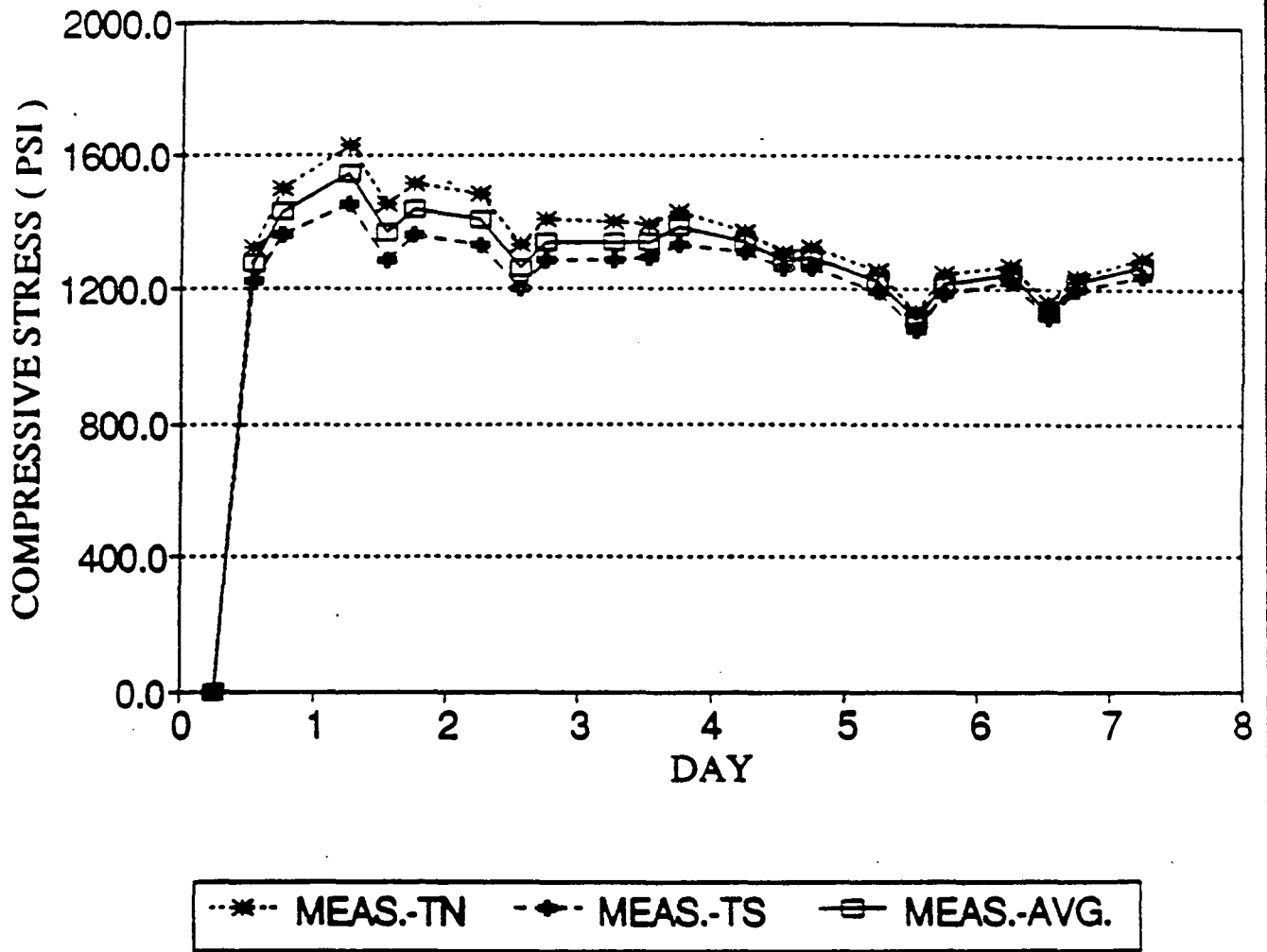
FIGURE 3.7 DEAD LOAD STRESSES BASED ON MEASUREMENTS GAGES 222T
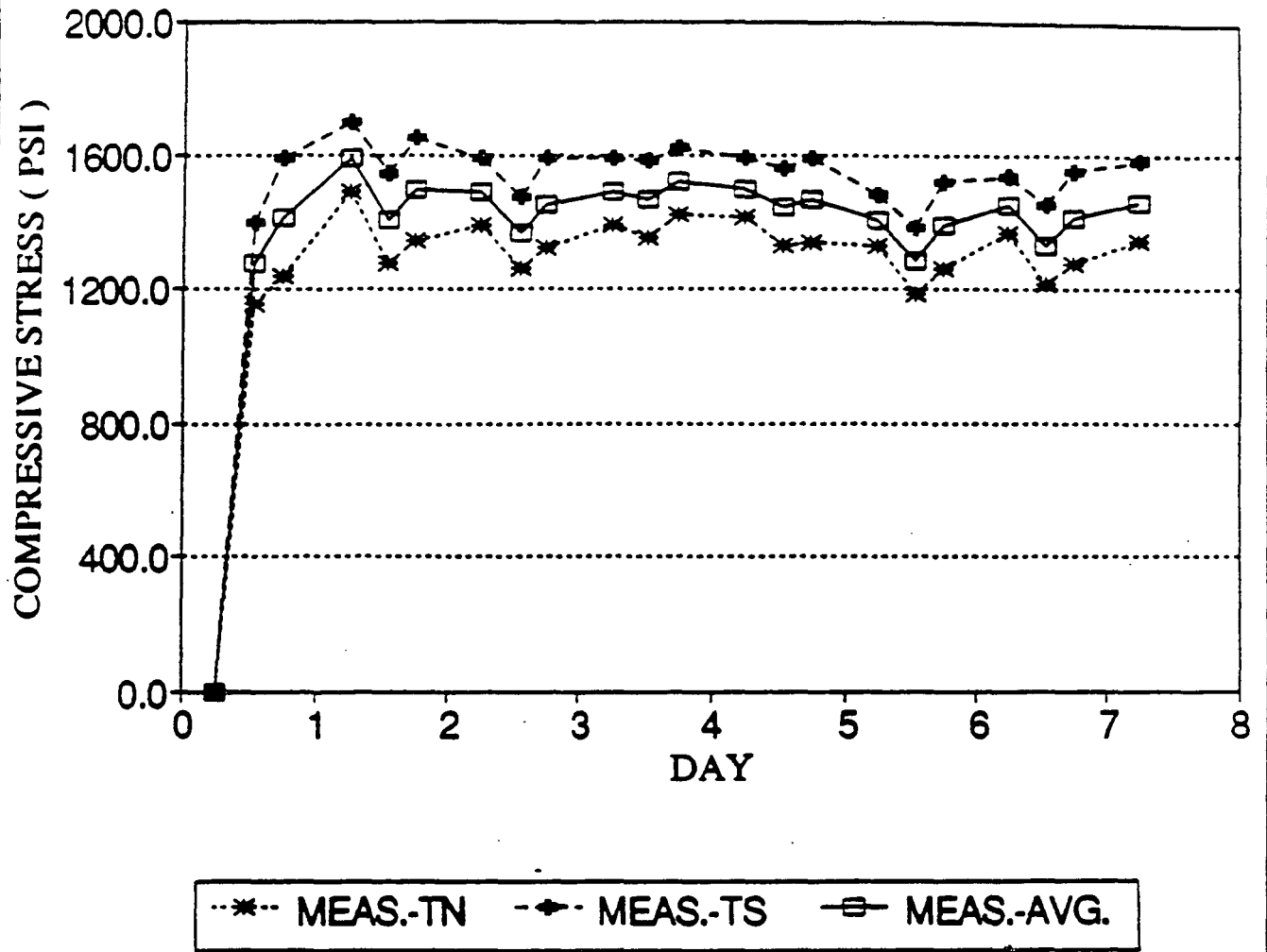
FIGURE 3.8 DEAD LOAD STRESSES BASED ON MEASUREMENTS
GAGES 232T

242T
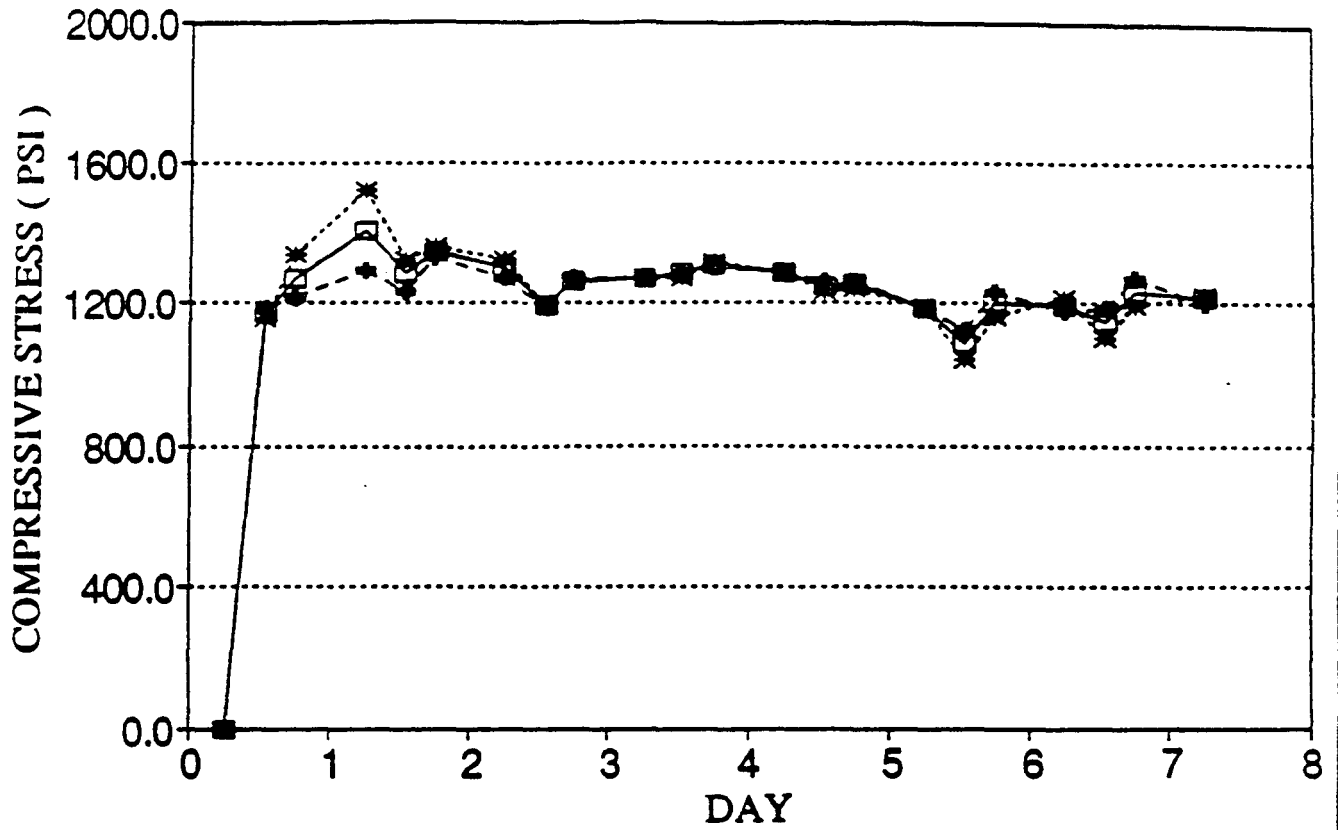
FIGURE 3.9   DEAD LOAD STRESSES BASED ON MEASUREMENTS
GAGES 242T

2_2T
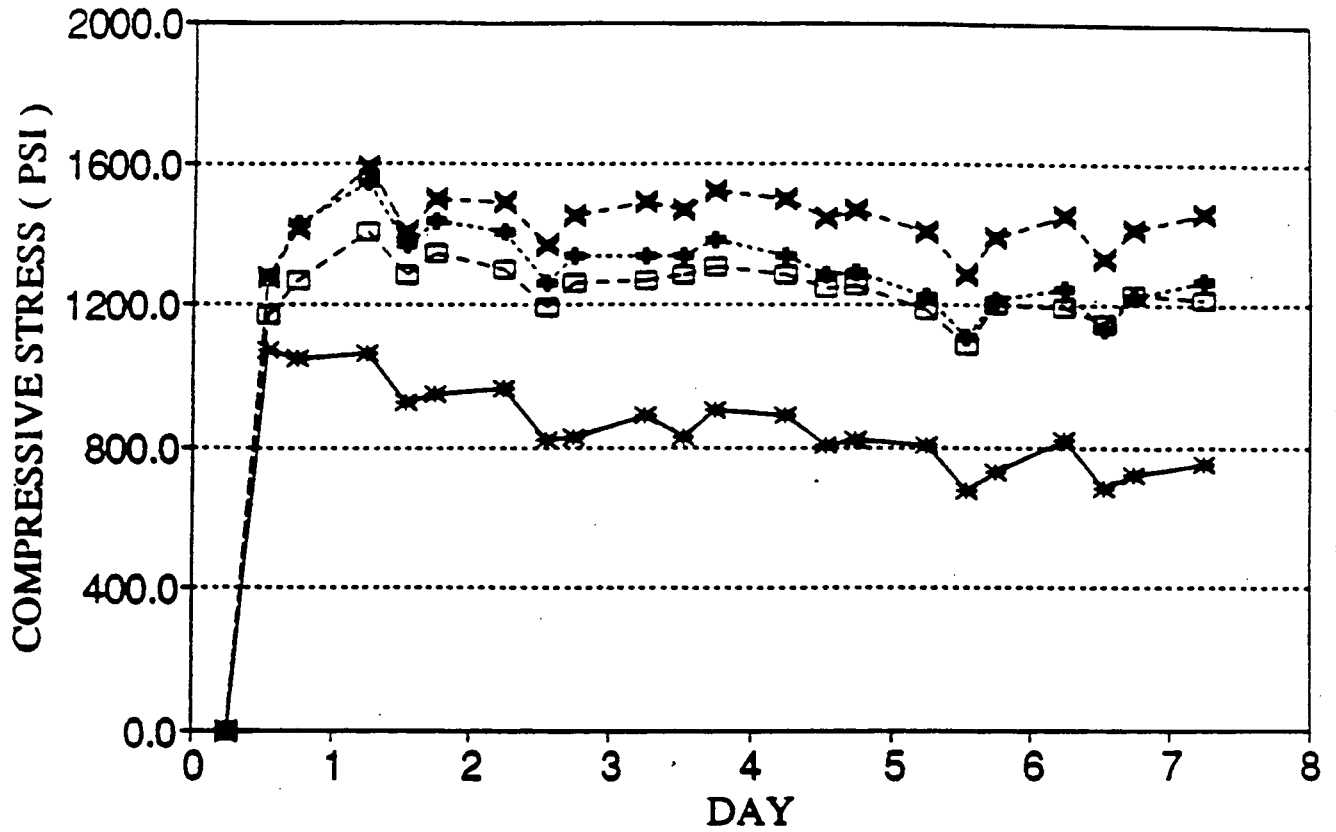
FIGURE 3.10   DEAD LOAD STRESSES BASED ON MEASUREMENTS
             GAGES 2_2T

312B
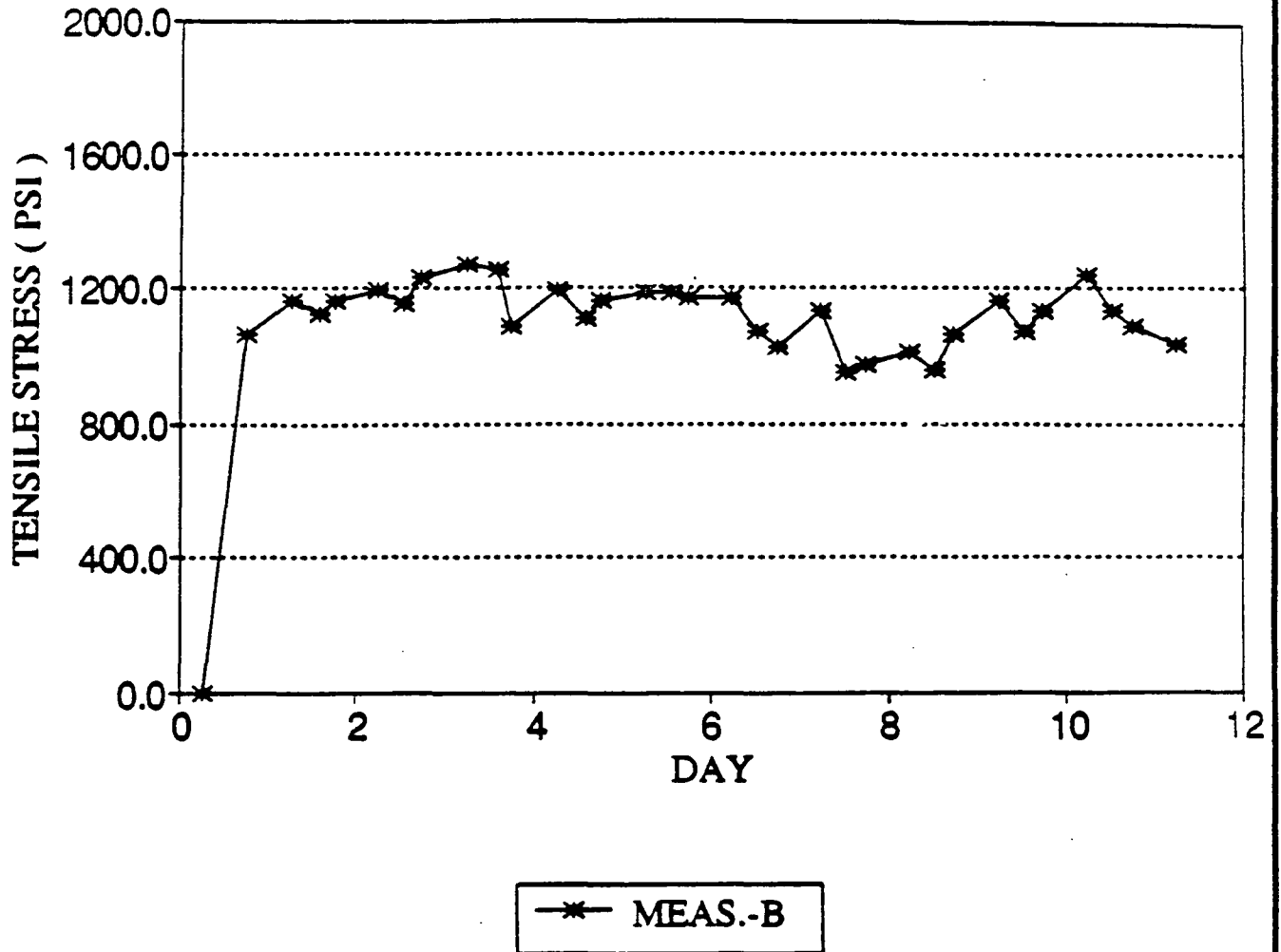
FIGURE 3.11   DEAD LOAD STRESSES BASED ON MEASUREMENTS
             GAGE 312B

322B
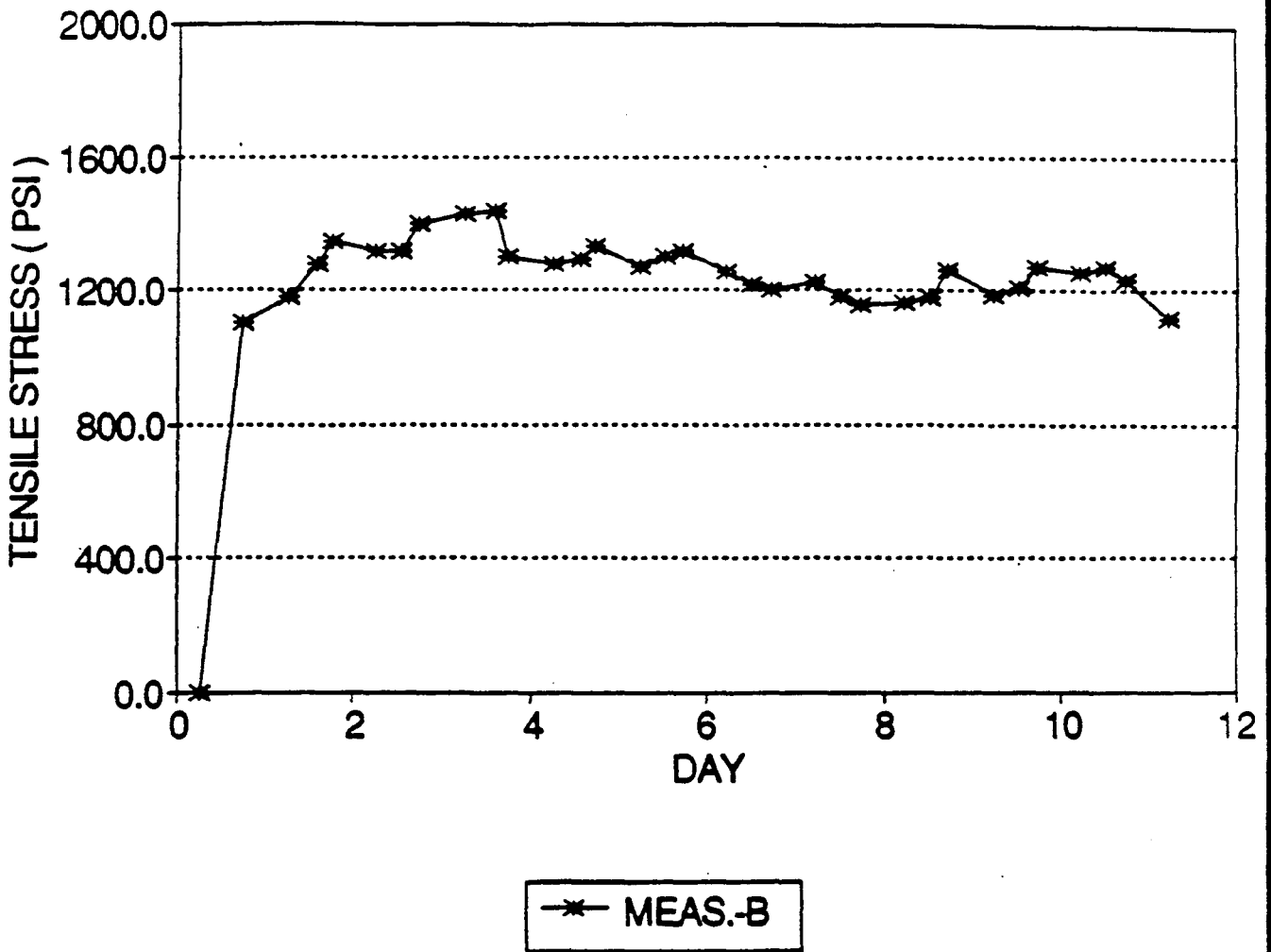
FIGURE 3.12   DEAD LOAD STRESSES BASED ON MEASUREMENTS
GAGE 322B

332B
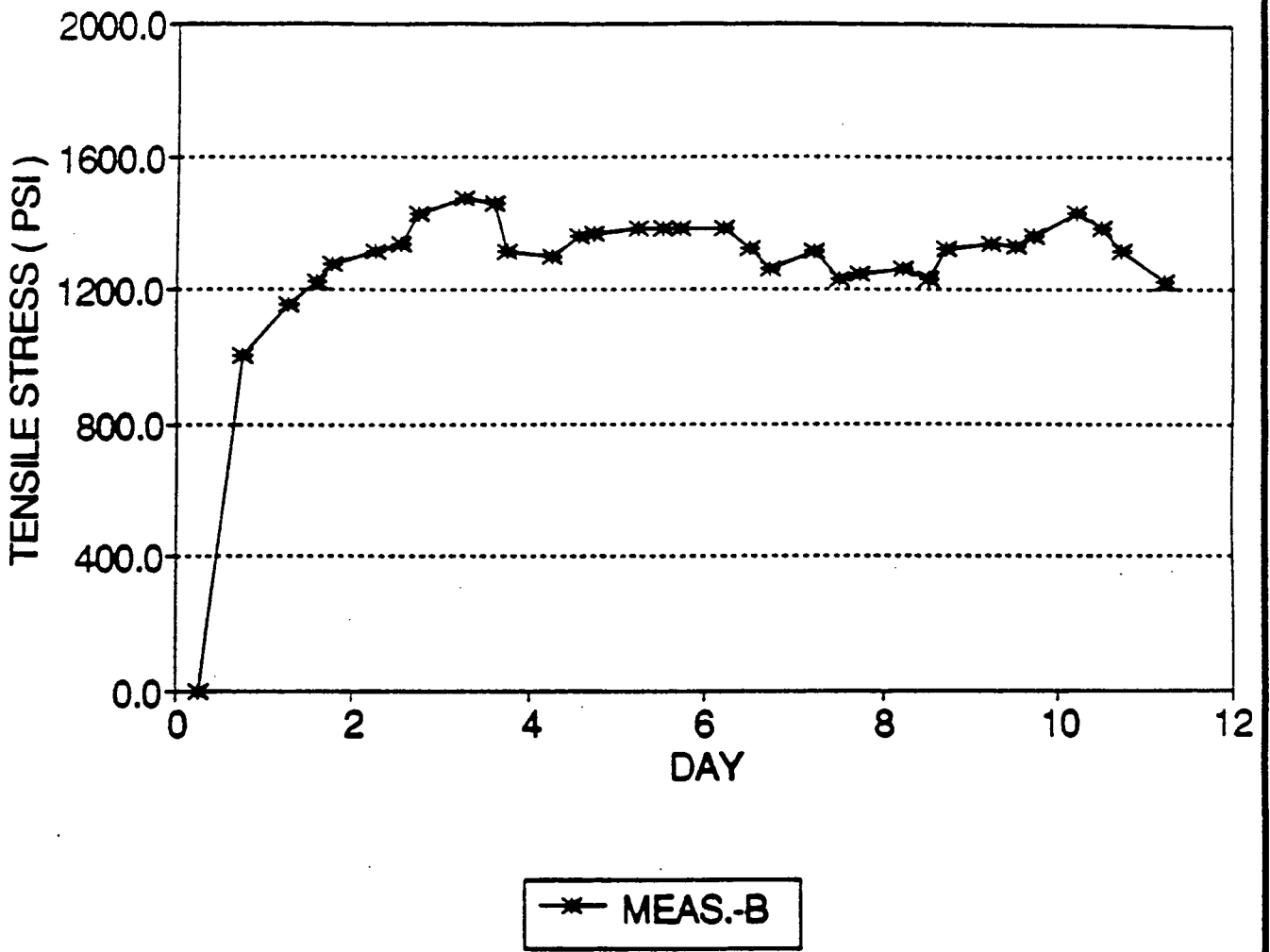
FIGURE 3.13   DEAD LOAD STRESSES BASED ON MEASUREMENTS
             GAGE 332B

342B
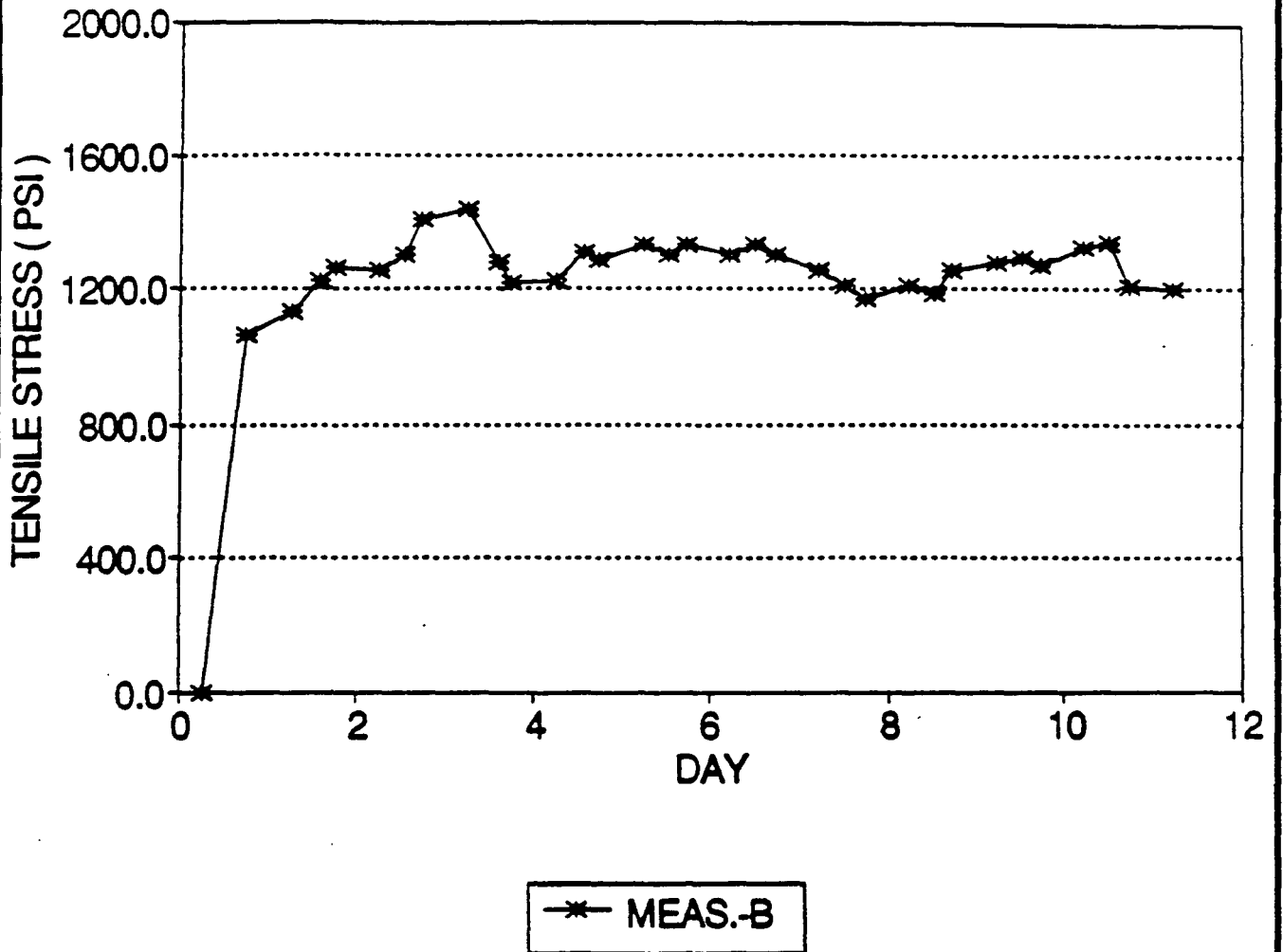
FIGURE 3.14   DEAD LOAD STRESSES BASED ON MEASUREMENTS
GAGE 342B

3_2B
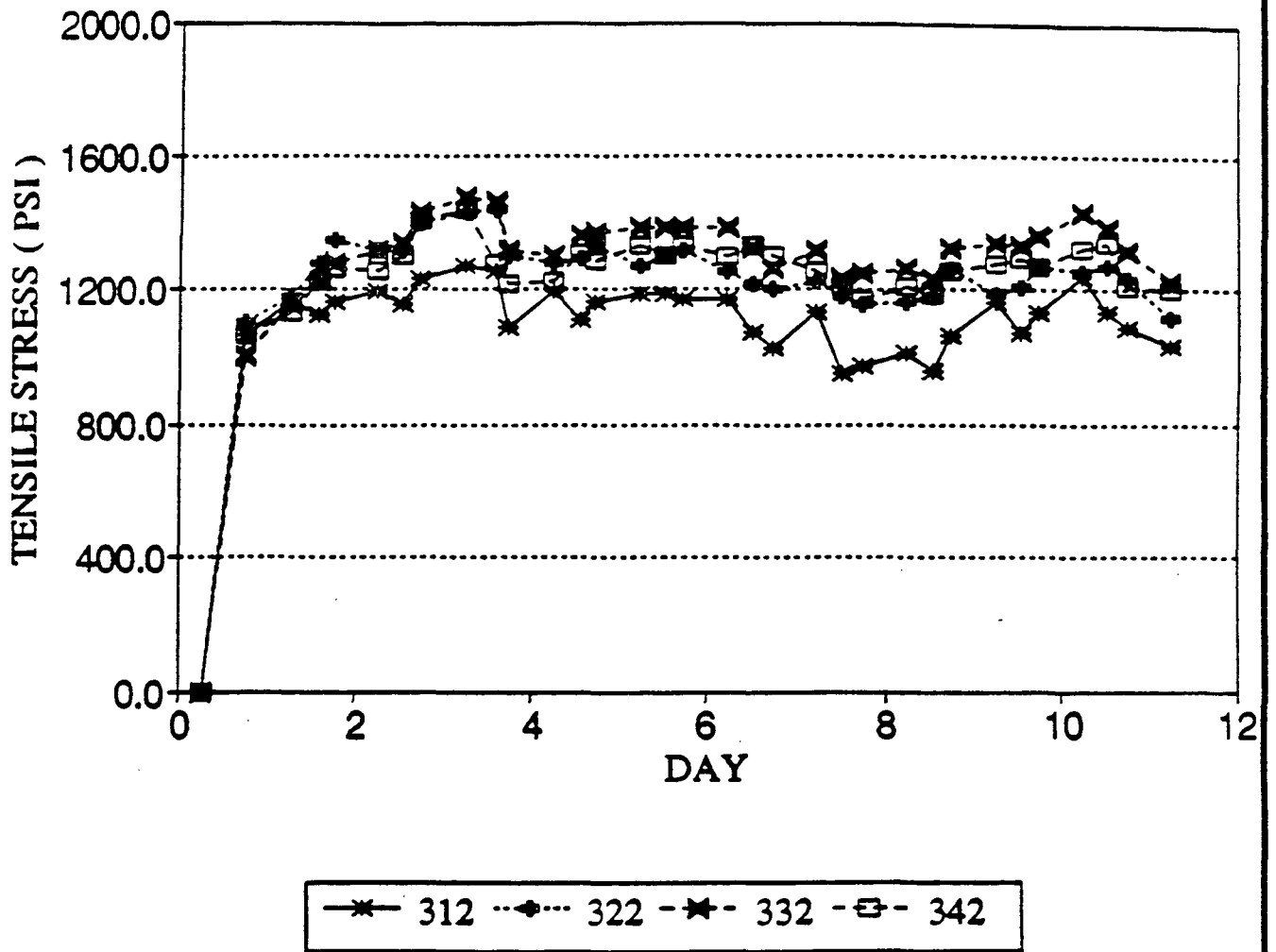
FIGURE 3.15   DEAD LOAD STRESSES BASED ON MEASUREMENTS
GAGES 3_2B

312T
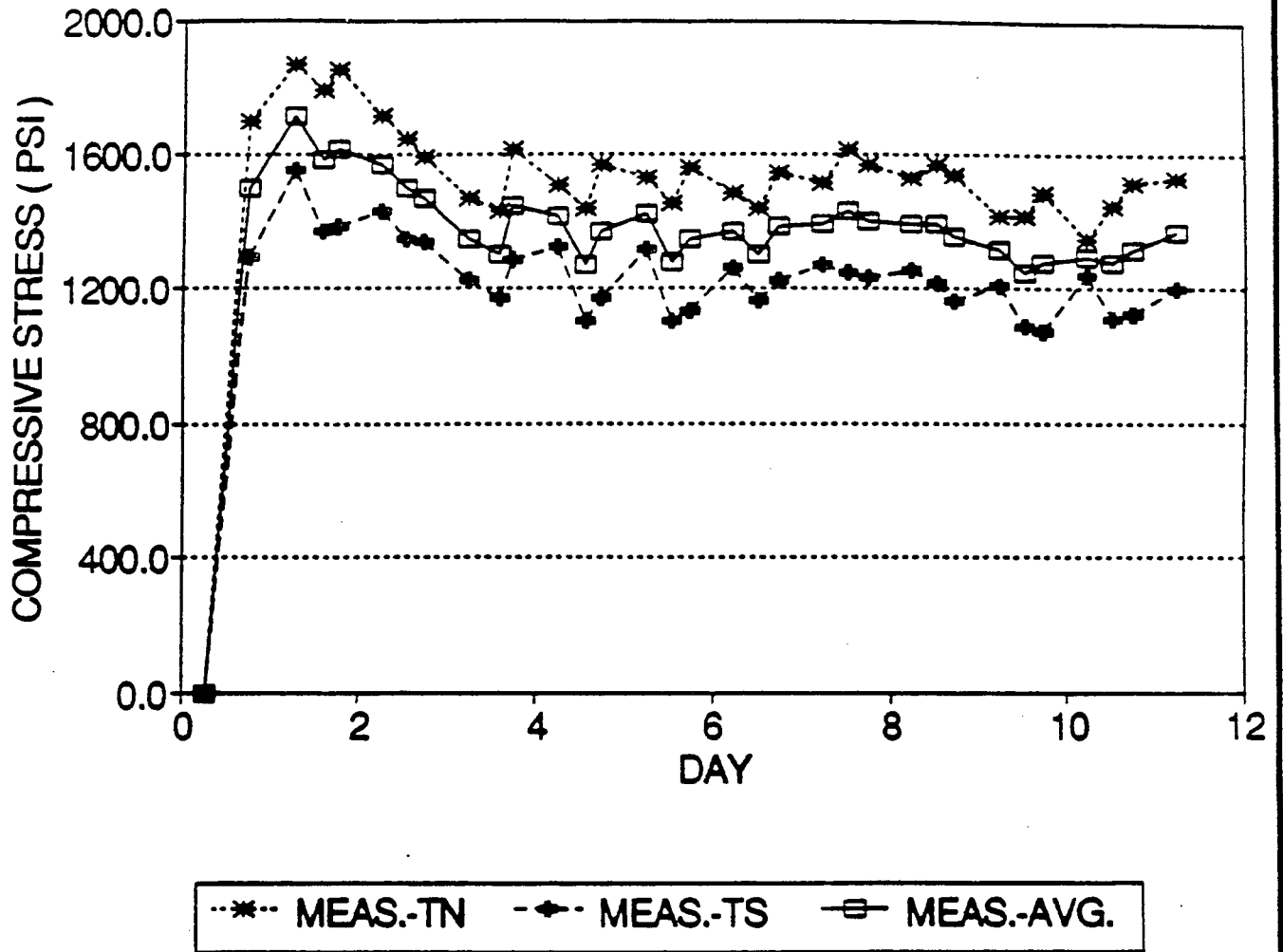
FIGURE 3.16   DEAD LOAD STRESSES BASED ON MEASUREMENTS
GAGES 312T

322T
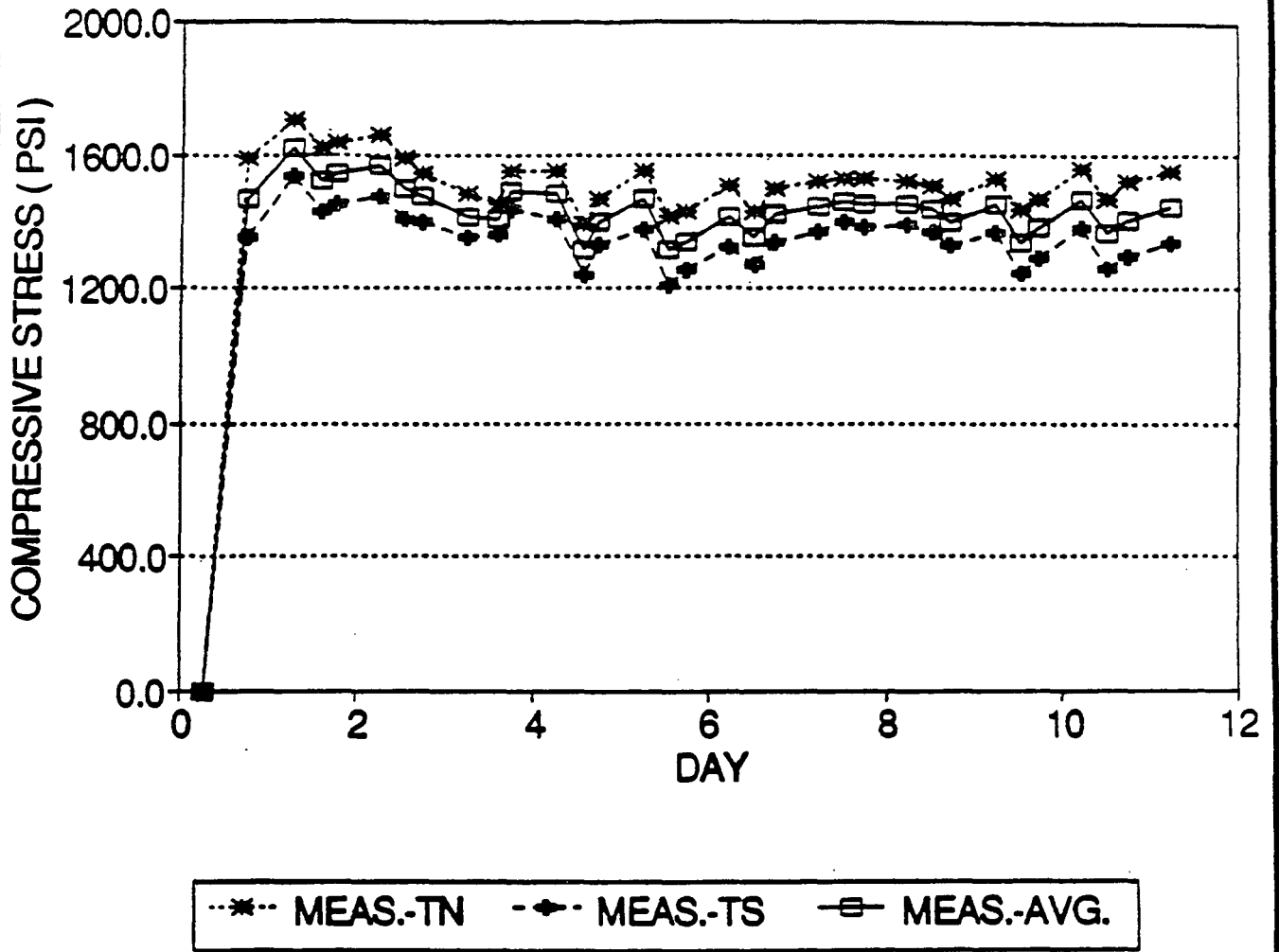
FIGURE 3.17   DEAD LOAD STRESSES BASED ON MEASUREMENTS
GAGES 322T

332T
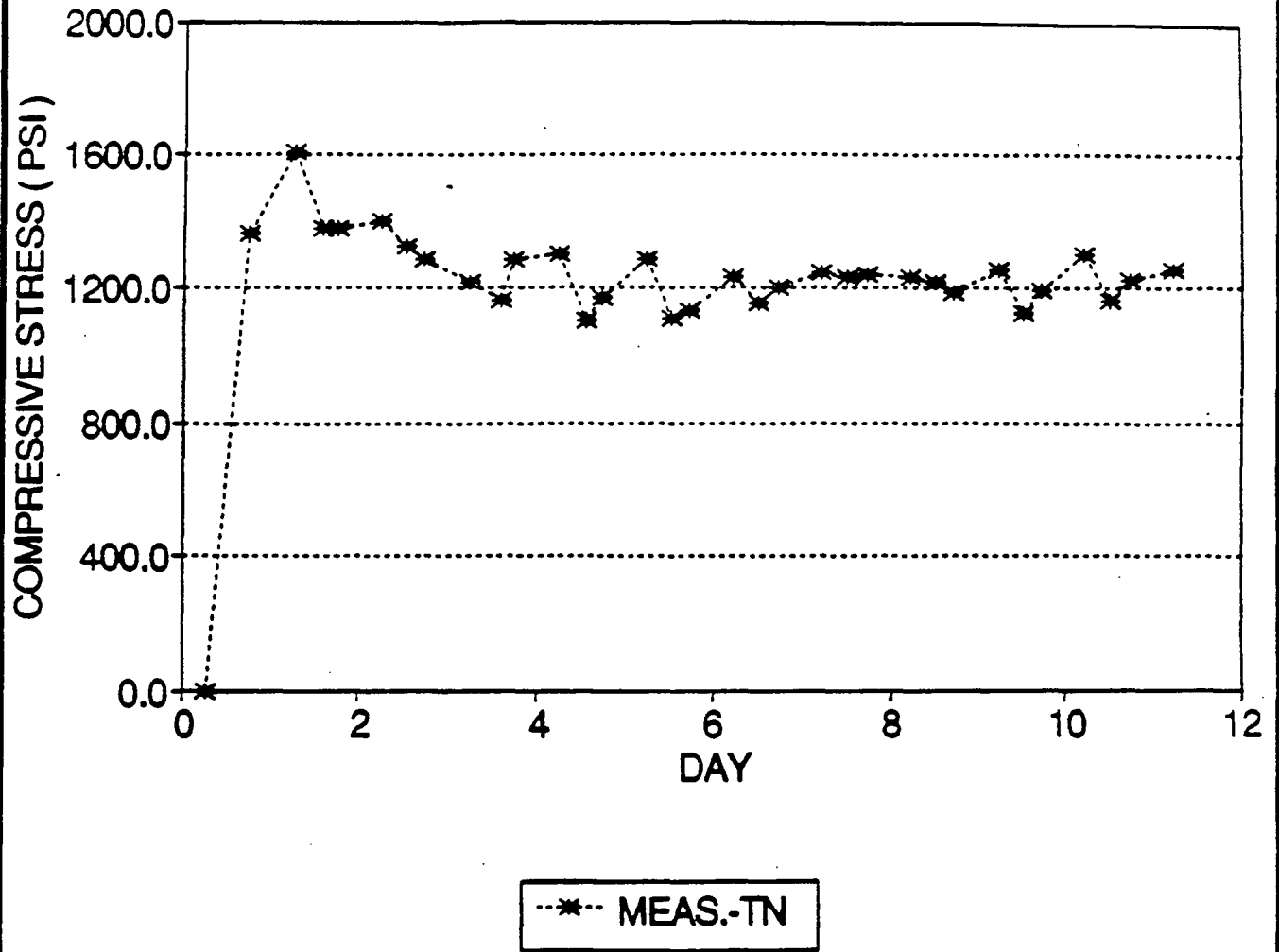
FIGURE 3.18   DEAD LOAD STRESSES BASED ON MEASUREMENTS
GAGES 332T
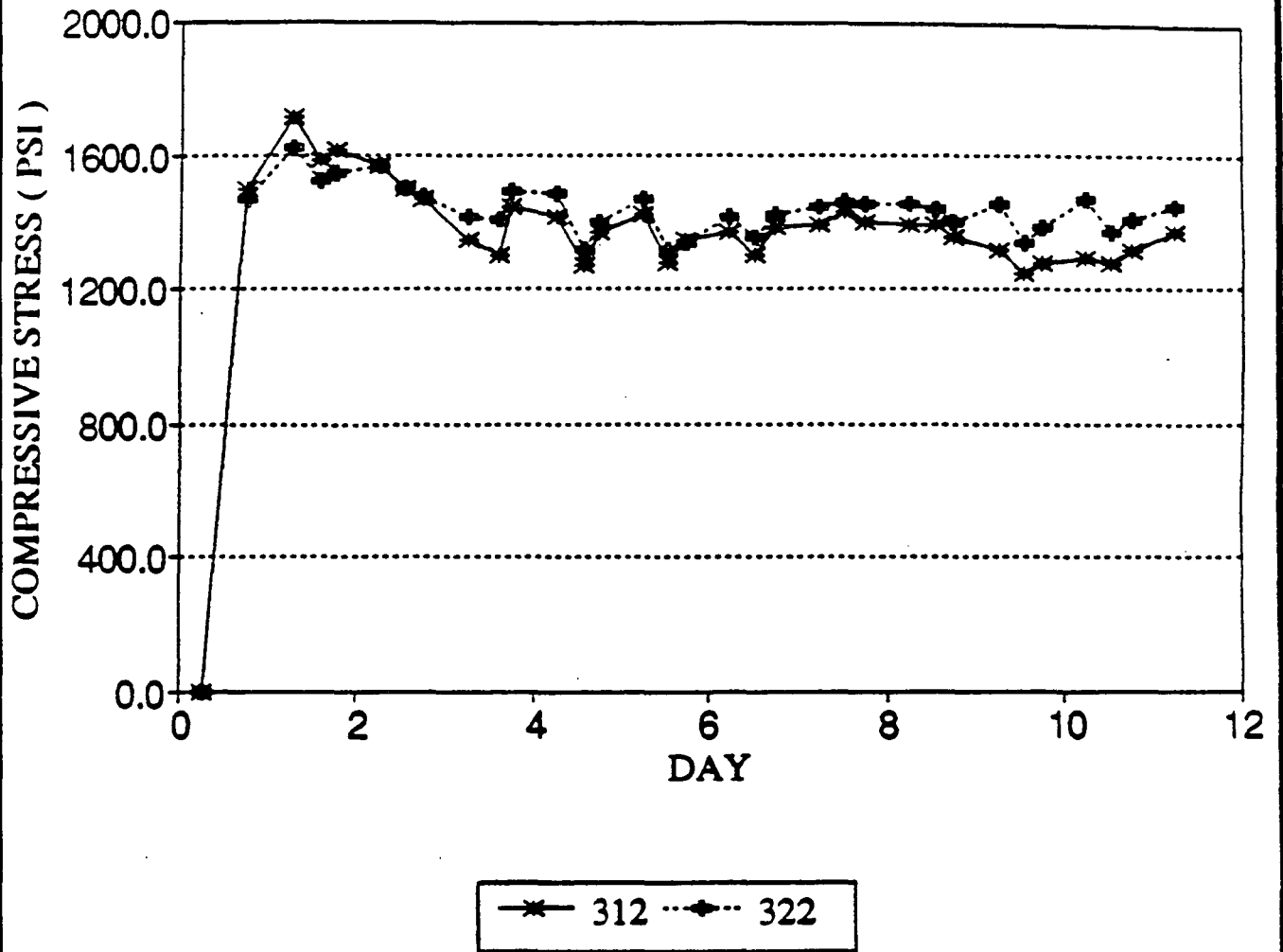
FIGURE 3.19   DEAD LOAD STRESSES BASED ON MEASUREMENTS
GAGES 3_2T
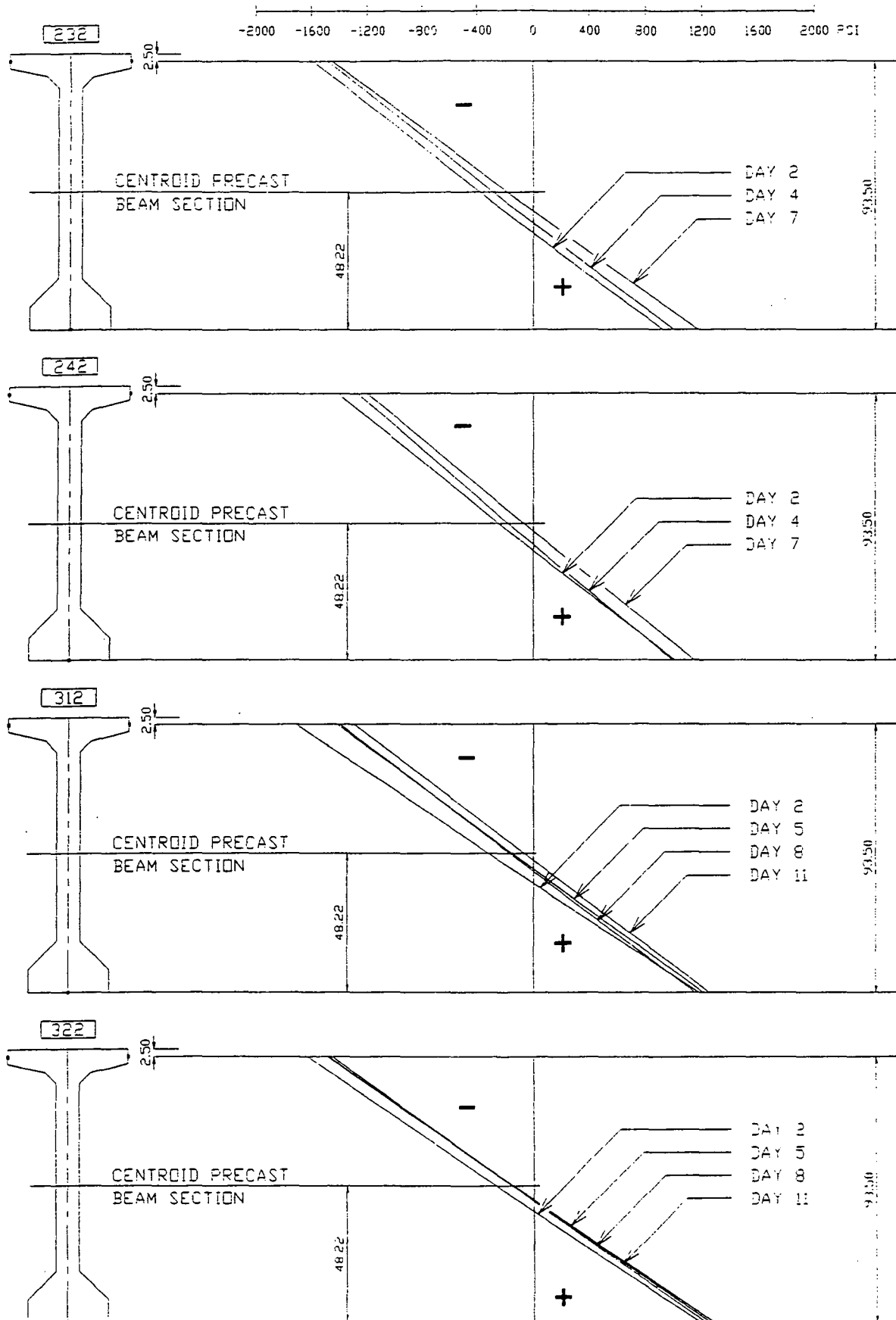
FIGURE 3.20   DEAD LOAD STRESS DISTRIBUTION AT MIDSPAN
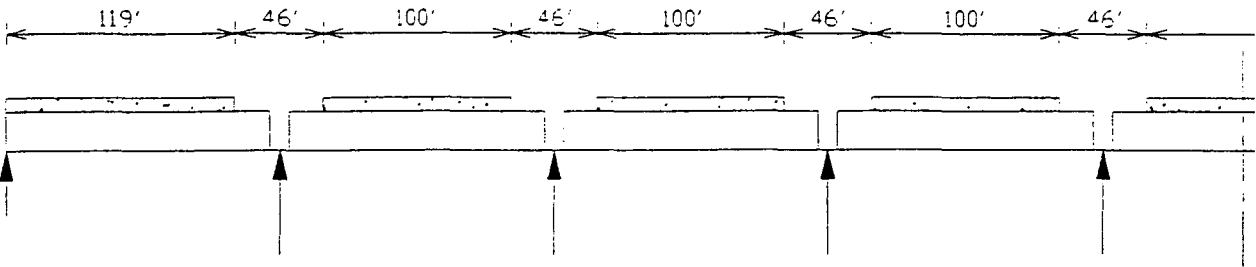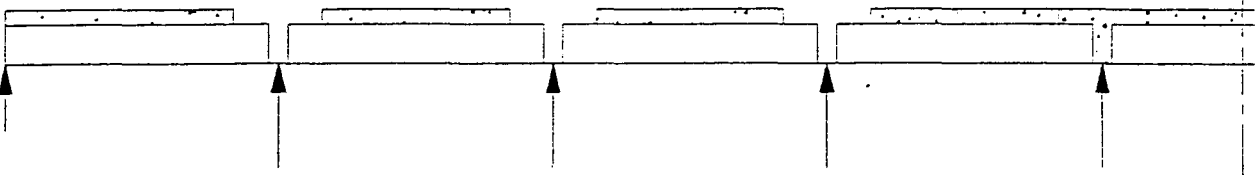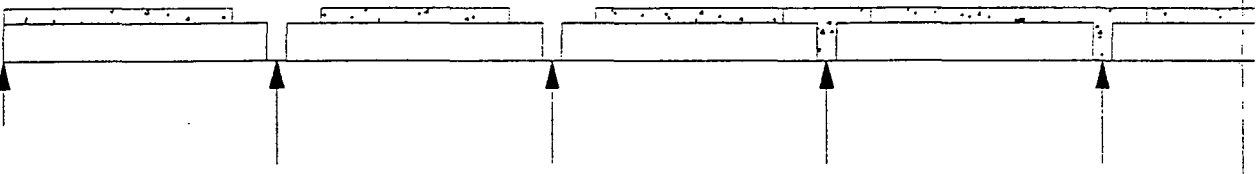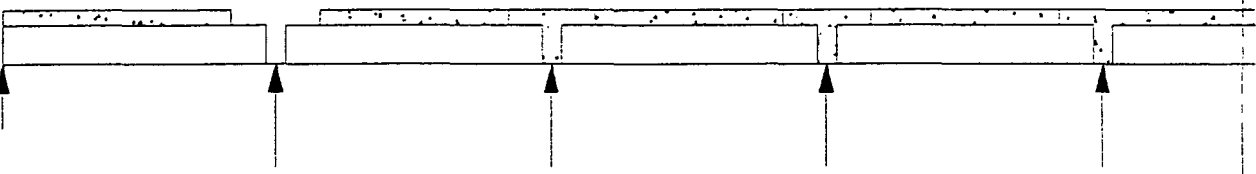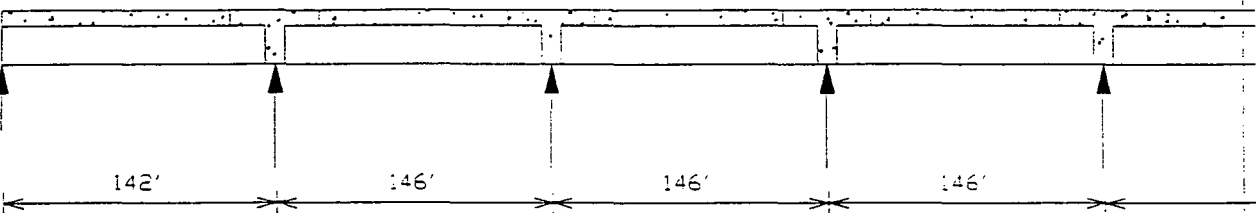
FIGURE 3.21   DECK CONCRETE PLACEMENT SEQUENCE USED IN ANALYSIS

23_B
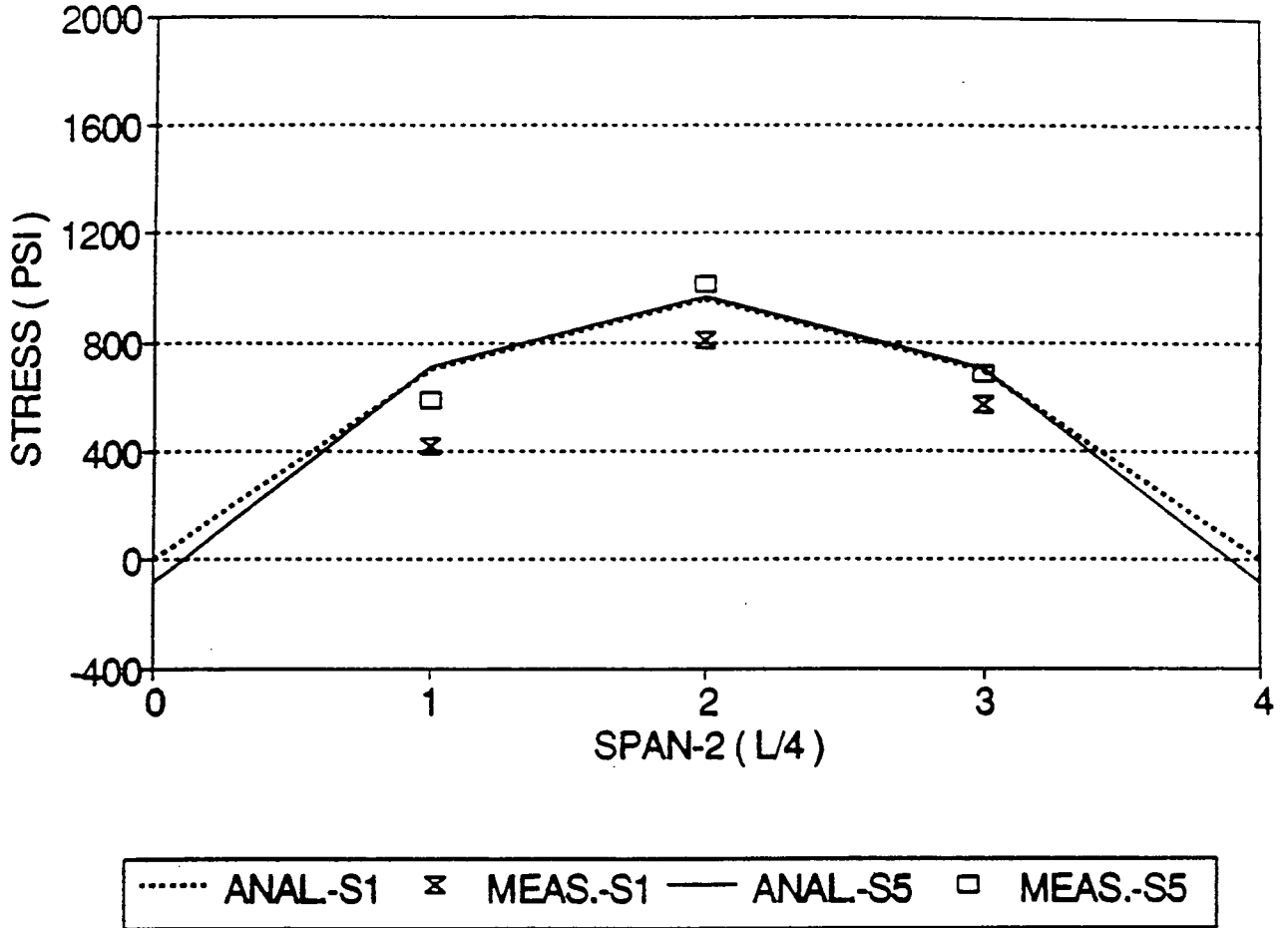
FIGURE 3.22 DEAD LOAD STRESSES GAGES 23_B

23_T
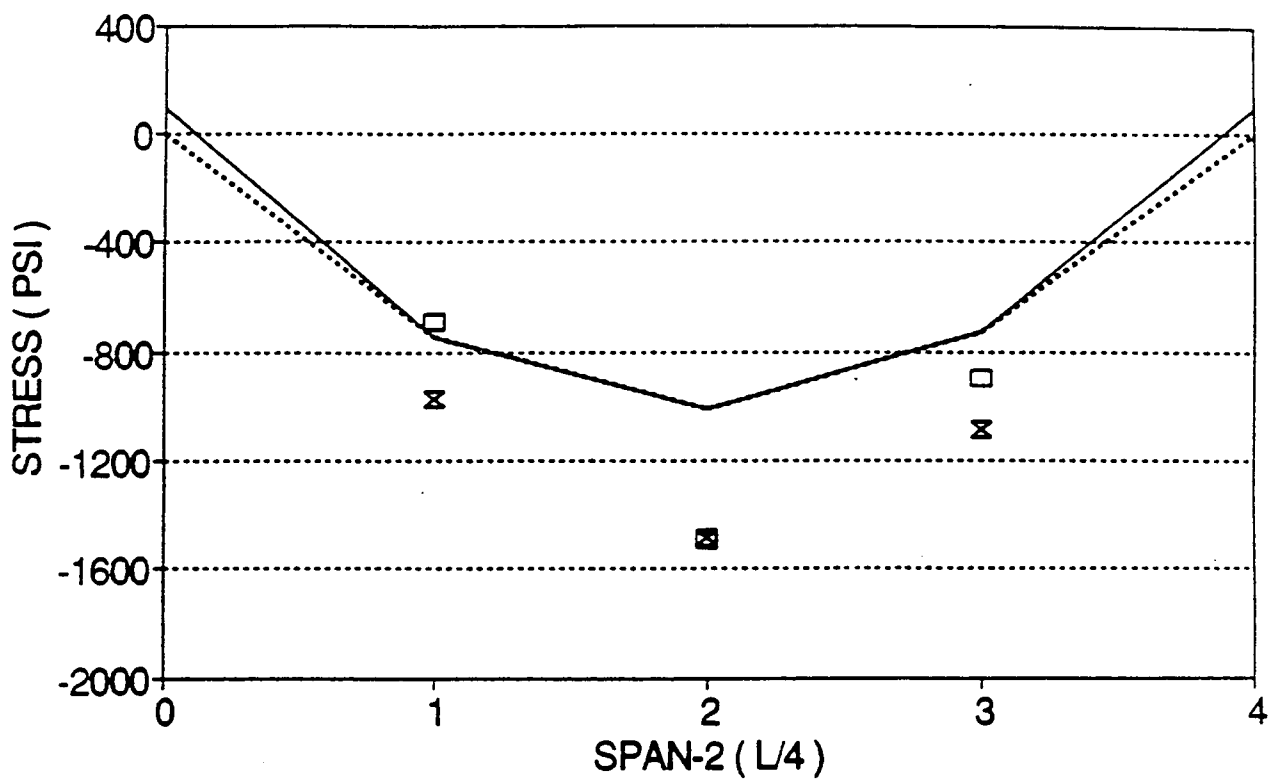
FIGURE 3.23   DEAD LOAD STRESSES   GAGES 23_T

24_B
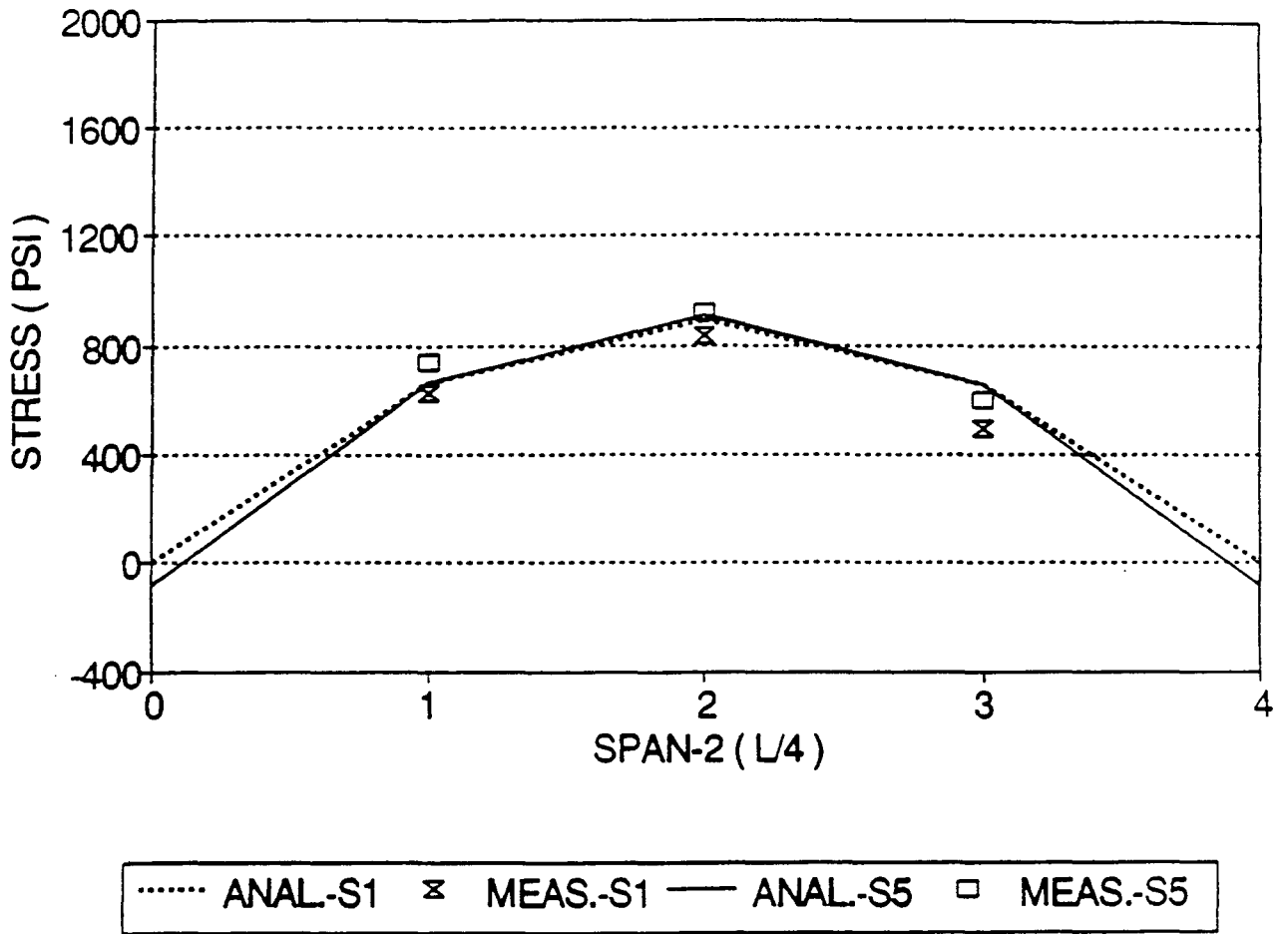
FIGURE 3.24   DEAD LOAD STRESSES   GAGES 24_B
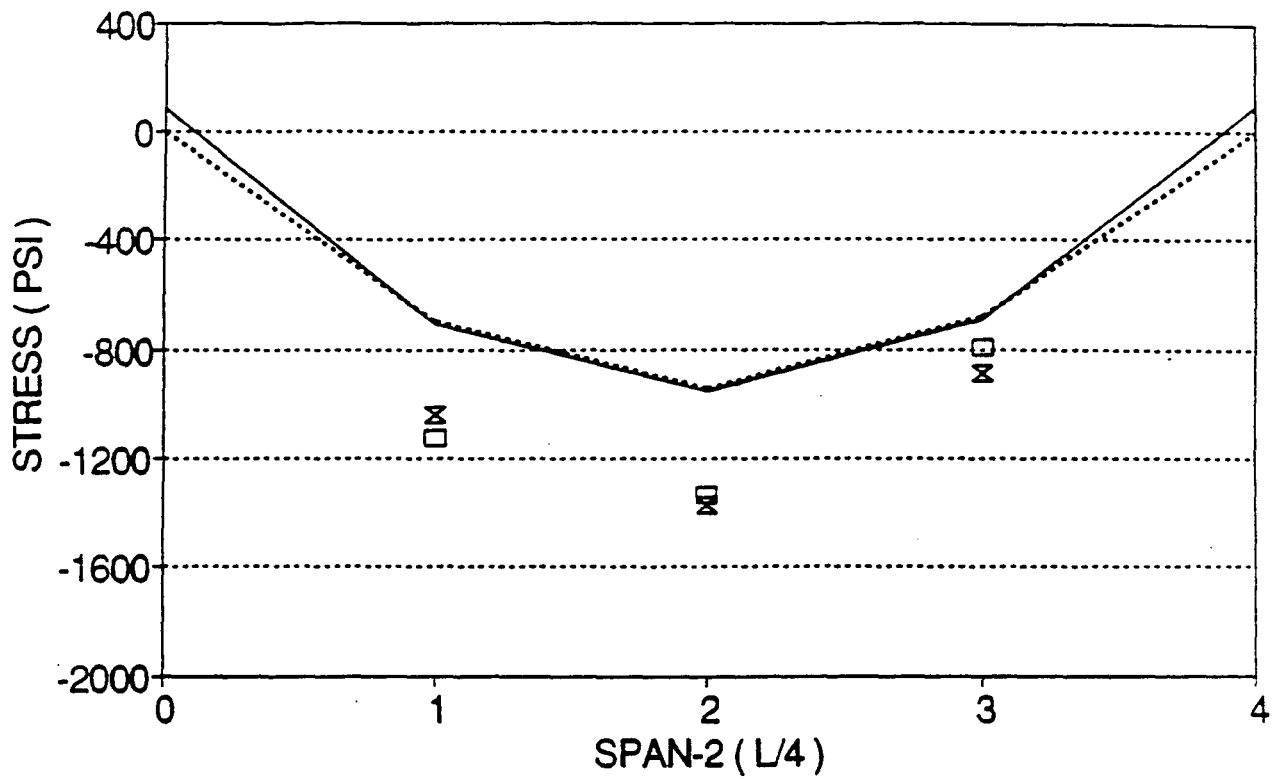
FIGURE 3.25   DEAD LOAD STRESSES   GAGES 24_T

TRUCK NO. 1

| 7'-0" | 13'-3' |

▼ 86.5 K

| # 4 | # 3 | # 2 | # 1 | AXLE NO. |

AXLE LOAD   26.9 K   27.0 K   15.0 K   16.6 K

WHEEL DISTANCE   4'-6'   4'-4'   11'=10'

TRUCK NO. 2

| 7'-3 1/4' | 14'-1 3/4' |

▼ 86.5 K

| # 8 | # 7 | ≠ 6 | # 5 | AXLE NO. |

AXLE LOAD   25.8 K   26.4 K   17.7 K   16.6 K

WHEEL DISTANCE   4'-5'   4'-6'   12'-6'
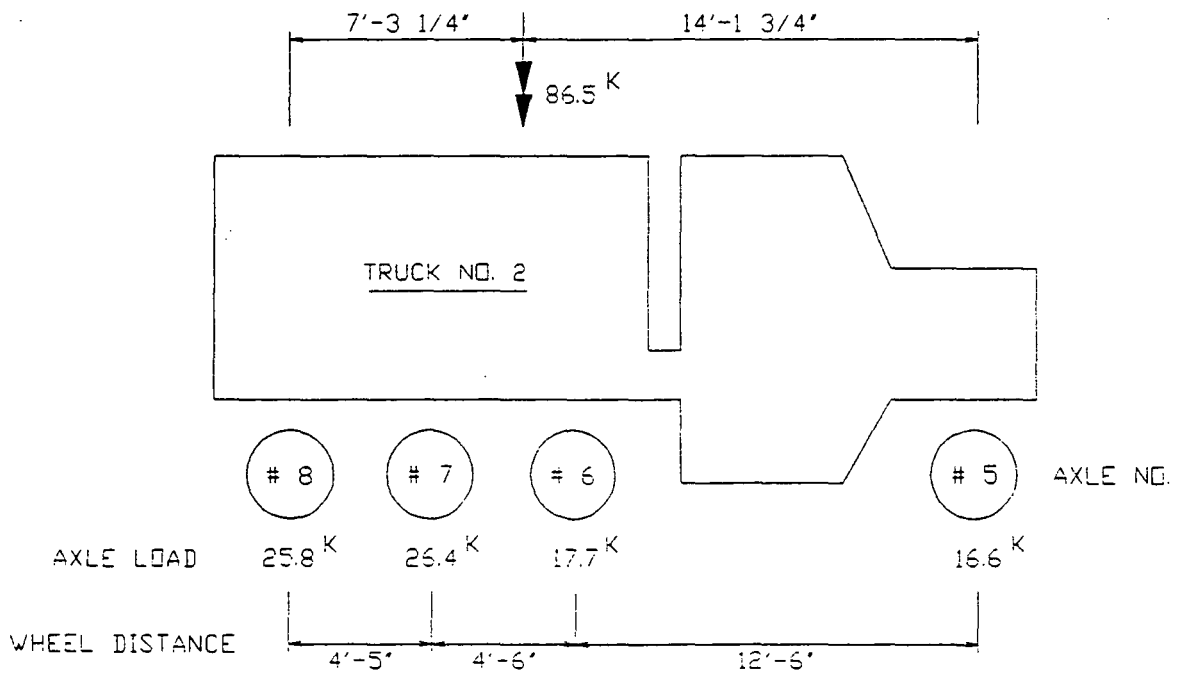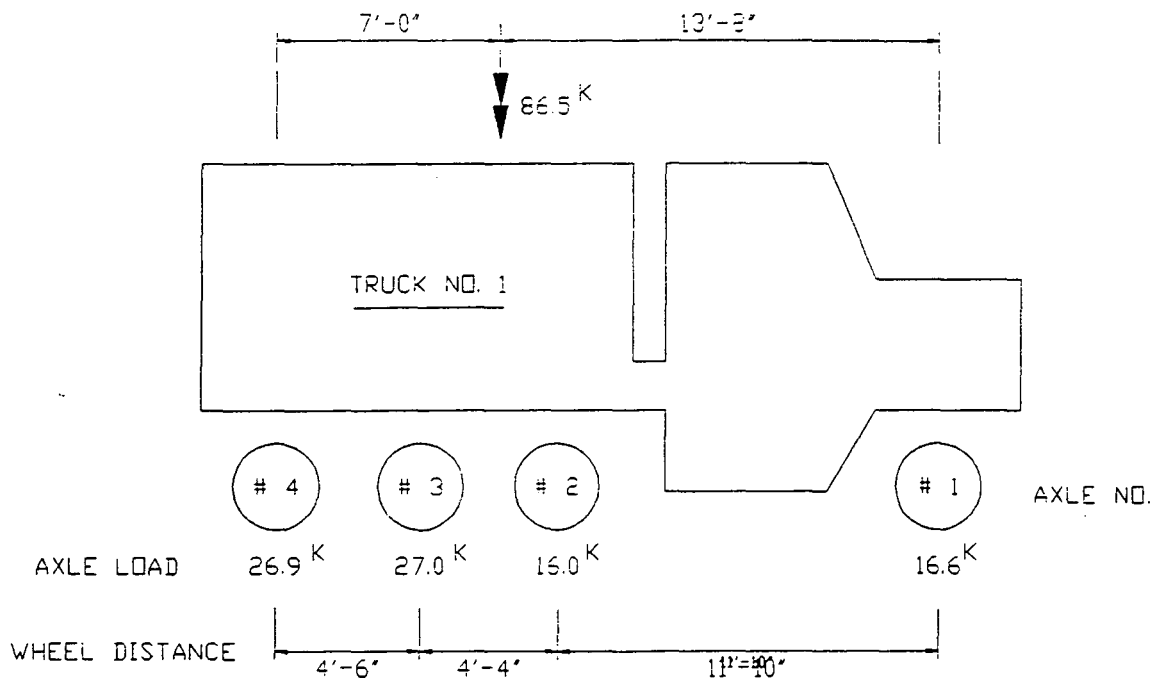
FIGURE 4.1   CHARACTERISTICS OF TEST TRUCKS
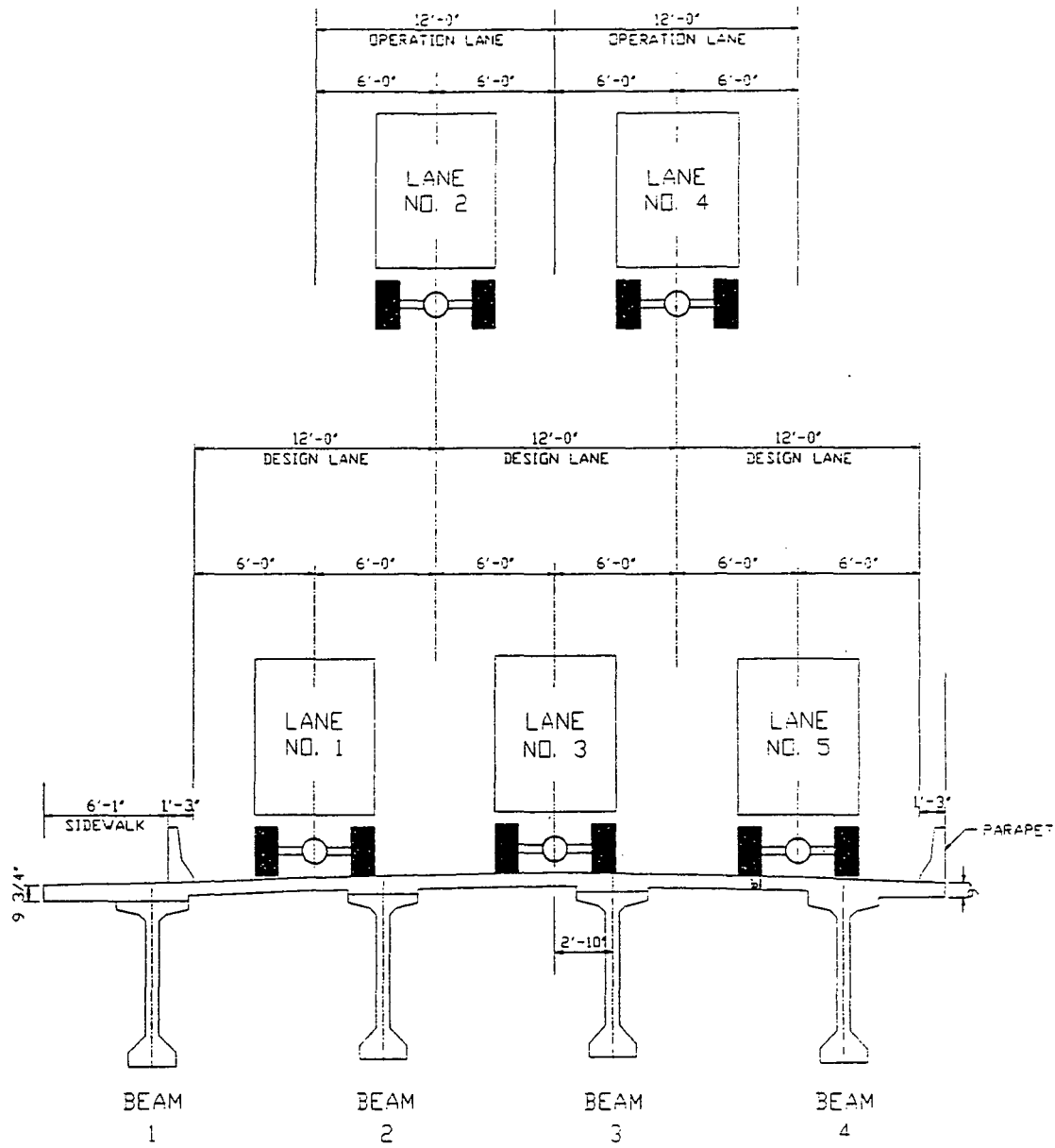
FIGURE 4.2 TEST LANES
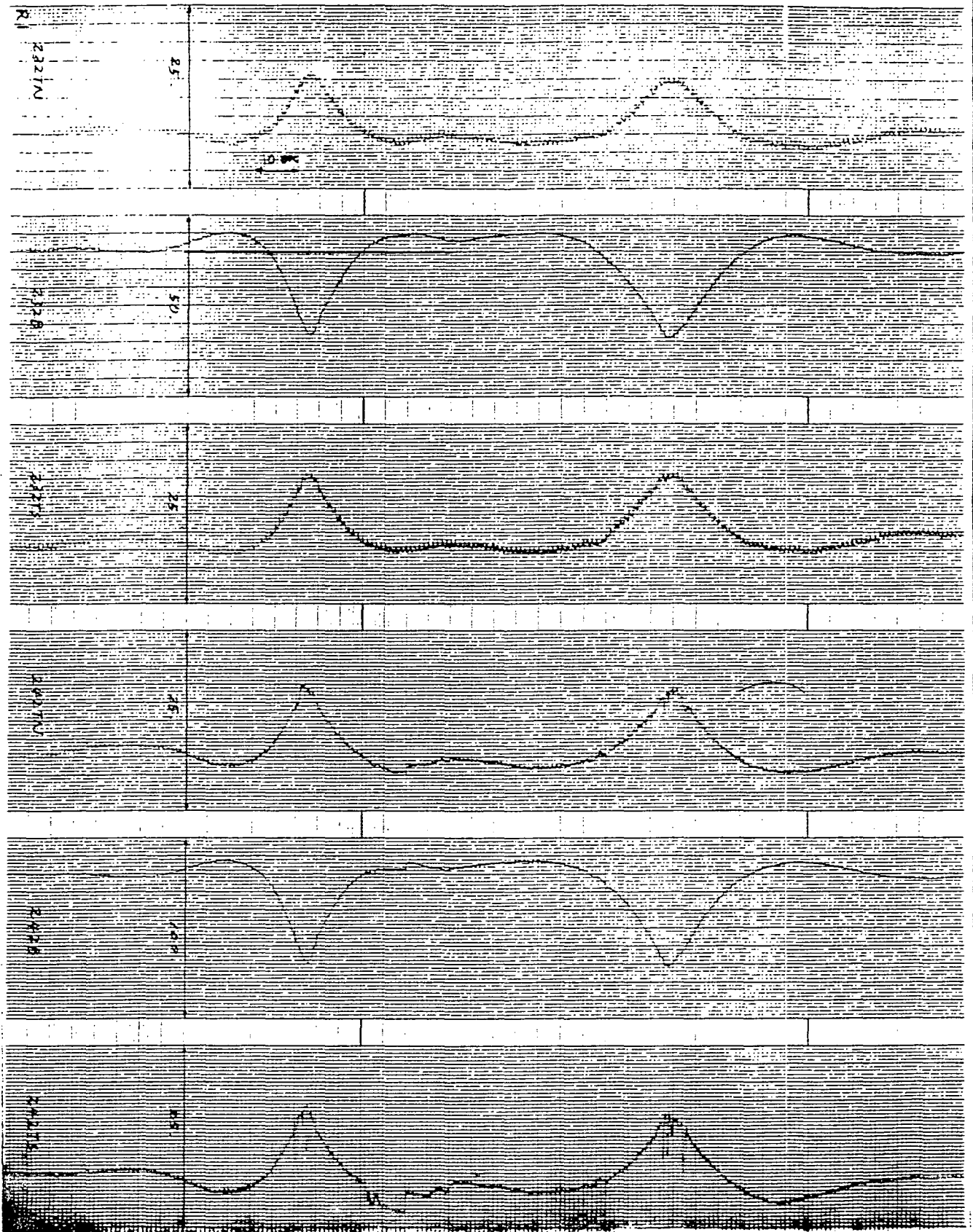
FIGURE 4.3   EXAMPLES OF STRAIN - TIME RECORDS
TEST-TRUCK RUN NO 1
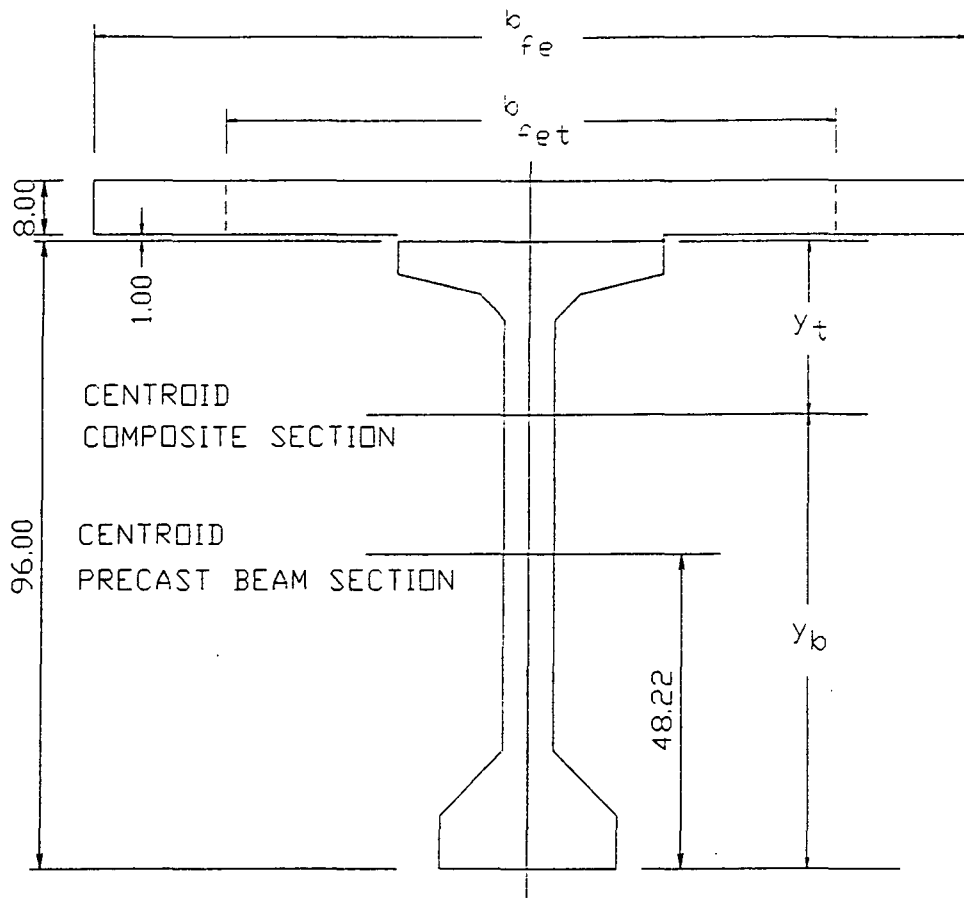
f'_{cs} = 4500 PSI f'_{cb} = 7600 PSI $n = \dfrac{E_{cs}}{E_{cb}}$ = 0.77

	A	$\overline{y}_b$	I
PRECAST BEAM SECTION	1277 IN.^{2}	48.22 IN.	1,522,000 IN.^{4}
COMPOSITE SECTION			
b_{fe} = 96 IN.		65.47 IN.	2,682,000 IN.^{4}

FIGURE 4.4   PROPERTIES OF COMPOSITE SECTION
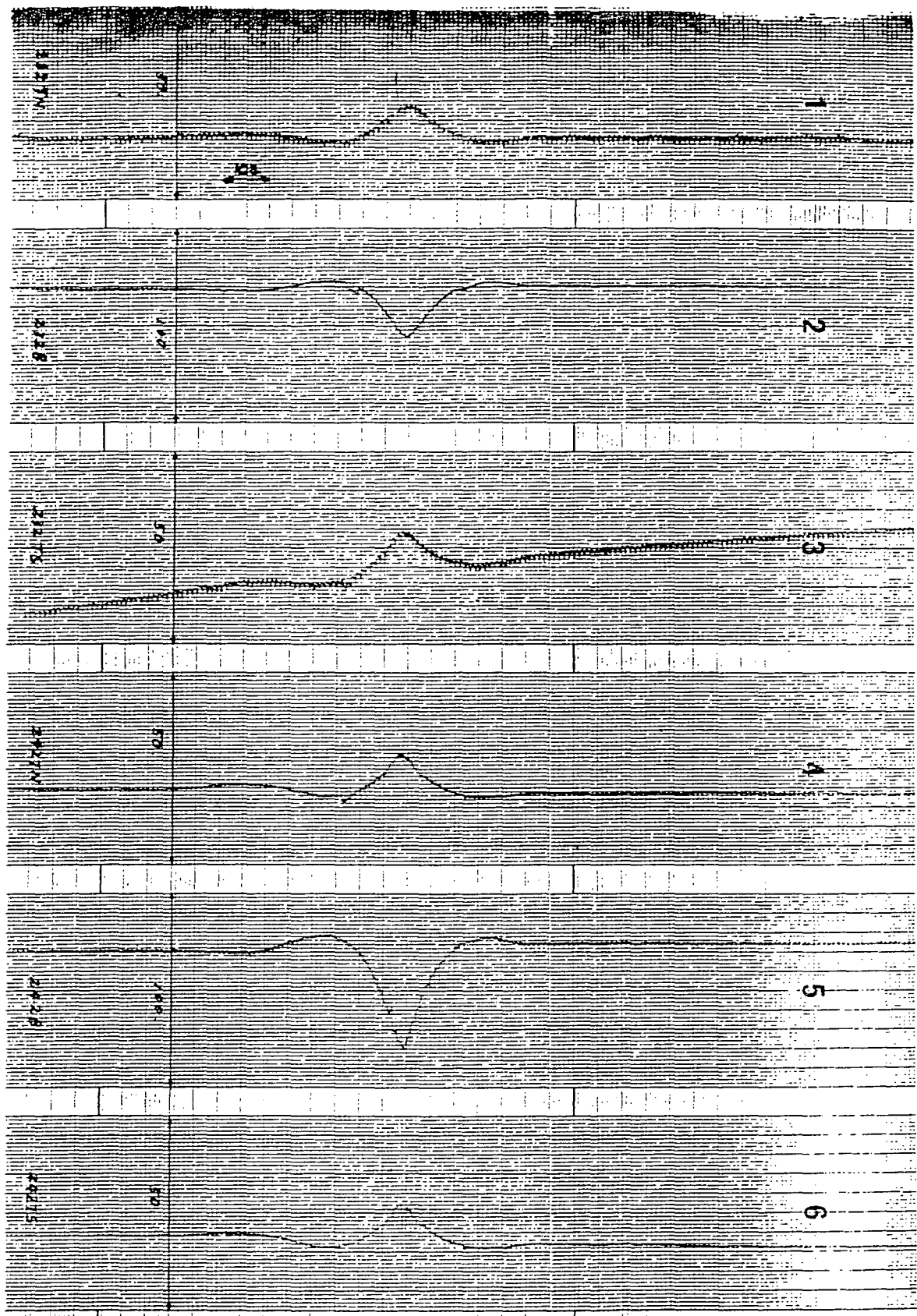
FIGURE 4.5   EXAMPLES OF STRAIN – TIME RECORDS
SUPERPOSITION TEST RUN NO. 1
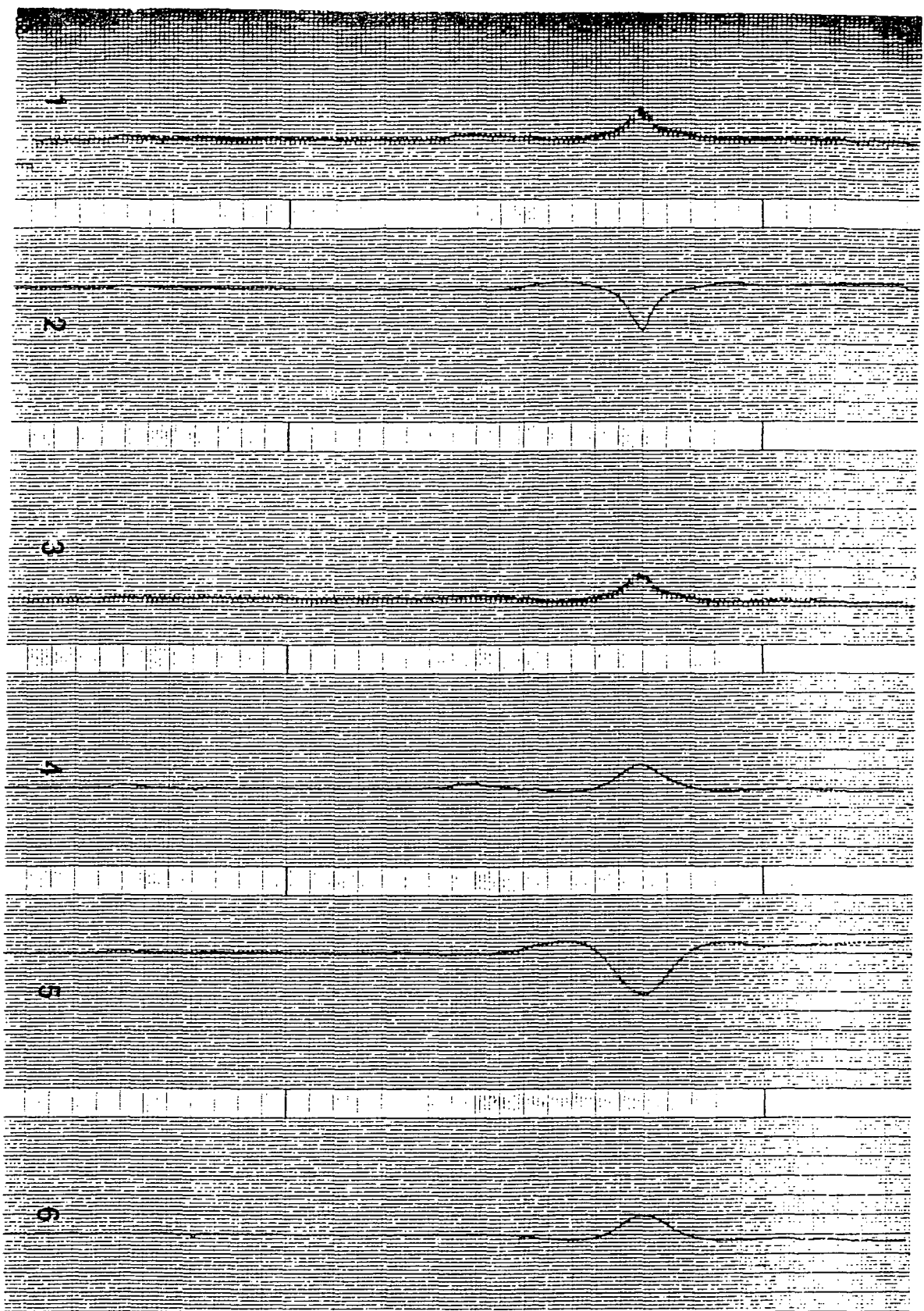
FIGURE 4.6   EXAMPLES OF STRAIN - TIME RECORDS
SUPERPOSITION TEST RUN NO. 2
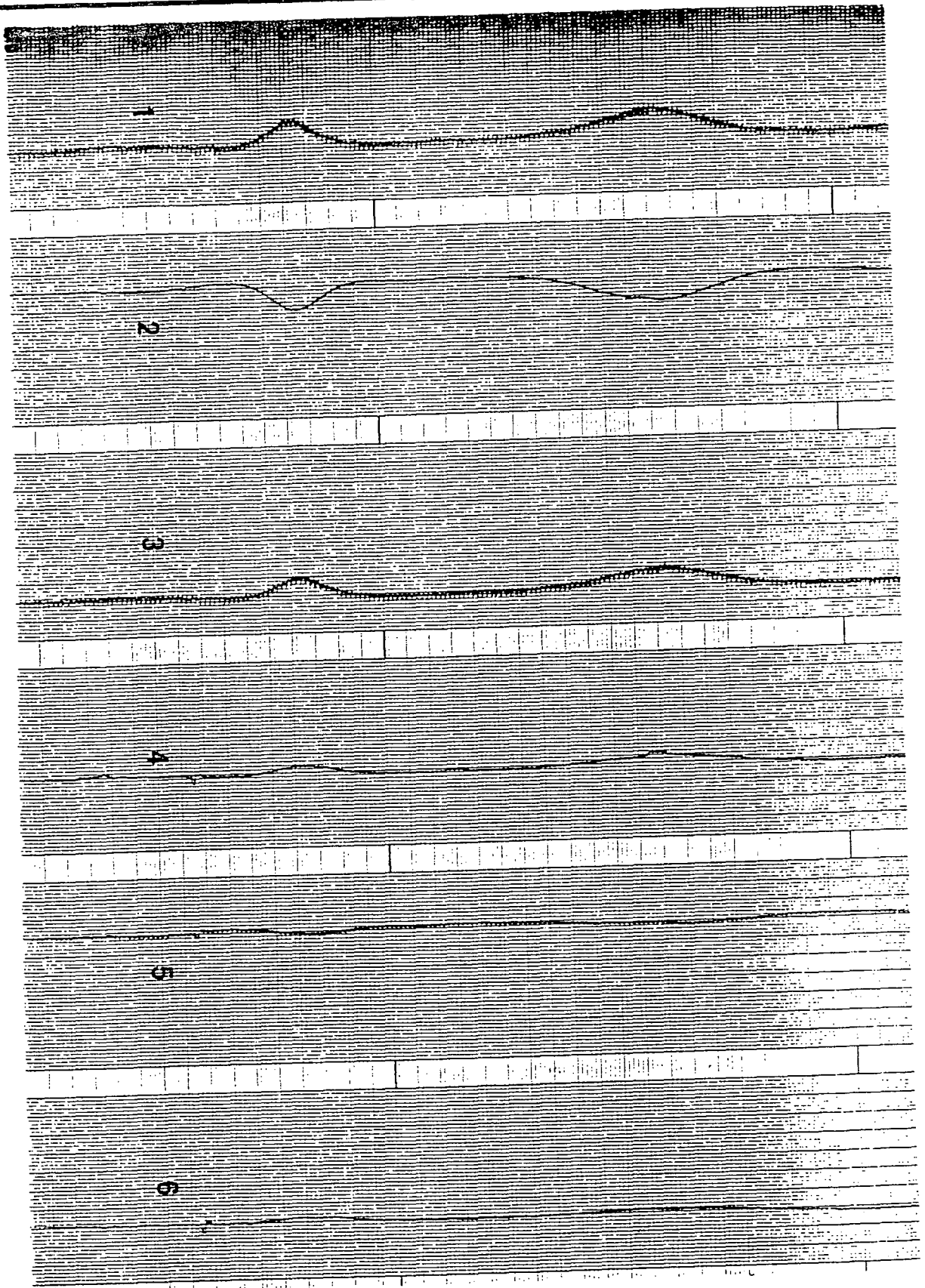
FIGURE 4.7   EXAMPLES OF STRAIN — TIME RECORDS
SUPERPOSITION TEST RUN NO. 3
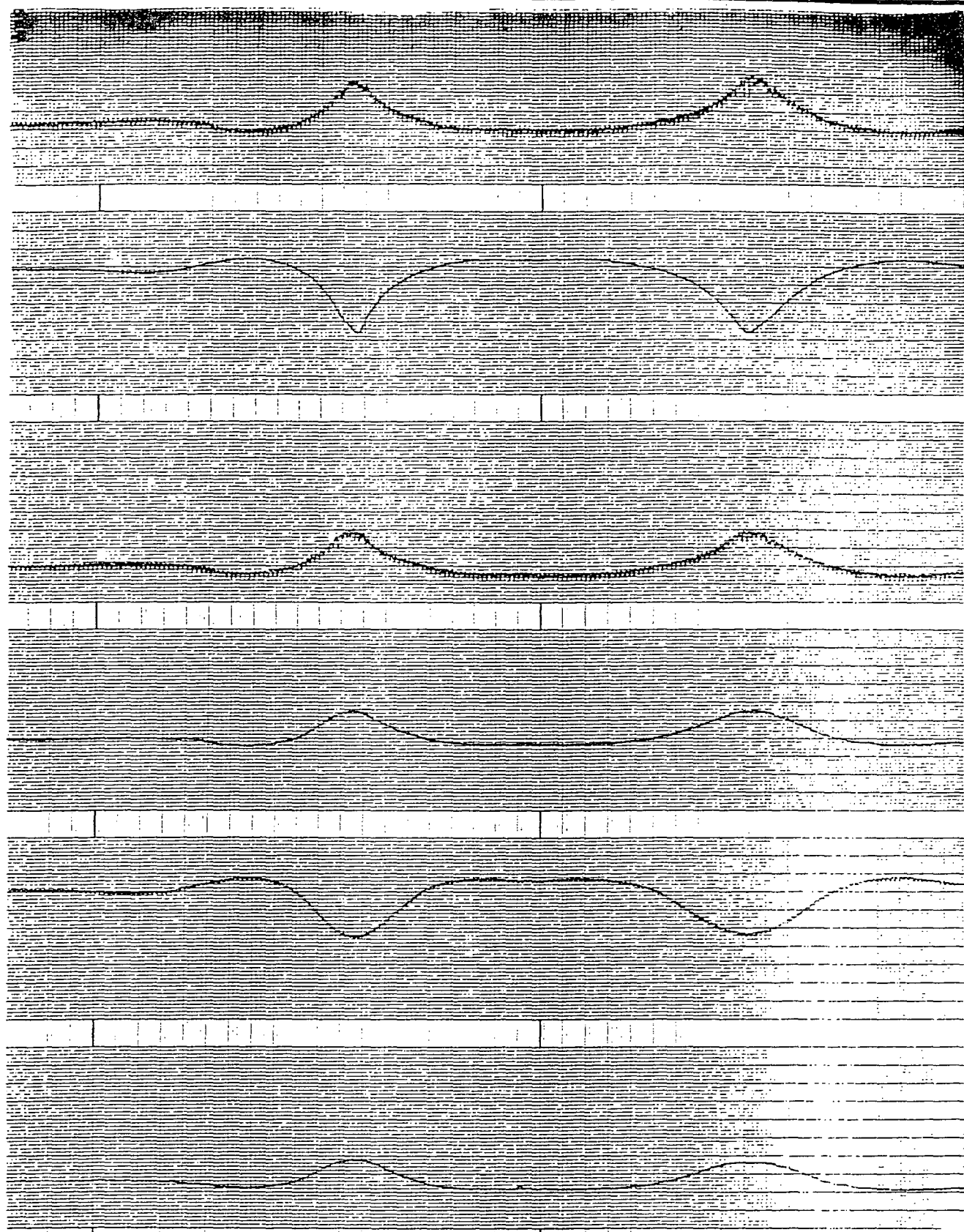
FIGURE 4.8   EXAMPLES OF STRAIN - TIME RECORDS
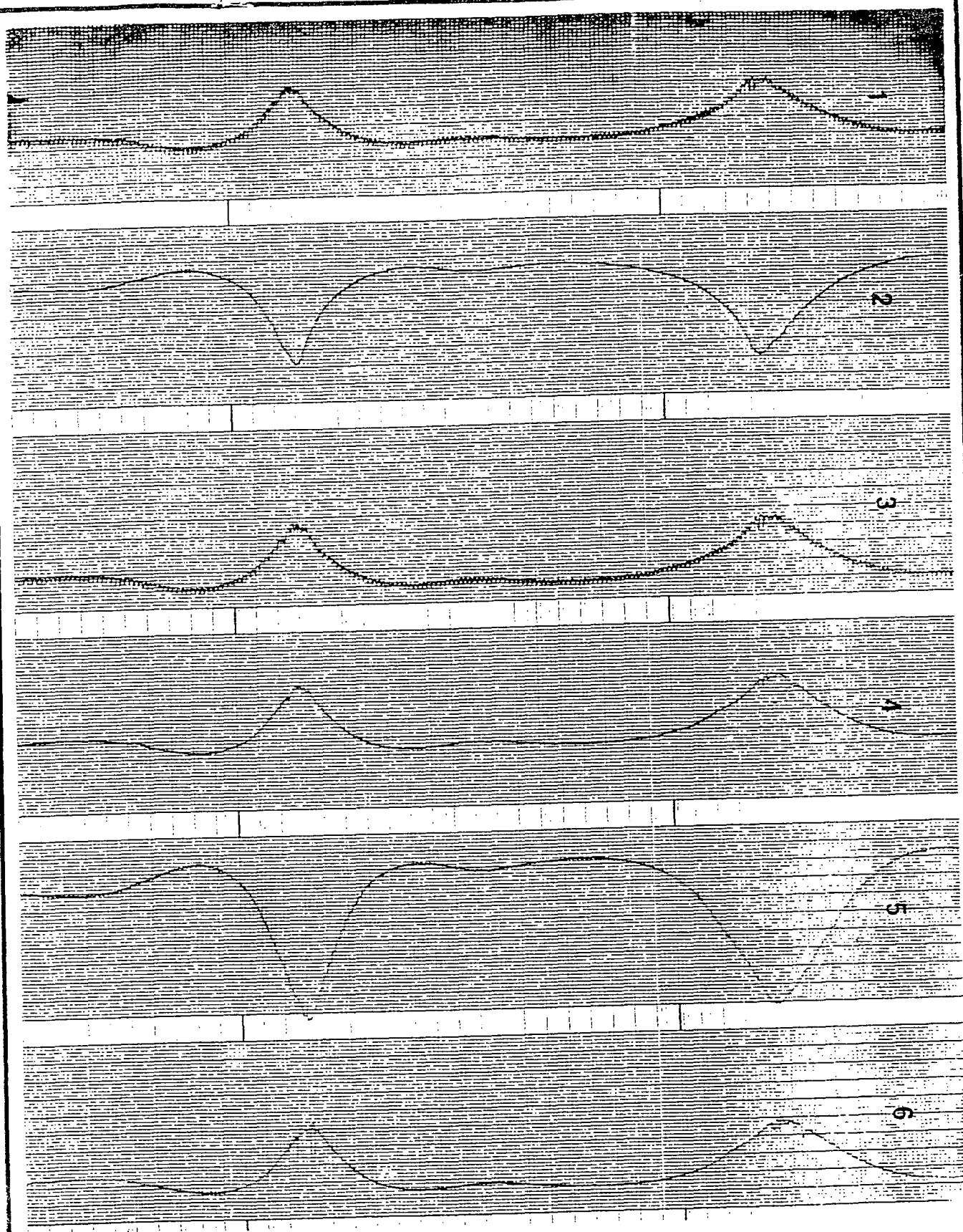SUPERPOSITION TEST RUN NO. 4

FIGURE 4.9   EXAMPLES OF STRAIN - TIME RECORDS
SUPERPOSITION TEST RUN NO. 5
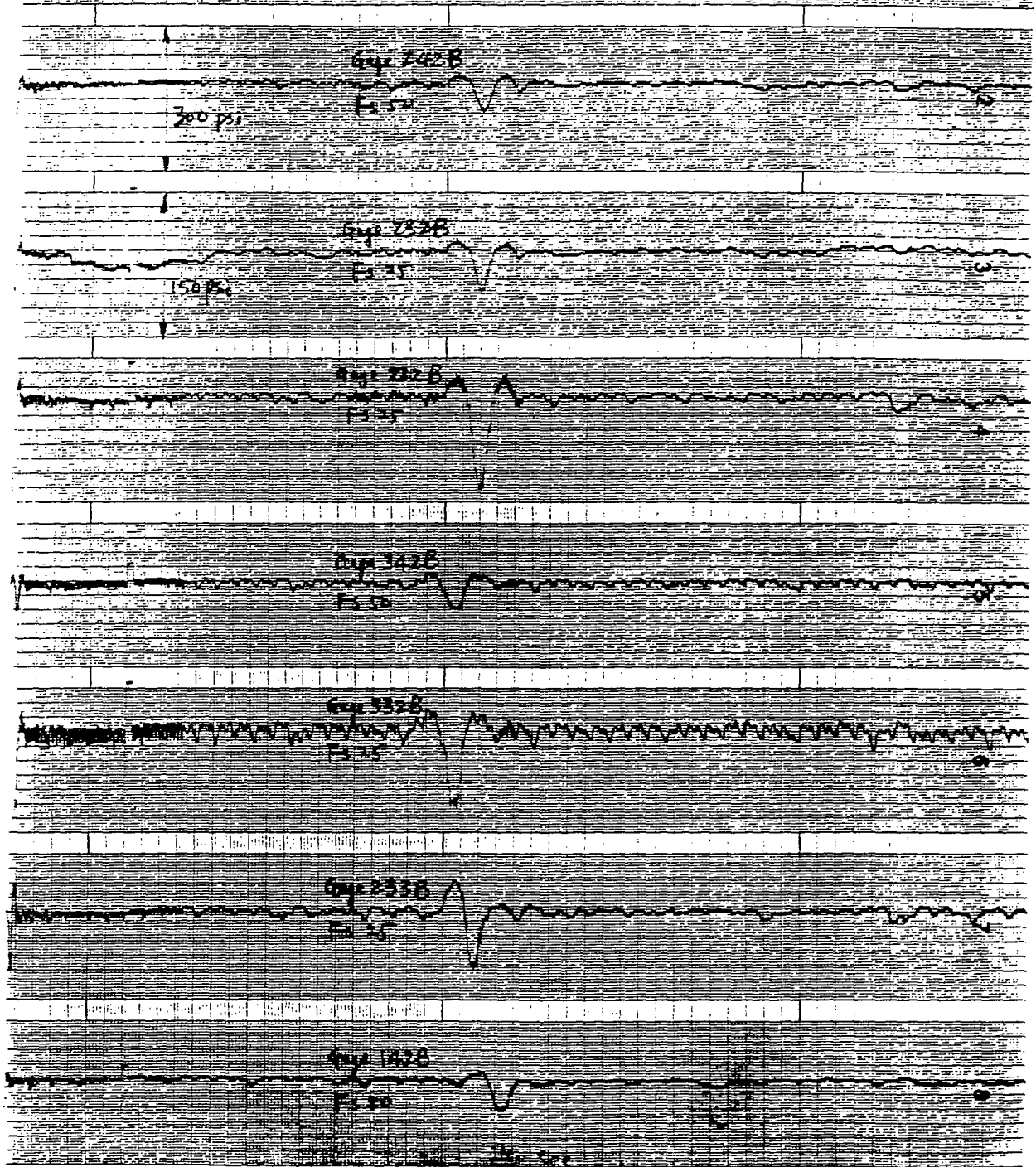
FIGURE 5.1   EXAMPLES OF STRAIN-TIME RECORDS
              DUE TO REGULAR TRAFFIC
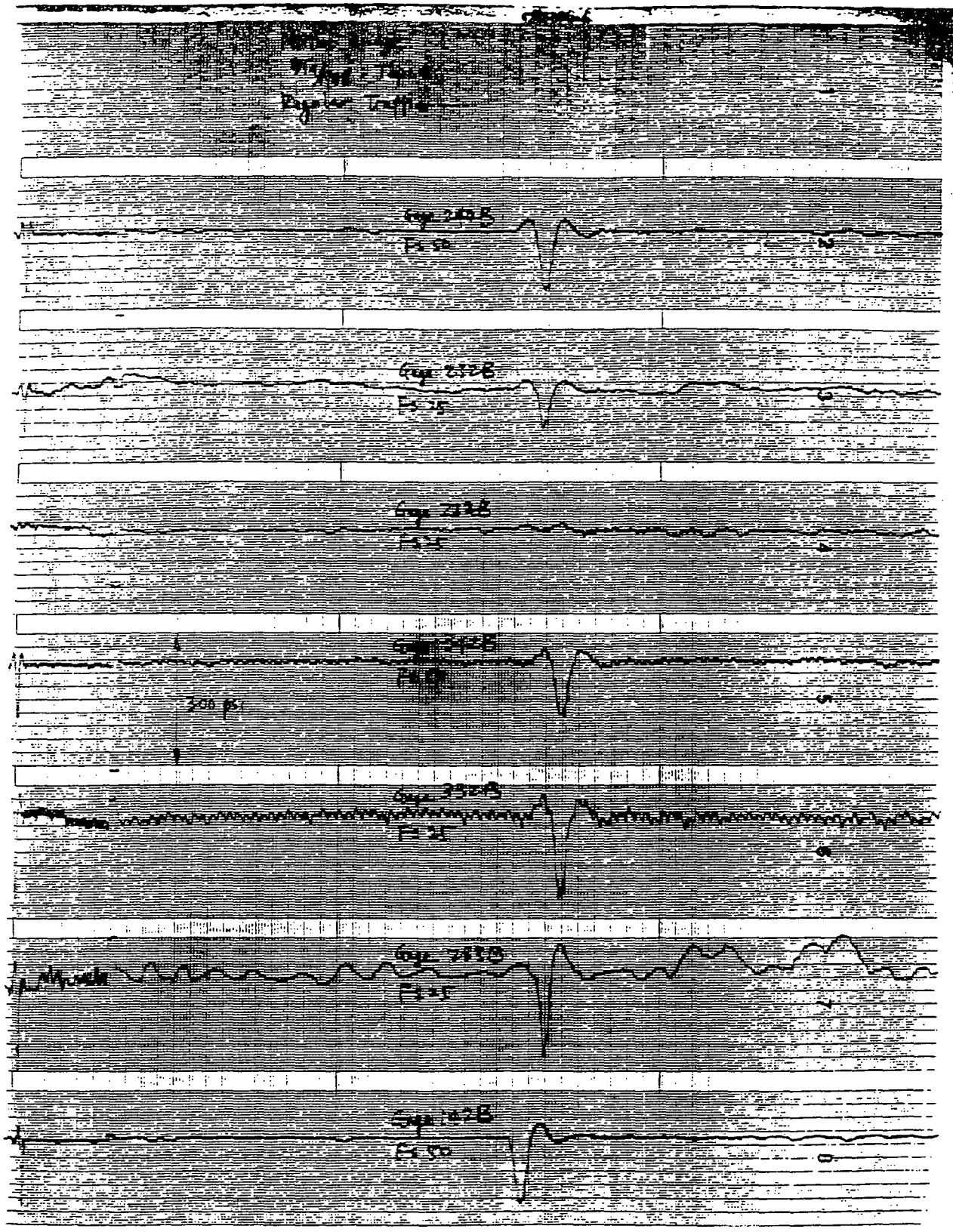   SINGLE TRUCK WESTBOUND IN LANE 2

FIGURE 5.2   EXAMPLES OF STRAIN-TIME RECORDS
DUE TO REGULAR TRAFFIC
SINGLE TRUCK EASTBOUND IN LANE 4

Milton Bridge
8/18/988 – Tape 4
Regular Traffic

Gage 242 B
FS 50

300 PSI

Gage 232 B
FS 25

Gage 222 B
FS 25

Gage 342 B
FS 50

Gage 332 B
FS 25
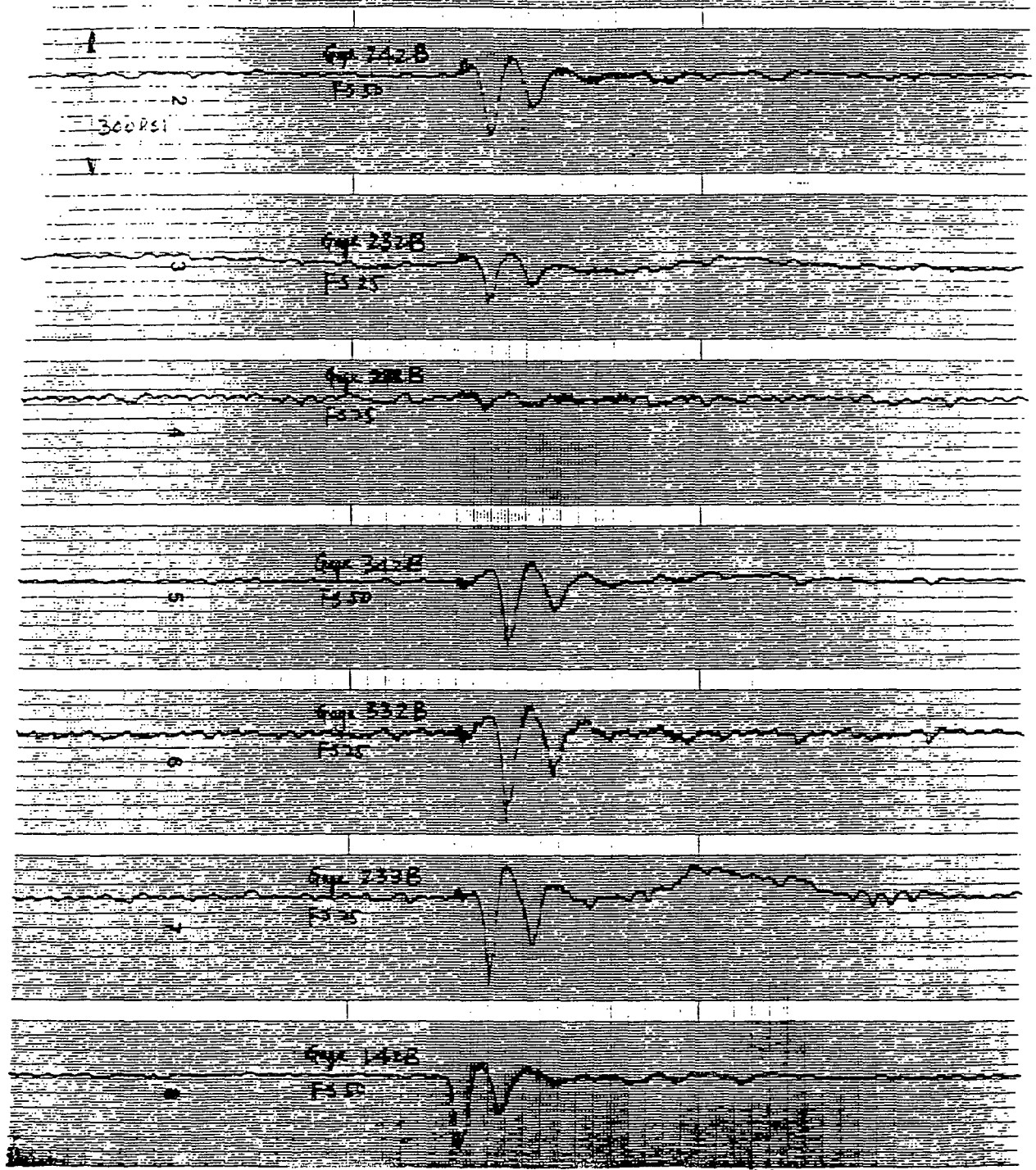
Gage 733 B
FS 25

Gage 142 B
FS 50

FIGURE 5.3   EXAMPLES OF STRAIN-TIME RECORDS
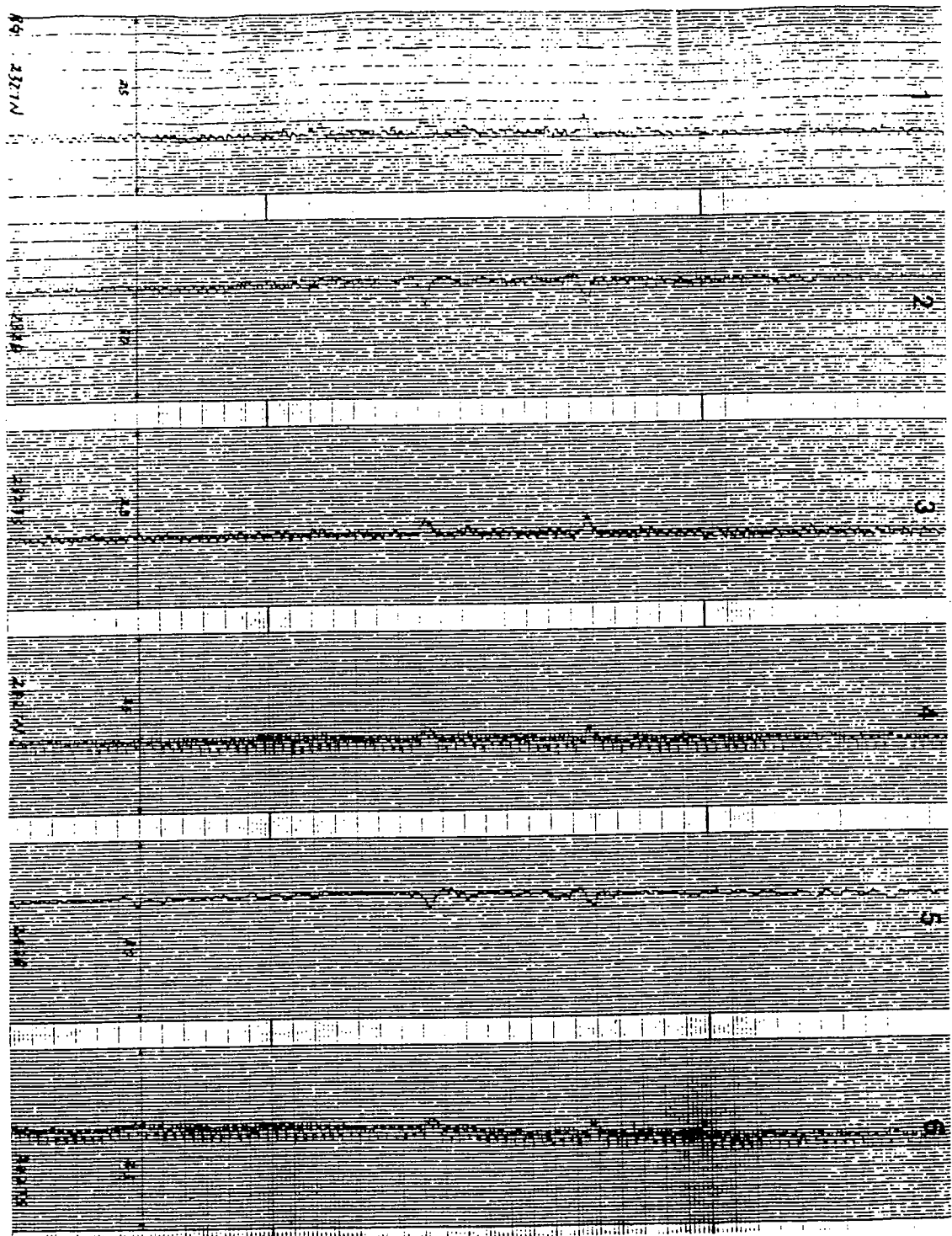DUE TO REGULAR TRAFFIC
TWO TRUCKS EASTBOUND IN LANE 4

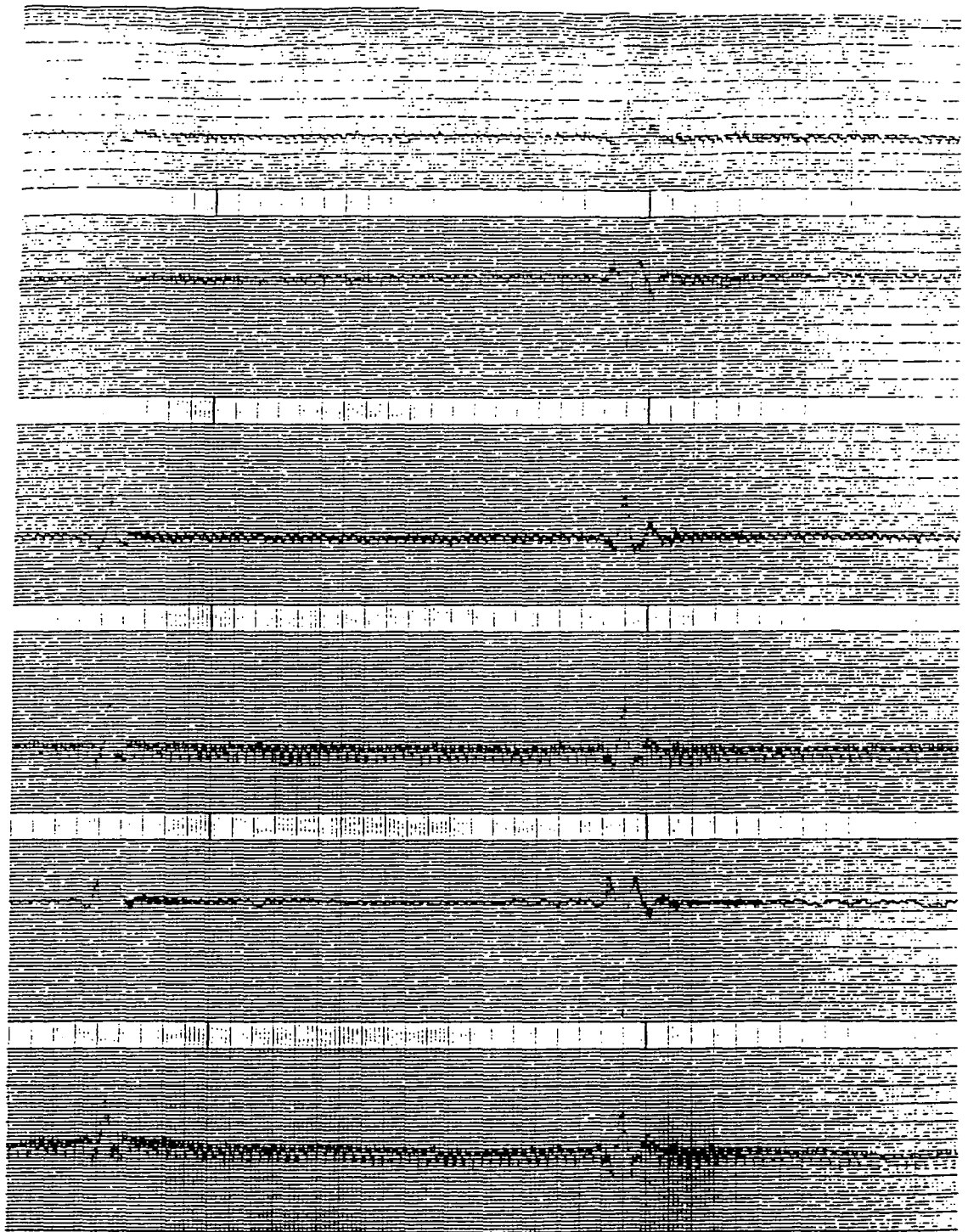FIGURE 5.4   EXAMPLES OF STRAIN-TIME RECORDS
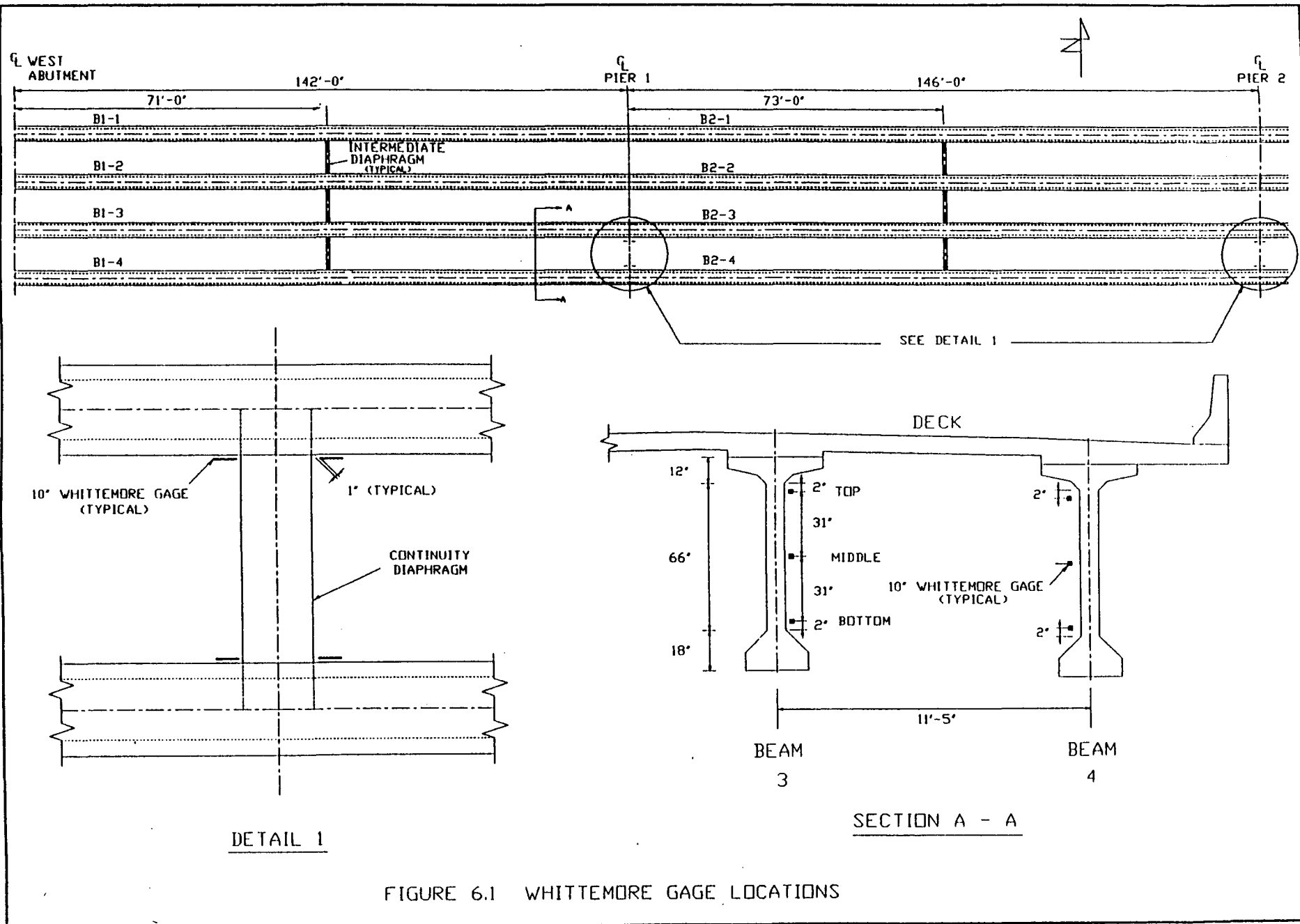DUE TO REGULAR TRAFFIC
EXAMPLE 1

FIGURE 5.5   EXAMPLES OF STRAIN-TIME RECORDS
DUE TO REGULAR TRAFFIC
EXAMPLE 2

CL WEST
ABUTMENT

142'-0"

71'-0"

B1-1

INTERMEDIATE
DIAPHRAGM
(TYPICAL)

B1-2

B1-3

B1-4

CL
PIER 1

146'-0"

73'-0"

B2-1

B2-2

B2-3

B2-4

CL
PIER 2

SEE DETAIL 1

10" WHITTEMORE GAGE
(TYPICAL)

1" (TYPICAL)

CONTINUITY
DIAPHRAGM

DETAIL 1

DECK

12"

31"

66"

31"

18"

2" TOP

MIDDLE

2" BOTTOM

2"

10" WHITTEMORE GAGE
(TYPICAL)

2"

11'-5"
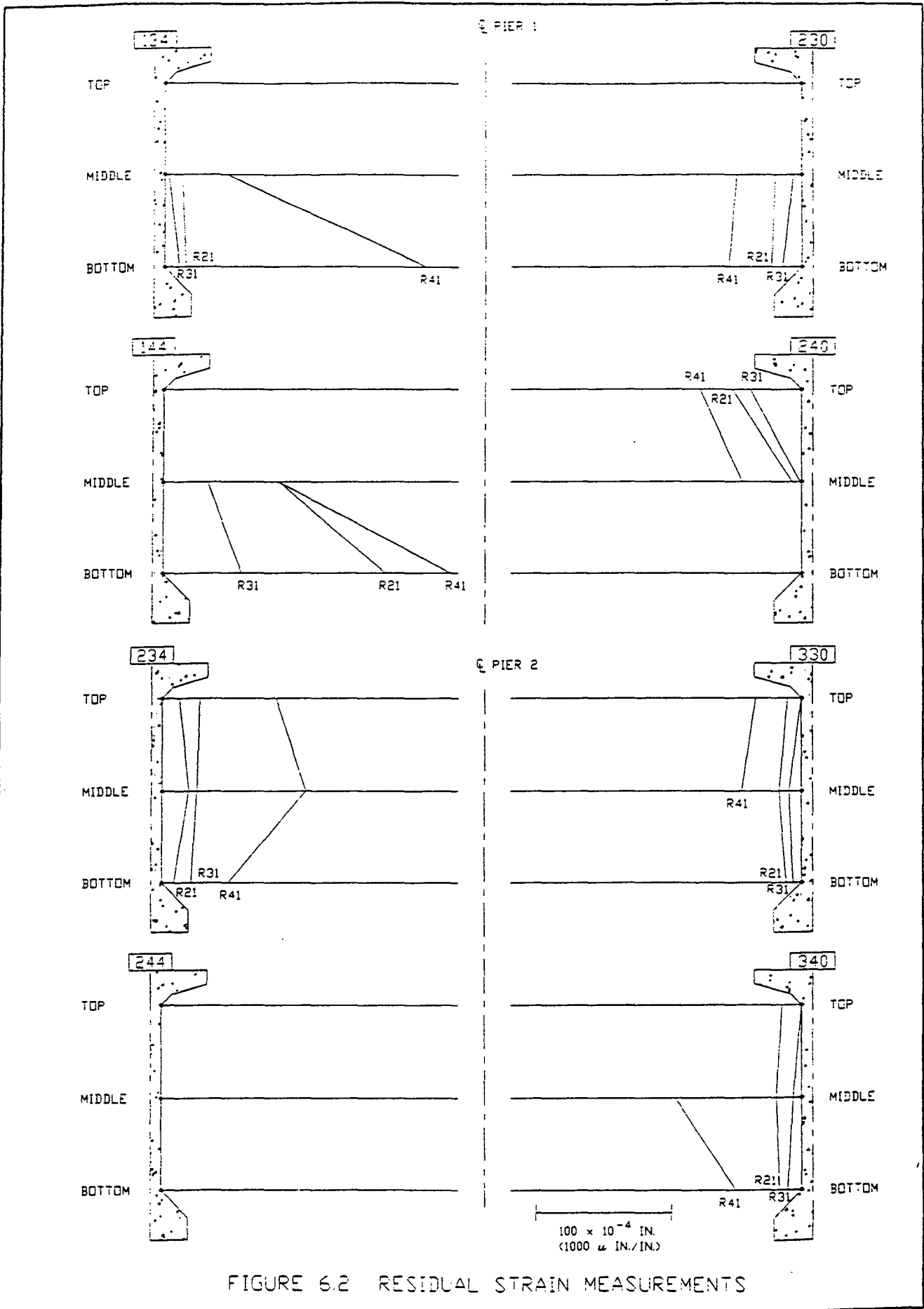
BEAM
3

BEAM
4

SECTION A - A

FIGURE 6.1   WHITTEMORE GAGE LOCATIONS

FIGURE 6.2 RESIDUAL STRAIN MEASUREMENTS